POLITECNICO DI TORINO –
UNIVERSITAT POLITÈCNICA DE CATALUNYA

Escola de Camins
Escola Tècnica Superior d'Enginyeria de Camins, Canals i Ports
UPC BARCELONATECH

MODELING OF CONCRETE DAM MOVEMENTS CAUSED BY EXPANSIVE PHENOMENA

Master Degree in Civil Engineering

Relators:

Ignacio Segura Pérez

Tai Ikumi Montserrat

Alessandro Pasquale Fantilli

Student:

Luca Cazzetta

July 2020

Torino - Barcelona

ABSTRACT

Expansive chemical reactions as Internal Sulphate Attack and Alkali-Silica Reaction are degradation phenomena that, under specific conditions, develop inside concrete structures. Concrete dams have been frequently diagnosed with such issues. Expansive reactions proceed for long time and eventually lead to different forms of deterioration and damage. Amongst the latter ones, movements of points of the dam have been attributed to the development of the reactions.

The main goal of this master thesis is to model the movements that are detected in concrete dams. The movements captured by auscultation systems, placed on the dams since an adequate number of years, are valuable hints of what happens inside the concrete. Points of the dams sometimes showed non negligible displacements, together with other deterioration mechanisms.

First the movements, in the vertical and horizontal direction, are obtained and analysed. These data, belonging to four Spanish dams (Graus, Tavascan, Paso Nuevo, Toràn), are then modelled with a mathematical exponential law, characterized by parameters that proved to be related to physical characteristics of the dams and to the physical-chemical nature of the reactions involved.

Robustness analysis was carried out, with the objective to find out whether the mathematical law that fitted the data is robust. The movements showed similar patterns among the different dams, that are composed of three characteristic phases: initiation, development and passivation. Fitting a specific portion of the pattern, and the whole dataset sometimes lead to similar results.

In the last stage parameters of the modelling of the movements are related, conceptually, to the physical and chemical aspects involved. Mathematical parameters of the model turned out to have a correlation with specific aspects of the anomalous dam behaviour, i.e. entity of the movements and their rates of development.

ACKNOWLEDGEMENTS

First of all I would like to thank Ignacio Segura, the Tutor of this Master Thesis, that despite the difficulties of this period, dictated by the COVID-19 outburst, has always been present, regardless of the distance, to support my work and guide it with his knowledge.

My gratitude is turned as well to Professor Alessandro Pasquale Fantilli, the tutor of my home university, for his advices in the moment of Erasmus experience interruption and its continuation in a telematic mode.

I desire to extend my thanks to Politecnico di Torino, for these great years of university life, and to the Universitat Politècnica de Catalunya, for hosting me in what turned out to be an unlikely too short period.

Then, I wish to thank all of my friends that have always been by my side in both good and difficult moments.

Finally, I want to say how grateful I am to my family, for what they are: my greatest gift.

LIST OF CONTENTS

LIST OF FIGURES

Number *Page*

LIST OF TABLES

Number *Page*

CHAPTER 1 - INTRODUCTON

1.1 Introduction

Dams represent a vital category of infrastructures inside a nation, for what concerns their role and their strategic importance. A great number of dams is built, and is being built, in concrete. It is therefore of clear remark the role that this material is called to serve.

Dams all over the world are built and maintained for various purposes, that very frequently include hydropower use or storage or irrigation and watering. The awareness of their fundamental role in the society and the understanding of the behaviour assumed by these gargantuan structures are prime necessities for who actually deals with them, as could be engineers.

Figure 1.1 – Dam of Paso Nuevo, one of the four investigated dams, in the province of Huesca, region of Aragon, Spain.

The issues of the expansions and volume changes that develop inside the concrete are, in this perspective, a delicate and important aspect, since they may lead to the degradation of the concrete fabric, that in turn could damage the structures, altering the macrostructural properties of concrete, and compromise their functionality and eventually their stability.

Inside 4 Spanish dams (Graus, Tavascan, Paso Nuevo and Toràn) that are located in the regions of Catalunya and Aragon, at North-East of Spain, the most harmful chemical reactions that developed over time were identified to be the ones that fall under the name of Internal Sulphate Attack (ISA) and Alkali-Aggregate Reaction (AAR), (Aguado et al., 1998, Araújo, 2008, Pardo, 2009). Of the latter one, in particular, the most diffused is the reaction with the silica compound of aggregates, named then Alkali-Silica Reaction (ASR).

As the abovementioned reactions proceed, their expansive character lead to a series of consequences, among which lay anomalous movements of points of the dam.

The principal objective carried out in this master thesis is the modelling of the movement data that are captured by the auscultation systems placed on the abovementioned dams. Specifically, the movements that have been registered, over many years, are the horizontal and the vertical movements. Several years of measurements are needed to be able to satisfactorily interpret the movements trend of the whole lifetime of the dams.

In a second stage movements modelling will be related to the main physical characteristics of the dams, such as height of the concrete blocks that compose the structure, and with the physical-chemical aspects of the deterioration mechanisms involved in the concrete mass deterioration

.

1.2 Scope and methodology

The movements of the dams have been acquired by means of auscultation systems that were put in place simultaneously to the end of construction of the dams and its commissioning. Unfortunately, often the auscultation systems were placed only some years after the commissioning of the dam. In these cases, the first part of the movements' history is missing. This issue is a non-trivial aspect in the case of Toràn dam, that despite being commissioned in year 1964, data are available only from year 2000. The modelling of the data resulted to be quite compromised, being the data set to be fitted too short (and of too late data). Additional assumptions have been stated for this dam.

One of the features of the modelling that was investigated deeply is the robustness of the modelling. The trends of movements with time and the actual evidences left by the degradation mechanisms were indisputably clear, and their analysis and diagnosis has been investigated deeply by many Authors. In this instance, the model proposed by Aguado, charged of the fitting of movements with an exponential law (Aguado et al., 1993) is questioned about its robustness, towards its capability to suit and predict recorded dams' movement measurements.

The questioned issues of the model robustness were the influence that different portions of the data have on the whole set of data. Specifically, data of the movements were split up in more parts, representative of the different parts of the displacements' evolutions, and each part was separately tested.

The last objective of the thesis corresponds to the physical modelling of the parameters of the model of the data movements. The parameters of the abovementioned exponential law are found to be related to physical and chemical aspects of the dams' deteriorations mechanisms, and a characterization of these relations are searched for.

The movements and their fitting have been analysed in detail on Matlab, a well-known computer software for numerical computation and statistical analysis. In the Matlab

environment data are analysed, modelled and eventually plotted. This powerful software allowed to carry a lot of operations and computations, among which the robustness analysis.

The physical modelling aimed to relate the parameters of the exponential movements model to physical characteristics, e.g. content of reactive minerals as pyrrhotite and pyrite. The purpose of this phase of modelling is the to be able to estimate movements potential intensities and their evolution in time, by an analytical model, but passing through physical aspects of the phenomena, that have a central role in the development of the deterioration mechanisms.

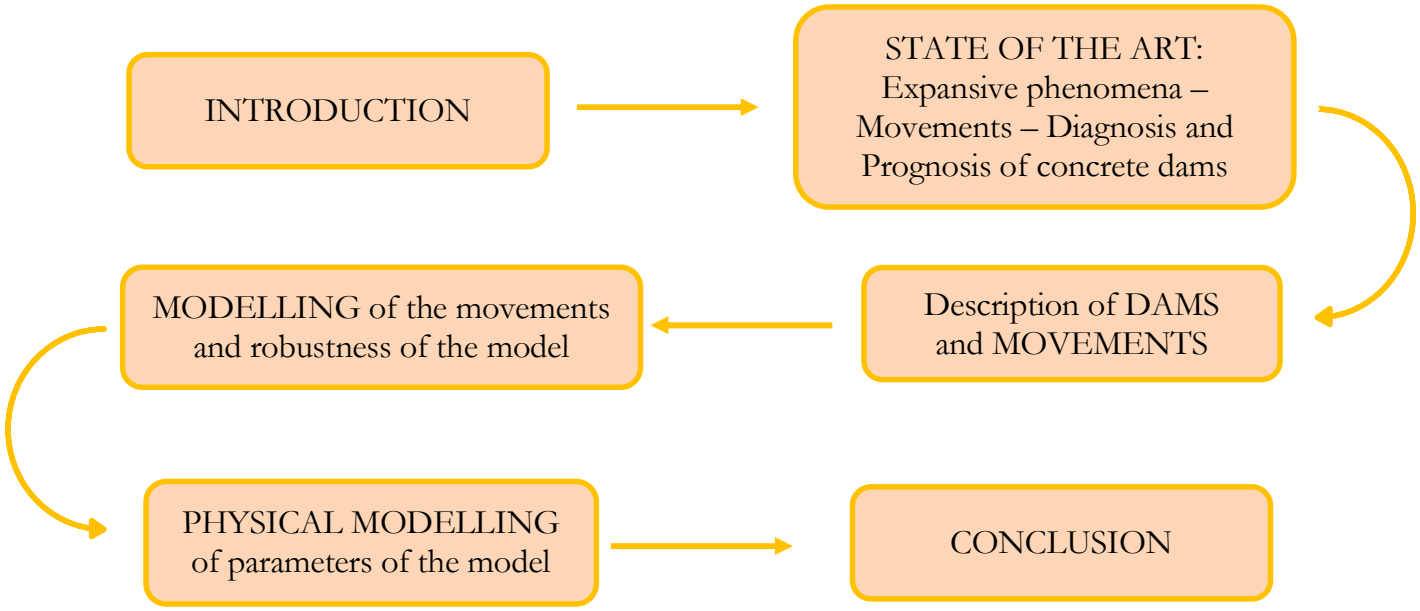

Figure 1.2 – Conceptual scheme of the thesis

CHAPTER 2 – STATE OF THE ART

2.1 Introduction

A great number of concrete dams are gravity dams, a classic structural scheme that works by countering the external actions by only its own weight. These massive structures are characterized by a huge quantity of concrete cast in-situ. Hence, all the components that make up the concrete are required in abundance. One of the components of concrete are the aggregates, and since a huge amount of them is required, it is usual strategy to extract them from sites as close as possible to where the dam will be built, in order to keep the costs under control (Casanova et al., 1996a). This scheme involves the use of aggregates that, according to their composition and their nature, could harmfully react with other components of the concrete. Hence the importance to characterize the aggregates (Ayora et al., 1998).

Whatever the structural type and the dimension, a lot of degradation phenomena are known to affect concrete, and amongst them lay those one that are related to the aggregates. With respect to this issue, two famous and well-known phenomena are the Internal Sulphate Attack and the Alkali-Silica Reaction. A lot of concrete structures are reported to be suffering of these diseases, and among them concrete dams (Pardo, 2009, Campos, 2012), that are likely to be severely affected, given their sizes and exposition to weathering agents.

The aforementioned reactions, Internal Sulphate Attack and Alkali-Silica Reaction (abbreviated ISA and ASR) are sets of detrimental chemical reactions that provoke expansion at a microstructural level, that pass on to the macrostructural scale mainly in form of cracking and fissures and cumulated non-recoverable movements. The progress of ISA and ASR reactions requires oxidizing agents (e.g. water and oxygen) and other specific conditions.

In this chapter, a review of the main aspects and effects of these two deleterious reactions, that develop inside the concrete without the need of external supply of sulphates (Divet, 2001) or alkali compounds, is presented.

First the expansive phenomena are described according to the advanced knowledge reached in this scientific field, together with the characterization and the evaluation of the consequences of their progress in concrete dams. Then, the modelling of their behaviour is revised, from both analytical and physical points of view.

2.2 Expansive phenomena in concrete dams

The expansive phenomena that were uncovered to be responsible, in the study cases of four Spanish dams, for damage and unusual behaviour are, as previously quoted, the Internal Sulphate Attack and the Alkali-Silica Reaction (Casanova et al., 1996b, Araújo, 2008). As well other reactions and phenomena happen inside the concrete mass, despite they are reported to be negligible compared to these former two in the case of concrete dams.

The eventuality of expansions that develop inside the mass of concrete is responsible for the cracking and fissuring that is much ordinarily found in concrete structures. Together with them come occurrences as spalling, pop-outs and staining, all typical diseases of such structures. ISA and ASR expansive phenomena are also responsible for the movements that are registered at the top level of the dams (Aguado et al., 1998, Araúlo et al., 2008) and that must be monitored to assure dam serviceability and static functions.

The expansive phenomena act at microscopic level and pass on to a macroscopic level. A well-established procedure of thorough description of the issues represented by the expansive reactions and their repercussions is outlined by Aguado et al. (1996, 1998). It consists in analysing the phenomena at three different levels: micro, meso and macrostructural, modelling each level with features that are characteristics of that scale. In the microstructural level, by way of example, the attention is focused on the chemical nature

of the reactions and of the reactants, e.g. oxidizing processes. In the intermediate meso-structural level the focus is drawn to the material of concrete. Usually this step is faced up with the help of numerical analysis, e.g. finite element modelling (Stankowski 1990, Casanova et al., 1997). Finally, at the macrostructural scale, the object of the modelling is the entire structure, from functional, structural and serviceability points of view. To evaluate the macrostructural effects is essential to pass through the microstructural ones (Aguado et al., 1996, Araúlo et al., 2008).

2.2.1 Internal Sulphate Attack

Sulphates and iron-sulphides are ordinary minor components of a wide variety of rocks and they are amongst the most abundant mineral types (Casanova et al., 1996a). Among the iron-sulphides present in nature, two of the most common ones are pyrite FeS_2 and pyrrhotite $Fe_{(1-x)}S$ (Janzen et al., 2000).

Internal Sulphate Attack is intended as the set of chemical reactions that develop inside concrete between the sulphate ions contained in the concrete pore solution and the constituents of the cement paste. The internal attribute suggest that the sulphates come from an internal source, i.e. the iron-sulphides contained in the aggregates, despite in some cases the sulphate supply can come from an external source (e.g. soil or liquids, Neville, 2002).

The ISA phenomenon is characterized by reaction products that have larger molar volumes than the reactants (Casanova et al., 1996a), and hence it is responsible of the expansions that are developed inside the concrete matrix. The expansions can be locally accommodated inside the concrete pores, or they can cause an internal state of stresses and strains when the voids are not sufficiently large to host the larger reaction products. In the latter case the state of stresses and strains could lead to crack the cement matrix (Skalny et al., 2002).

Numerous are the cases where the ISA has been detected and identified as the cause of expansive and deterioration phenomena in concrete structures all over the world (Guirguis et al. 2018).

The Internal Sulphate Attack is divided into two expansive phases. In a first stage the aggregates and the iron-sulphides enveloped in the lithotypes are oxidized: oxidizing agents, e.g. oxygen and water, react with pyrite FeS_2 and pyrrhotite $Fe_{1-x}S$ to form iron hydroxides and sulphuric acid (Oliveira, 2011, Schmidt et al., 2011, equations 1 and 2):

$$pyrite\ oxidation: \qquad 2FeS_2 + 2H_2O + \frac{9}{2}O_2 \rightarrow Fe_2O_3 + 2H_2SO_4 \qquad (1)$$

$pyrrhotite\ oxidation$:

$$Fe_{1-x}S + \left(\frac{10-3x}{4}\right)H_2O + \left(\frac{4-3x}{2}\right)O_2 \rightarrow (1-x)Fe(OH)_3 + H^+ - SO_4^{2-} \qquad (2)$$

In the last equation regarding the pyrrhotite oxidation to form iron hydroxides and hydrogen and sulphate ions, the value of x may vary from 0 to 0.125.

In equations (1) and (2) reported above, the main oxidizing agent is the oxygen, given the highly alkaline pH conditions of the inside of the concrete (Belzile et al., 2004). Hence the kinetic of the reaction depends on factors such as the O_2 diffusion coefficient D $[m^2/s]$ (Oliveira, 2011).

In figure 2.1 is reported the Backscattered Electron image (BSE) of cement matrix from the concrete of a dam with highlighted iron-sulphides inclusions (Schmidt et al., 2011).

In a second stage, once the iron-sulphides have oxidized, the sulphates that are released as sulphuric acid and as ions react with the cement hydrated components. This stage is characterized by complex chemical reactions a molar volume increase significantly higher than the one occurred during the development of equations (1) and (2). The sulphates reacts with portlandite, calcite and with gypsum to form delayed ettringite (Tangit-Hamou et al., 2005, Araúlo, 2008):

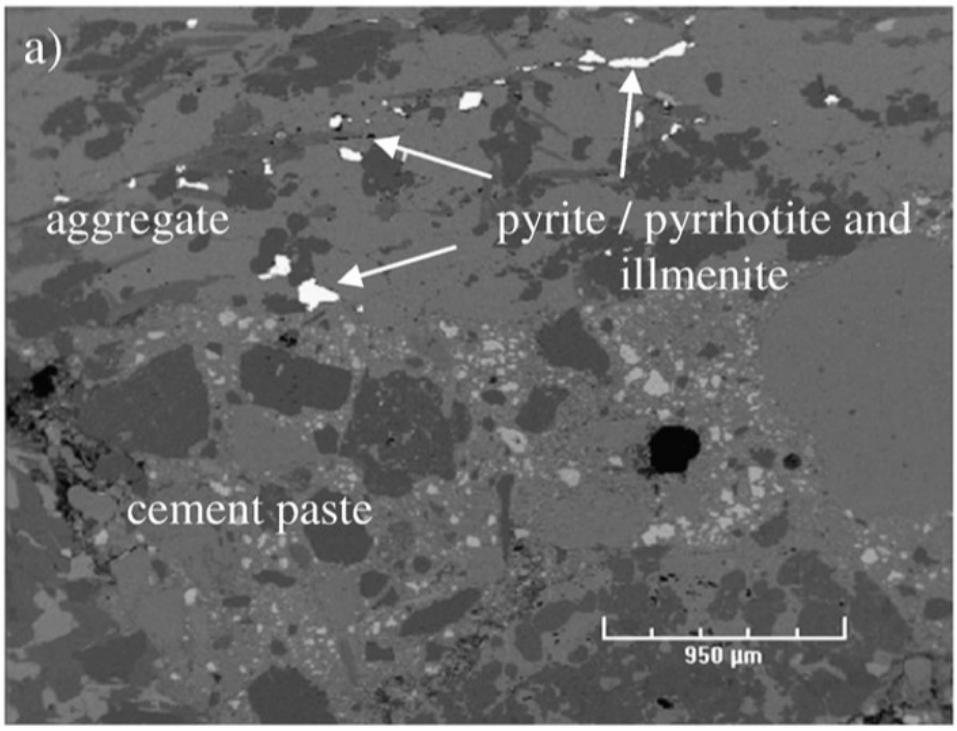

Figure 2.1 – Backscattered Electron image (BSE) of concrete matrix from the concrete of a dam that highlight the presence of pyrite and pyrrhotite (Schmidt et al., 2011).

$$gypsum\ formation: \quad H_2SO_4 + CaCO_3 + 2H_2O \rightarrow CaSO_4.2H_2O + CO_2 \qquad (3)$$

$$gypsum\ formation: \quad H_2SO_4 + Ca(OH)_2 \rightarrow CaSO_4.2H_2O \qquad (4)$$

$$ettringite\ formation: \quad 3CH + C3A + 3S + 29H \rightarrow C_6AS_3H_{32} \qquad (5)$$

Where: $CH = Ca(OH)_2\ (portlandite)$, $C3A = 3calcium\ aluminate$, $S = SO_4^{2-}\ (sulphate)$, $A = Al_2O_3$, $H = H_2O$.

The final reaction product is the secondary ettringite: $C_6AS_3H_{32}$ =($CaO.Al_2O_3.CaSO_4.32H_2O$), different from the primary ettringite formed during the early plastic setting stage of concrete mixing.

The oxidation process is greatly exothermic and it produces, together with the sulphate attack to cement paste, local volume expansions. The two-stages ISA phenomenon is a

slow process and takes years in order to show its signs. In some cases, after many decades its effects are not yet fully developed and the reactions are still going on. The two phases of the ISA development, the first oxidation of the pyrite (FeS_2) and pyrrhotite $(Fe_{1-x}S)$ iron-sulphides with the formation of sulphuric acid and iron hydroxides and diffusion of sulphate ions SO_4^{2-}, and the successive attack of the sulphate to the cements paste with the eventual formation of secondary ettringite $CaO \cdot Al_2O_3 \cdot 3CaSO_4 \cdot 32H_2O$ from C3A, gypsum and water (Hamou et al., 2005), have two different impact on the expansion of the concrete volume. The second phase (sulphate attack) is characterized by reaction products that have bigger molar volumes than the first phase ones (oxidation).

The expansions depend mainly upon the amount of reactive aggregates and on the availability of the oxidizing agents. Moreover, an important role is covered by iron-sulphides types, by the enveloping rocks sizes and lithotypes (e.g. siliceous or carbonatic), by pH and by environmental agents as temperature and relative humidity (Oliveira, 2011).

The dependence of the reaction kinetics and development has been deeply investigated and modelled, and remarkable reference could be found in Aguado et al, 1993, 1996, 1998, Ayora et al., 1998, Chinchón et al., 1995, Casanova et al., 1996, 1997, Schmidt et al., 2011, Oliveira, 2011, and many others.

2.2.2 Alkali-Silica Reaction

Alkali-Silica Reaction is a set of chemical reactions that are developed inside concrete, between the alkali hydroxides contained in the pore fluids of the cement and the reactive forms of silica that are contained in the aggregates (Swamy, 1992). The product of this reaction is a gel substance of complex chemical nature.

ASR is a category of AAR, that stands for Alkali-Aggregate Reaction. Siliceous aggregates are not the only one that are reactive with the alkaline components of the cements (e.g. carbonates), but in this chapter only them are addressed.

The reactions involved in this mechanism need three main components to proceed: alkali hydroxides, that are obtained from the alkali content of the cement (mainly Na_2O and K_2O), but also from the aggregates (Bérubé et al., 2002), siliceous reactive minerals, that are contained in the aggregates, and water. Many rocks are known to contain silica, e.g. in form of amorphous SiO_2, hence the problematics related to the ASR expansive issue is quite diffused in concrete structures.

Water has two fundamental roles in the development of the ASR expansive phenomenon. In a first stage it is the carrier of the alkali ions (Na^+, K^+ and Ca^+) and hydroxyl ions (OH^-) to the spots where the reactions are likely to start, i.e. the siliceous aggregates borders. In a second stage, once the reactions are developed and the gel is formed, water constitute the absorption feature by the gel the allow its expansion.

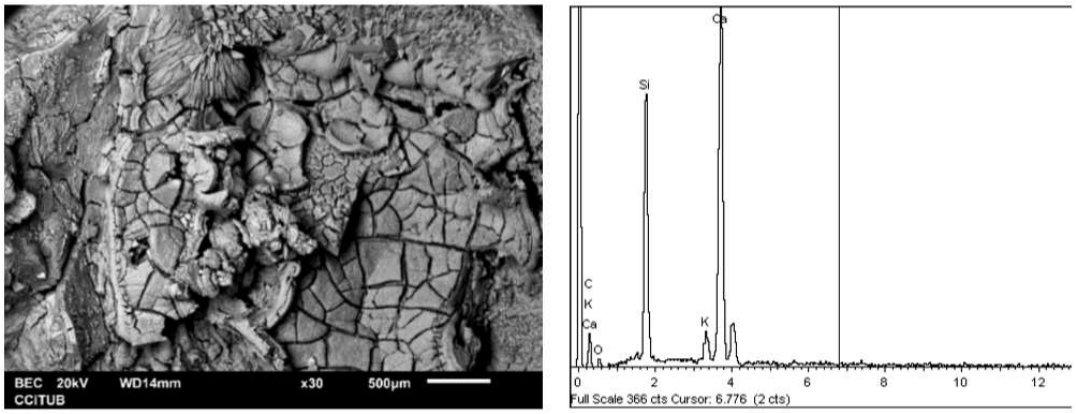

Figure 2.2 – Massive ASR gel reaction product formation captured by SEM and composition characterization through EDX spectroscopy (from Aguado et al., 2020).

The factors that mainly affect the ASR evolution and intensity are the water availability, the environmental effects, characteristics of the aggregates (grain sizes and content of reactive silica among others), and of the cement (pH of the pore fluid), temperature and its variations, and the microstructure of the concrete (pore fluids are the medium of the mass and ions transfer).

The ASR phenomenon is known to be expansive and it has been studied by many researchers (Stanton, 1940; Hobbs, 1988; Swamy, 1992; Fournier and Berubé, 2000). Many laboratory tests have been developed to identify the presence of deleterious ASR and the potential expansion that it can cause. To cite some of them, accelerated mortar bar test and non-destructive tests, that aim to evaluate the potential expansivity of a certain mixture in particular conditions (technical regulations can be found in RILEM committee, Lindgård et al., 2011; EN 206-1, 2001; ASTM C1260-07, 2007, and many others).

Similarly to the ISA mechanism, the ASR is a very slow phenomenon that may need many years in order to fully develop. In the case of concrete dams, usually after 30-40 years its effect are not yet fully exhausted.

2.3 Consequences of the expansive phenomena

The expansive phenomena in a concrete dams can be separated in two branches: the 'expected' expansions, that are due to temperature variations and environmental effects and hence have a seasonal trend, being followed by shrinking and cyclic repetitions, and the 'anomalous' expansions, that are caused by chemical reactions that have expansive character and are cumulated over time. The former ones, despite being of interest from an engineering point of view as well, are not regarded in this thesis. Hence from now on, when referring to expansive phenomena, the 'anomalous' expansions are considered only.

The expansive phenomena that act inside the concrete mass, i.e. ISA and ASR, have a series of consequences on concrete structures. Typical degradation features are 'map' and oriented cracking, movements at the top of the dams and other evidences as coloured stains and superficial deposits of reaction products. When the expansions are not accommodated in the concrete voids, strain develops and stresses arise, and as soon as they overcome the concrete matrix local strength, cracks are initiated. As the reactions proceed, the cracks propagate and the volume changes. Many models in literature describe the expansion phenomena, but they are usually referred to a specific reaction (ISA or ASR). For example

Léger et al. (1996), Furusawa et al. (1995) modelled the ASR reactions, while few literature is available regarding the modelling of the ISA, for example regarding the oxidation mechanism: Yagi and Kunii (1955) with the UCM (Unreacted Core Model) and Oliveira et al. (2012), with the NUMC (New-UMC). The coupling of the two effects is still a partly unexplored field.

Since the aggregates are distributed in all the concrete mass, the expansive phenomena are diffused inside it. Nevertheless, in a concrete structure as a dam, different conditions of stresses, humidity, temperature and oxygen exposition in the body of the dam would lead to differential expansions according to the position (Oliveira, 2011).

Two cracking pattern usually arise in concrete dams affected by ISA and ASR: map cracking, where the cracks don't have a preferential direction but are randomly distributed in the concrete mass (as can be appreciated in figure 2.3), and oriented cracking, when the cracks follow a precise direction according to the states of stresses that are developed in the concrete dam, be them compressive, tractive or torsional.

Figure 2.3 – Mapped cracking on the downstream face of the Tavascan dam, located in the Pyrenees region, Spain. (from Aguado et al, 2018).

The damage of the ISA and ASR mechanisms also reveal itself in form of cumulated displacements. Local expansions cumulate along the dimension of concrete structures and it results in movements of the parts that are less constrained. In the case of dams, the movements are observed at the top level, where the state of constraints is more free, with respect to the base/foundation level, in the vertical direction, and towards the downstream face of the dam.

The movements caused by the expansive phenomena are recorded by auscultation systems, that allow in time to investigate the extension of the movements and the direction.

Many Spanish dams have been reported with such deterioration processes, e.g. Graus, Tavascan and Toràn (Araúlo, 2008) and Paso Nuevo dam (Río et al. 2008), and many others.

2.3.1 Diagnostic phase

The diagnostic phase in the circumstance of ISA and ASR expansive phenomena embraces all the actions that aim at discovering and characterise the problems related to them in concrete dams. The abovementioned expansive phenomena bring with them characteristic features. With the correct means of investigation they can be successfully outlined, since they show up with particular signs.

Clear evidences of ISA and ASR come from visual inspection, laboratory testing and identification of anomalous behaviour. Once accurately defined, they allow to recognize the actual problem that affect a concrete dam. Measured movements at the top level and at the service gallery level are in this optic precious information of the major expansive phenomena involved. Displacements recorded in the vertical and horizontal directions, for a sufficiently long number of years, allow to differentiate the effects of the two phenomena:

- ISA expansions are influenced by the supply of oxygen, since it is the primary oxidizing agent (Rodrigues, 2015). Being the oxygen supply much higher in the

downstream face than in the upstream face (that is submerged for most of the height), the kinetics of the reaction inside the dam is differential. The concrete in the downstream face is exposed to much higher oxygen concentrations (9.37 mol/m^3 versus 0.26 mol/m^3 of the upstream face (Oliveira, 2012)), and it will expand much more quickly. This earlier expansion is confined in the first portion of superficial concrete. The differential expansion lead to a turning movement of the dam and the points located at the top of the dam will move toward the downstream face. Huge horizontal movements toward the downstream face are signs of big and fast ISA related expansions, the differential movements between blocks are symptoms of how much the phenomenon is diffused.

- ASR expansions are governed by the water availability in the concrete mass, for the reactions to proceed and for the alkali-silica gel to absorb it and expand. The content of water in a generic cross-section of a concrete dam can be supposed to be quite constant, except the last meters of the downstream face, that are in contact with the atmosphere, whose relative humidity is lower (Bazant and Wittman, 1982), as depicted in figure 2.4. The development of the ASR is more homogeneous along the profile of the concrete dam than the ISA one, therefore the expansions due to the ISA are evenly distributed and affect mainly the vertical direction, that is the less constrained one (Araúlo, 2008). As for the ISA, also for the ASR the speed of movements happening and differential movements between blocks are signs of the speed of reactions progress and their diffusion.

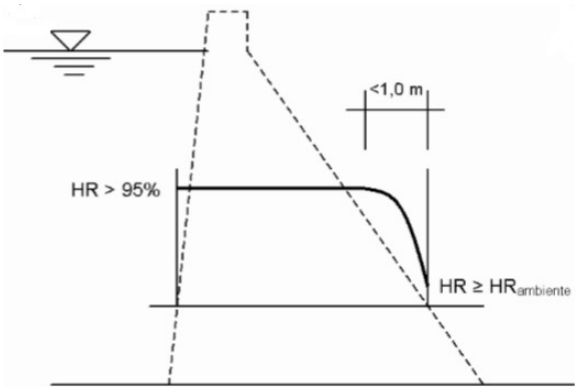

Figure 2.4 – Profile of the relative humidity along a concrete dam cross-section (Bazant and Wittman, 1982).

Laboratory tests are valuable means of diagnosis of the actual deterioration process that is going on in a concrete element. They are carried out on aggregates, on concrete cores extracted from the dams, on concrete samples made in laboratory, and on other specimens. Among the large amount of tests, the main ones are: optic microscopy, X-Rays Diffraction, X-Rays Efflorescence, SEM microscopy and EDX analysis, petrographic examination, accelerated expansion tests, non-destructive tests, mechanical and physical tests, permeability tests and others (Araúlo, 2008, Swamy, 1992). Laboratory tests are well-established and reliable, each test having its own advantages and drawbacks. Nevertheless, the step from laboratory to field conditions is delicate.

The huge size of a gravity concrete dam would require a very ample number of tests to be conducted. In this thesis, only the movements recorded at the top of the dam are considered as diagnostic instruments.

Once the diagnostic phase is carried out, a more or less clear picture of the particular dam situation can be outlined and the detected specific problems and it can be assessed whether they have severe repercussion or are under control. Corrective measures can be undertaken and an effective management plan can be drawn.

2.4 Modelling of the expansive phenomena

2.4.1 Purposes

Whatever the expansion phenomena, i.e. ISA or ASR, the generated increment of volume is also responsible for internal action that, at a macro scale, are reconducted to map cracking (or oriented cracking according to the state of stress generated by the internal expansions), and to non-recoverable movements (Campos, 2012). Different phenomena can be modelled with different models that have common assumptions. In general, articulated models take into consideration many parameters and rely on few specific assumptions, and they are usually troublesome to apply. Simpler models instead rely upon many assumptions that simplify the modelling of the otherwise complex phenomenon.

Many models exist in literature, regarding different aspects related to concrete dams. For example the NUMC model (Oliveira, 2012) that describe the kinetics of the oxidation of the reactive iron-sulphide bearing aggregates in function of the geometry of the particles and their physical characteristics, as reactant and oxidizing agents concentrations.

Modelling of the movements is an important step in the light of being able to predict their future behaviour. It is also fundamental in order to be able to relate aspects of the model to physical and chemical causes that are involved in the ASR and ISA, from a quantitative point of view.

2.4.2 Analytical and physical modelling

Models of the phenomena are available at different scales, i.e. microscale, mesoscale and macroscale. In the regards of this thesis, a model describing the evolution of the displacements measured at the top of the dam has been used and investigated. The mentioned model is the one proposed by Aguado (1993) that is able to characterize both vertical and horizontal movements. It follows an exponential law, as can be appreciated in equation (6):

$$y = A + B \cdot \left(1 - \exp\left(-\left(\frac{t}{C}\right)^{p}\right)\right) \tag{6}$$

The meaning of the parameters will be explained in chapters 4 and 5.

The movements registered at the top of the four dams show a common trend. They all have three main phases:

1) 1st phase: Initiation. The expansion phenomena take place. This phase could start immediately or need some time before its beginning, according to many factors, being howsoever the reactions of slow character.

2) 2nd phase: Growth/Development. After the first initiation phase, where the gradient of expansion keeps increasing, the gradient here reaches the maximum value. The expansions proceed at the maximum speed, and at the end the phase the speed of reactions starts to decrease.

3) 3rd phase: Passivation/Stabilization. After many years, the reactions are almost all consumed and the reactive minerals are nearly all reacted. The movements quite entirely took place and the gradient is approaching to zero.

The physical modelling aim to relate physical parameters of material and of the structure (e.g- quantity of reactive aggregates, access to oxidizing agents, geometry of the concrete blocks) to characteristics of the movements (e.g. maximum expected movement, time after which the trend of movement change, represented by the parameter C – inflection point of the model of equation (6) – as it will be explained further on).

CHAPTER 3 – DESCRIPTION OF THE DAMS AND OF THE MOVEMENTS

3.1 Introduction

The control of the movements is a significant issue in the stability and serviceability evaluation of a dam. Excessive movements could have serious consequences on the safety of the structure, or on its functionality, and therefore must be carefully taken in consideration. Displacements are clues of what kind of phenomena are or have been developing, so they are of primary importance in the light of diagnosing the actual deterioration processes in activity, together with their intensity and direction. It is then fundamental to undercover the causes of the movements.

The four Spanish dams that were the core of the analysis have been monitored and registered since many years. A huge amount of data and information belongs to a dam and its construction. This pulls with it a great number of instrumentations and control devices that are mandatory to be installed on and inside them. The number of monitoring devices varies according to the type of dam, the dimensions, the construction process, the age as well as the local site-dependent conditions, e.g. the foundations. The monitoring device must be adapted to the particularities and the importance of the dam (Lutz et al., 2006).

In this work, the attention was focused to the data regarding the horizontal movements and the vertical ones, recorded at the top level. As well the movements registered in the service galleries are, when available, taken into consideration, since they may as well be relevant for the diagnosis of the internal events.

Although the structures of the dams could be similar in shape and size, each of them is unrepeated and behaves in its own peculiar way, under the hydraulic and structural and functional points of view. For each dam a specific scenario must be outlined.

Nevertheless, in all the four dams, the same degradation phenomena have been detected (Araúlo, 2008, Río et al. 2008), i.e. sulphate attacks and alkali-silica reactions, that operate

in similar ways in the four different scenarios. In figure 3.1 the typical map cracking of the expansive phenomena can be appreciated, close to a vertical joint separating two blocks, in the Graus dam (Aguado et al., 1991).

Figure 3.1 – Map cracking of the concrete near a vertical joint that separate two adjacent blocks of Graus dam, typical of the ASR and ISA expansive phenomena (Aguado et al., 1991).

As already mentioned, the movements recorded at the top of the dam are valuable information for the diagnosis of the events that have been happening inside the dam, and together with other investigation techniques, e.g. concrete core extraction and laboratory analysis, they allow to accurately depict each dam situation. Following this, effective countermeasures can be taken, when necessary.

ENDESA and ACCIÓN companies were responsible for the monitoring of the movements of the dam at the top level during the years of dams' commissioning.

3.2 Investigated dams

The dams investigated in this master thesis are, as already mentioned, gravity dams, and a typical transversal cross-section is as pictured in figure 3.2.

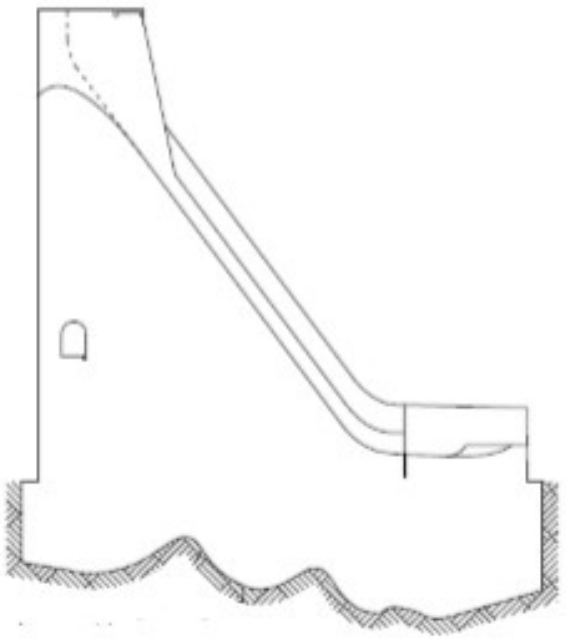

Figure 3.2 - Typical gravity dam transversal cross-section. the cross-section in this figure belongs to a central block of the Tavascan dam.

The Graus and the Tavascan dams are gravity dams not far from each other, as can be seen from figure 3.3, from the view obtained by Google Earth. Toràn dam is a bit farther, but still the ground on which they all lay on is from the same geological formation, mainly composed by shales and limestones (Díez-Cascón y Bueno, 2001). Previous studies confirmed that the origin of the anomalous dams' behaviour is attributed to the iron-sulphides alteration (Chinchón et al., 1995, Casanova et al., 1996b; Aguado et al., 1998), contained in the aggregates used in the concrete. Similar considerations are made for the Paso Nuevo dam (Río et al. 2008). Lithotypes of the surrounding area have been found responsible of carrying iron-sulphides minerals.

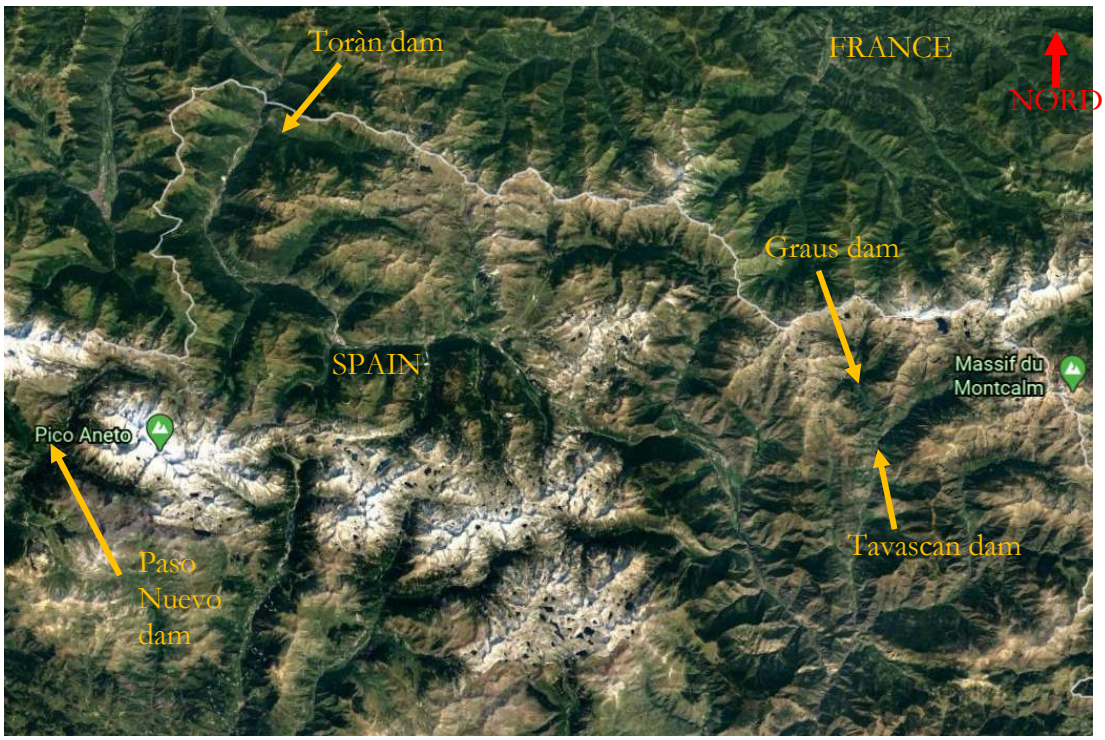

Figure 3.3 – Satellite 2-D view of the region where Graus, Tavascan, Paso Nuevo and Toràn dams are located (from Google Earth). The grey line is the national border with France.

In figures 3.4 are represented the front and the plan view of the Graus dam. The dam is divided in 7 blocks separated by vertical joints. The spillway is situated in block 3 and occupies partly the adjacent blocks 2 and 4. Concrete blocks have similar height, except the lateral ones (1 and 7), that are shorter. Geometric and other main data are reported in table 3.1.

Tavascan dam is divided in 4 blocks as represented in figure 3.5, displaying the plan view (A), the front view (B) and the cross-section of a central blocks, typical of the gravity dam scheme, characterized by the presence of the spillway.

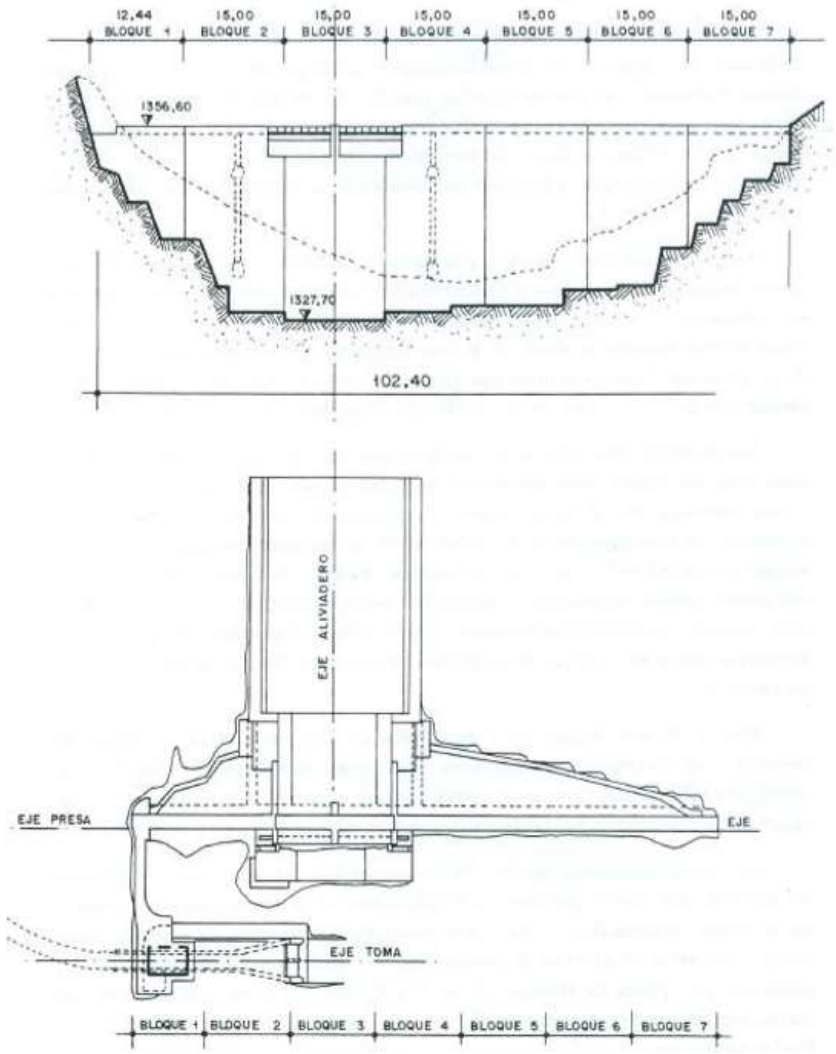

Figure 3.4 - Front and plan view of the Graus dam

	Characteristics	Year of commissioning	Top length [m]	Maximum height [m]	Number of blocks	Maximum spillway capacity $[\frac{m^3}{s}]$	Volume of the impounding $[hm^3]$	Function	Owner
DAMS:	**GRAUS**	1971	100	28.90	7	205.0	0.33	H	Endesa Generacion
	TAVASCAN	1966	57	29.5	4	216.7	0.64	-	Endesa Generacion
	PASO NUEVO	1969	195	73	12	330.0	3	H	Acciona Energia
	TORAN	1964	65	40	8	71.0	0.78	H	Endesa Generacion

Table 3.1 – Main characteristics of the dams.

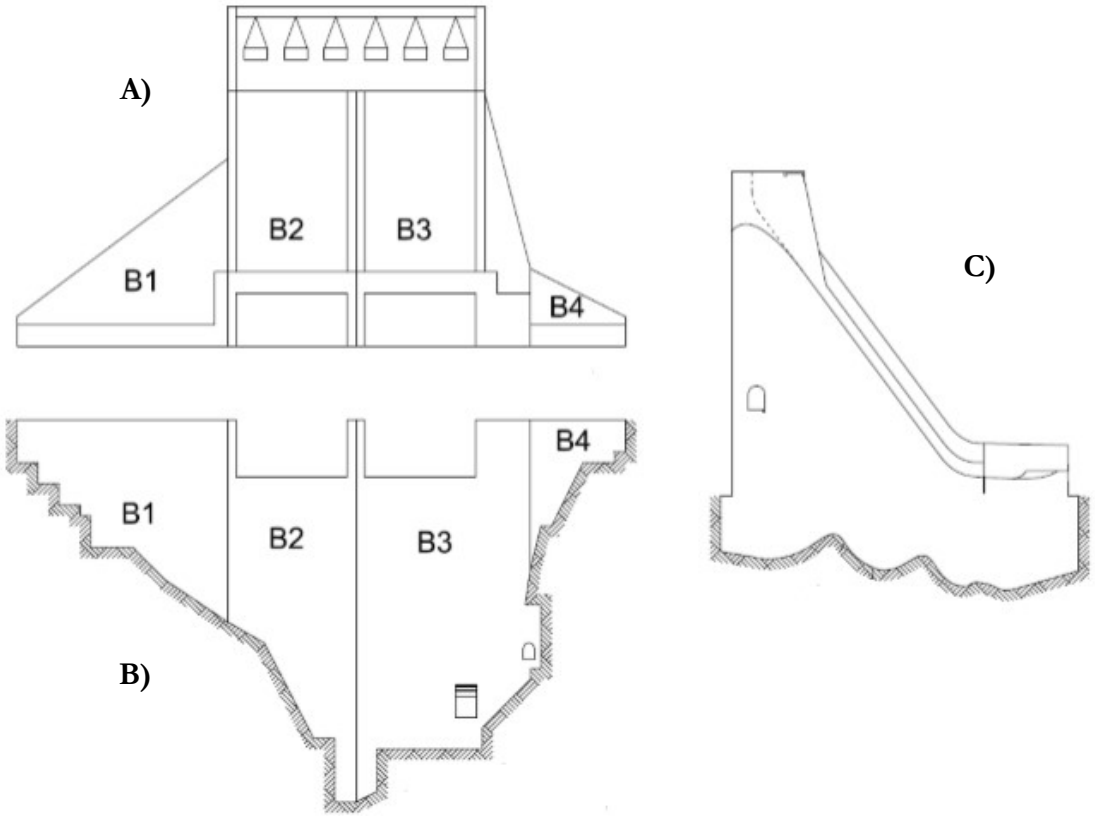

Figure 3.5 - Tavascan dams, divided in 4 blocks: A) plan view, B) front view from the upstream face, C) typica cross-section of the central blocks.

The Paso Nuevo dam is represented in figures 3.6 and 3.7. The blocks are divided by the vertical joints, displayed with dashed lines. The spillway is located at the top of blocks 4, 5 and 6. In the front view are reported the 4 service galleries. From this view it's possible to see the organization of the dam monitoring devices. They include collimation and levelling measurements stations, drains, automatic and manual manometers, inverted pendulums, filtration monitoring devices, micrometers and deflectometers, temperature and pressure measuring devices, among the others.

Collected data include, besides displacements at the top level and other measurements, water level variations, temperature trends (of the air and of the water), pressures at galleries levels measured by manometers, joints movements (opening or closing), chemical analysis of the water.

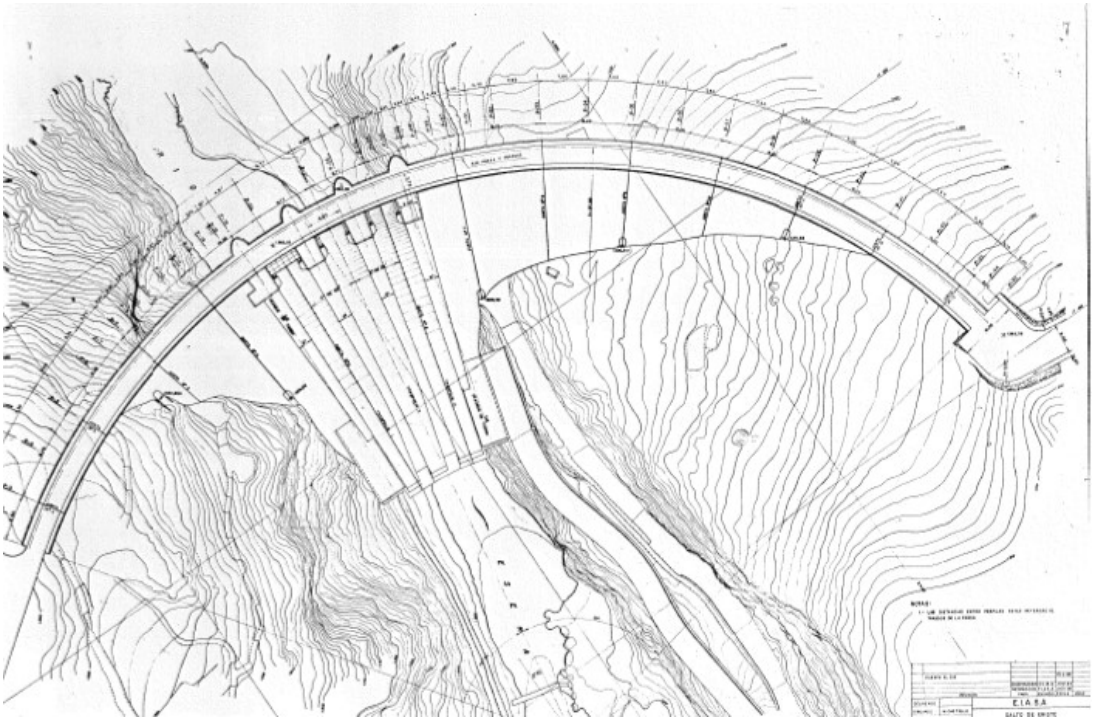

Figure 3.6 - Plan of Paso Nuevo dam, representing the blocks separated by the vertical joints and the contour lines of the surrounding area.

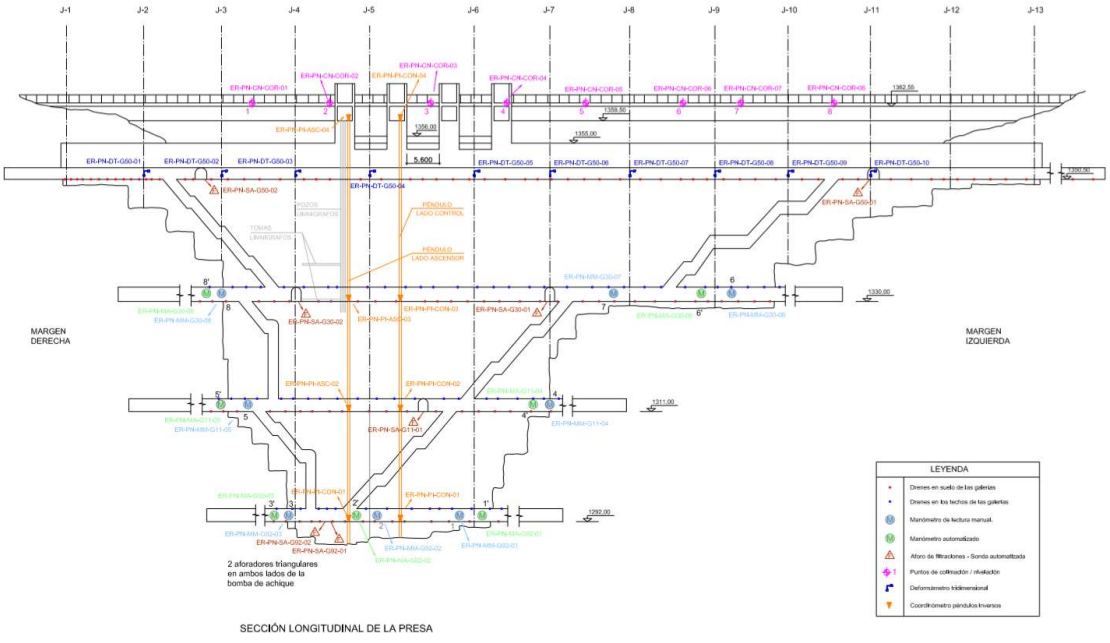

Figure 3.7 – Front view of the Paso Nuevo dam (seen from the upstream face). Vertical joints are indicated by dashed lines, separating the blocks. The movements monitoring devices stations are shown by pink circles.

The Toràn dam front view is pictured in figure 3.8, together with a characteristic cross section. The dam is made up of 8 blocks and two main service galleries. The spillway is located in the two central and biggest blocks. Lateral blocks are considerably smaller.

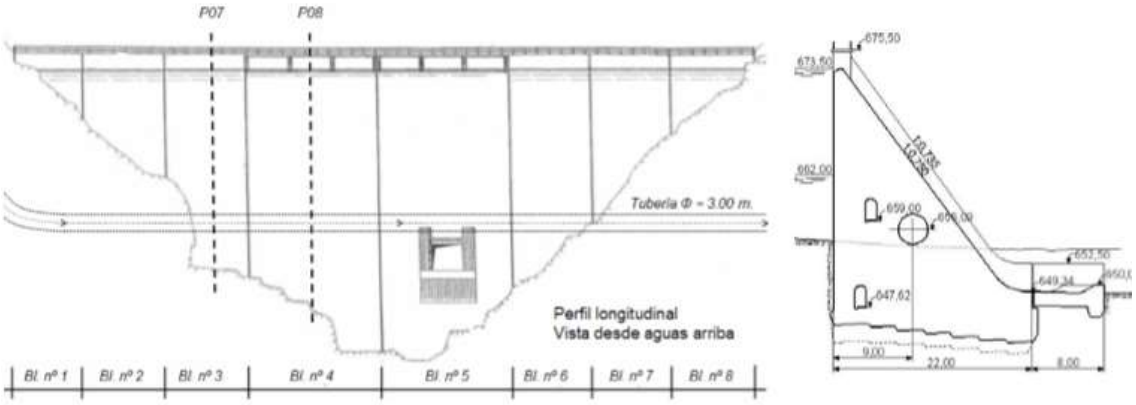

Figure 3.8 – Front view of the Toràn dam and the typical cross-section belonging to the central blocks. The spillway is located in central blocks, that are the largest ones.

3.3 Movements of the dams

In this chapter the movements of the dam that have been captured by the auscultation systems are going to be introduced. The dam monitoring device is a set of measurement systems, that allows the judgement of the behaviour of a dam and its foundation subjected to the applied loading, be it external or internal. It is necessary that monitoring of the situation is carried during the construction and the impounding, and then during all the time in which the dam will be operative, in order to be able to detect any signs of abnormality and take action straightaway (Lutz et al., 2006).

The monitored movements are those of levelling (vertical direction) and collimation or alignment (horizontal direction). They have been monitored at the top level of the dam, where their magnitude was the highest, and they are reported in the following chapters. In figure 3.9 one can appreciate the horizontal movements toward the upstream face, at the top of Graus dam (Aguado et al. 2014).

Many causes could be the trigger of the movements of a dam, e.g. an inadequate foundation level. Usually movements are triggered by more causes, that concatenate and superpose their effects, and it could be a troublesome work to precisely identify these causes. A lot of uncertainties envelope their knowledge. In spite of that, a scientific approach, which relied upon field inspections, extended laboratory testing and well-established experience, allowed to discover what were the reasons of the movements in the four analysed dams (Aguado et al., 1993, 1998, 2014, 2018, Araúlo, 2008).

The first consideration from the analysis of the movements is that a big portion of them is non-recoverable (Aguado et al., 1993). The portions of the movements that are considered non-recoverable are labelled as 'anomalous', differently from the recoverable parts of them. While the latter ones are due to the temperature and seasonal variations and trend of the water level of the basin and its temperature oscillations, the former ones are found to be due to unexpected phenomena that evolve inside the concrete mass.

In the four dams, they coincide with the Internal Sulphate Attack and, with usually lesser extent, with the Alkali-Silica Reaction. Despite them, other reasons usually tend to superpose to these two phenomena, for example the presence of the spillway in the central blocks, that could be liable of haltering or favouring the movements.

Expansive phenomena happen at a local scale and, cumulating until affecting the dam scale, they provoke differential displacements of each block, being the latter ones separated by vertical joints. It's therefore important to monitor each block of the gravity dams when possible, in order to seize the diffusion of a problematic, or, in alternative, its specificity. Frequent are in fact the special conditions to which a block is subjected (in terms of stress, surrounding confinement, hydraulic conditions, soil-structure interaction, or others), that are responsible of its distinct behaviour. Nevertheless, expansive phenomena, as ASR, can be generalized to the whole concrete body of the dam (Aguado et al., 1998).

Figure 3.9 – View of the top of the dam from the downstream face of Graus dam. The movements of the railings at the level of the central blocks are directed toward the upstream face (Aguado et al., 2014).

The reference system set in the measurements considers positive the measurements in the vertical plane that move upward, and as negative the ones downward. In the horizontal direction the positive measurements are the one directed towards the upstream face. The Tavascan dam is the only one of them for which the measurements are available since the first day of commissioning, immediately after the construction phase has ended. The other dams have sets of movements data that do not cover all their lifetimes, because the auscultation systems were installed in a second moment. In the Graus dam it has been installed about 10 years after the commissioning, in the Paso Nuevo after 15 years, in the Toràn dam after about 35 years.

3.3.1 Horizontal movements

Horizontal movements measured at the top of the dams were always reported to be in the direction of the upstream face. The explanation of this trend is to be found in the existence of the Internal Sulphate Attack affecting the concrete mass.

As described in chapter 2.2.1, the ISA needs an oxidizing agent in order to proceed, together with water. Without oxidizing agents, being mainly oxygen O_2 in these cirmustances, the iron-sulphide bear by the aggregate wouldn't be weathered and oxidized (1st phase of the ISA). Hereafter, being the iron-sulphides (i.e. pyrite and pyrrhotite) not oxidized, sulphates would not be released in sufficient quantities and the Internal Sulphate attack doesn't take place.

On the other hand, when oxidizing agents are available in adequate quantities, the oxidation of the iron-sulphides passes off. Now, being the concentration of oxidizing agents (i.e. Oxygen O_2) much higher in the downstream face with respect to the upstream face, the former one experiences more oxidation and it experiences it quite more quickly. Such differences in the entity and in the speed of oxidation results in differential expansions, being much more ample in the downstream face. As a consequence, a turning movement is produced at the top of the dam and it will move upwards and toward the upstream face, as one can see in figure 3.9.

The intensities of the horizontal displacements varied from dam to dam and from block to block. In figure 3.10 the collimation movements of the Graus dam are displayed. Blocks 4 and 5, that are the central and tallest ones, have recorded higher movements, while blocks 1 and 7, that are the lateral and shortest one, attached to the abutment margins, are characterized by very small movements.

An immediate consideration that can be assessed is that the collimation movements in the Graus dam have started to stabilize since at least 10 years. The trend of the displacements is very similar in all the blocks, suggesting that the phenomenon that caused them has hit

the blocks in a similar way, and the differences between them are imputable to the different geometric configurations of the blocks (Aguado et al., 2014).

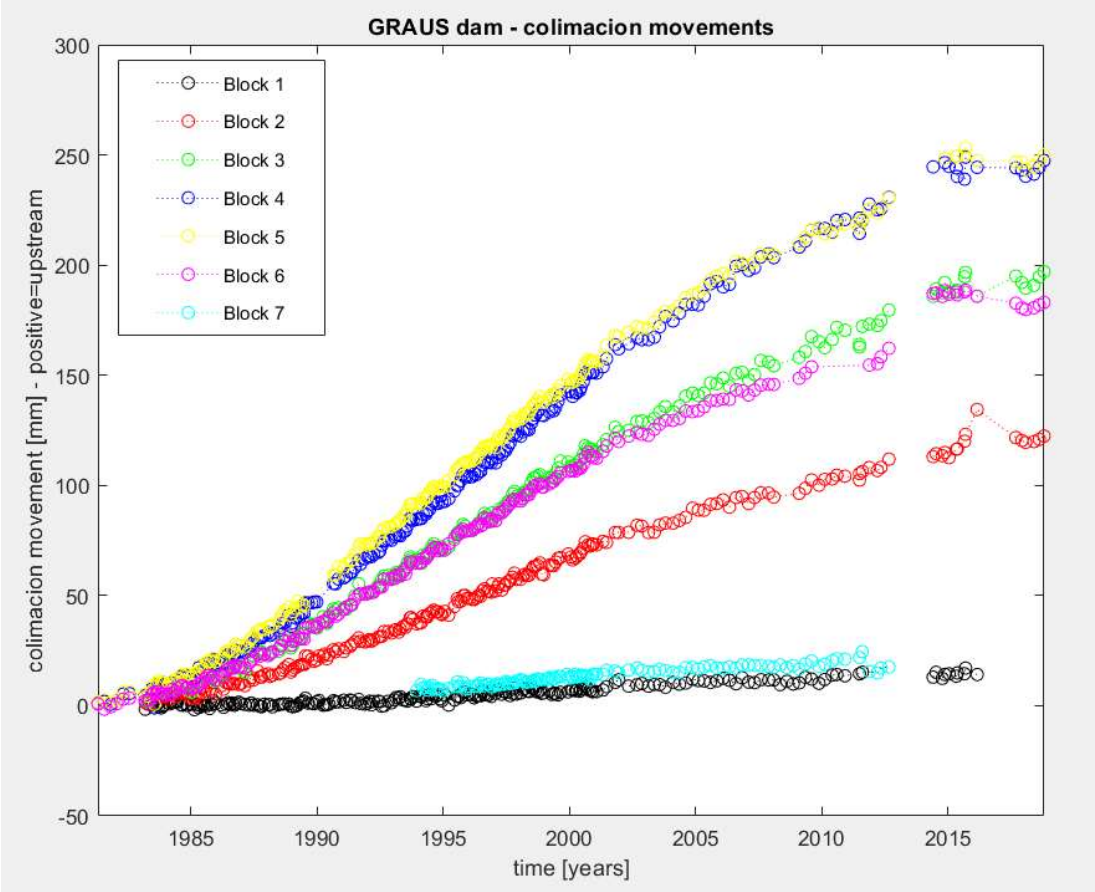

Figure 3.10 - Collimation displacements of the 7 measurements stations installed on Graus dam.

The expansive reactions, once considered responsible for the anomalous movements, could be thought to be generalized and diffused to the whole body of the concrete dam, with some local exceptions.

In the following figures the horizontal displacements of the dams of Tavascan (figure 3.11), Paso Nuevo (figure 3.12) and Toràn dam (figure 3.13) are reported. By looking at the data of the collimation movements, it's immediate to see that the they have entered the stabilization phase descripted in chapter 2.4. In the cases of blocks 4 and 5, in addition, decreasing movements are observed.

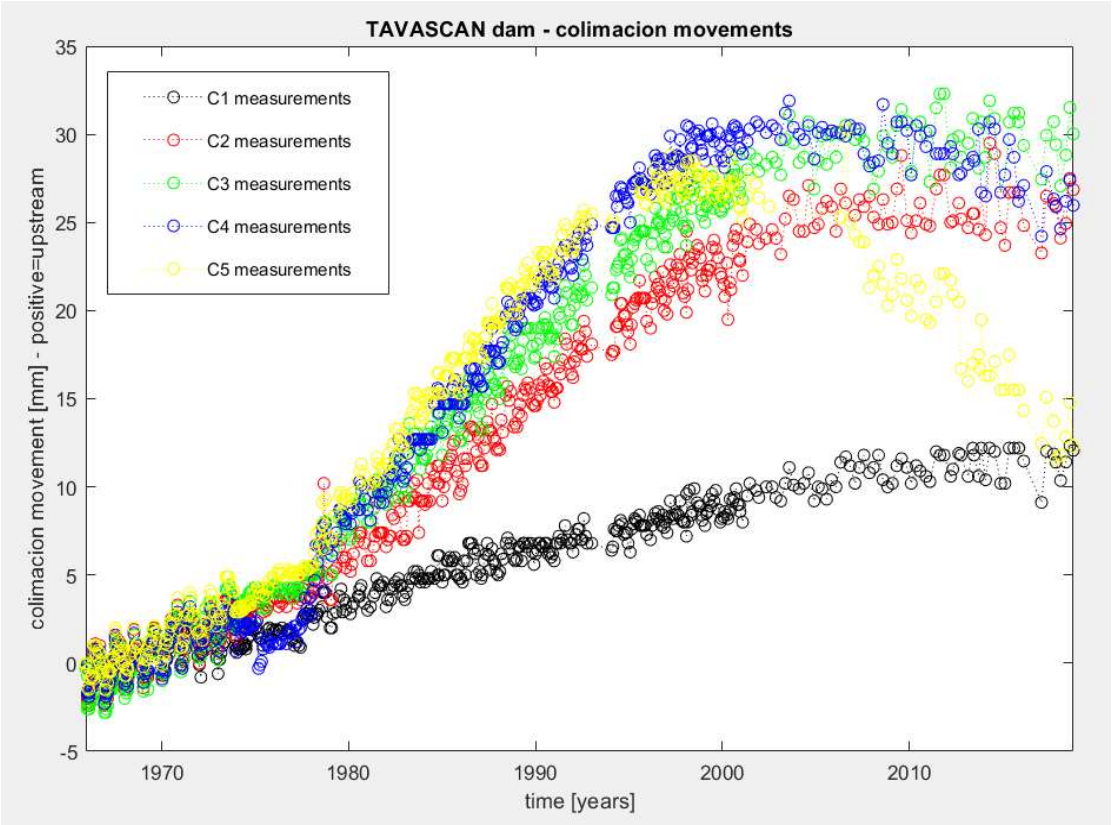

Figure 3.11 - Collimation movements of the 5 measurement stations of the Tavascan dam.

The trends of movements of blocks 4 and 5 could in some way affect the fitting operation of the exponential curve given by equation (6). The behaviour of Tavascan horizontal displacement is somehow similar to the one of Graus dam: blocks shows a similar trend in terms of time after which the stabilization is happening. Also the magnitude are similar amongst blocks, leading to think about a diffused effect that could be generalized to the whole dam.

What is markedly different from the collimation movements of the two dams (Graus and Tavascan) is the magnitude. While in Graus dam they eventually reach up to 250 mm, in the Tavascan dam they arrive at just 30 mm. The action of the ISA degradation and expansion in the latter dam has been characterized by a lower intensity (Aguado et al., 2016).

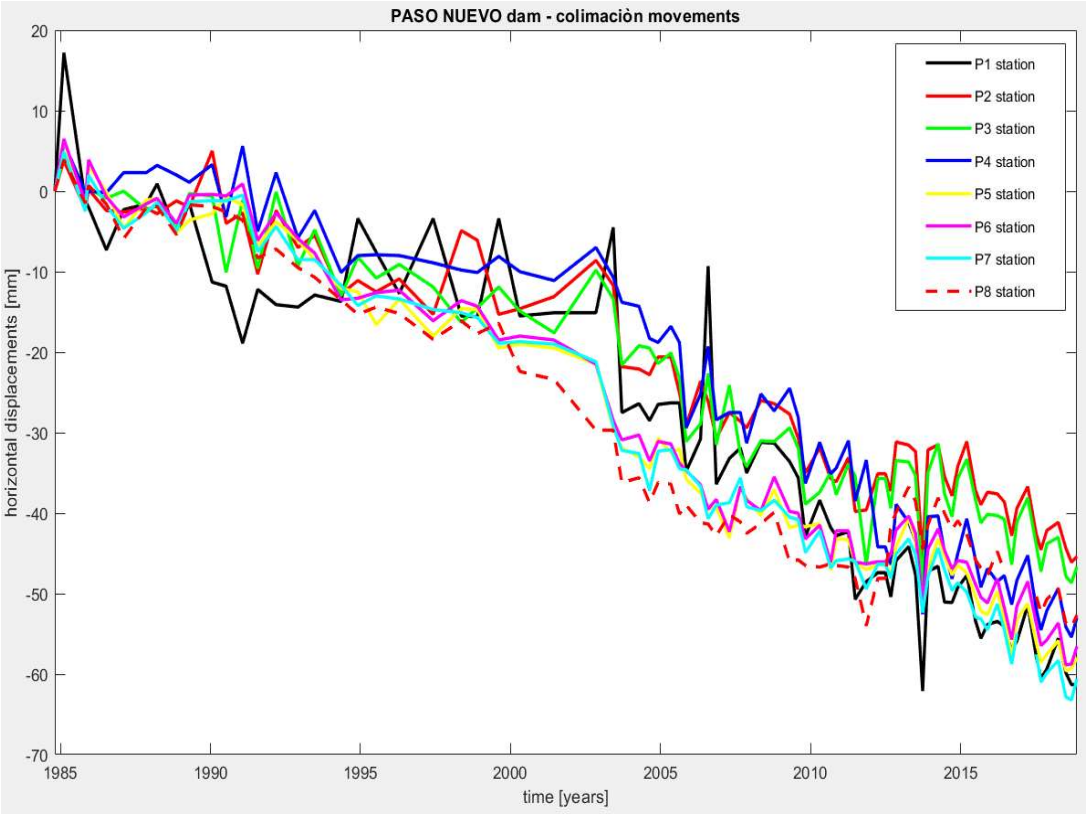

Figure 3.12 - Collimation movements of the 8 measurement stations of the Paso Nuevo dam.

The Paso Nuevo and the Toràn dams have registered horizontal movements that show negative signs. In this case (except block 1 of Toràn dam) the reference system used considered the positive movements in the opposite direction with respect to before, being positive the movements toward downstream.

The horizontal movements of the Paso Nuevo dam, differently from the previous two dams, shows trends that are not yet going to stabilize but seem to belong to the 2nd phase of the reaction development. Some exceptions are present, for example block 3 (measurement station P1) shows big movements despite being one of the shortest blocks (Aguado et al., 2020). In past studies of the Paso Nuevo movements, relations between the magnitude of the movements and the slenderness and height of the blocks didn't produced any significant result (Aguado et al., 2020). In this case, a generalized phenomenon is acting and it is superposed to specific and local problems.

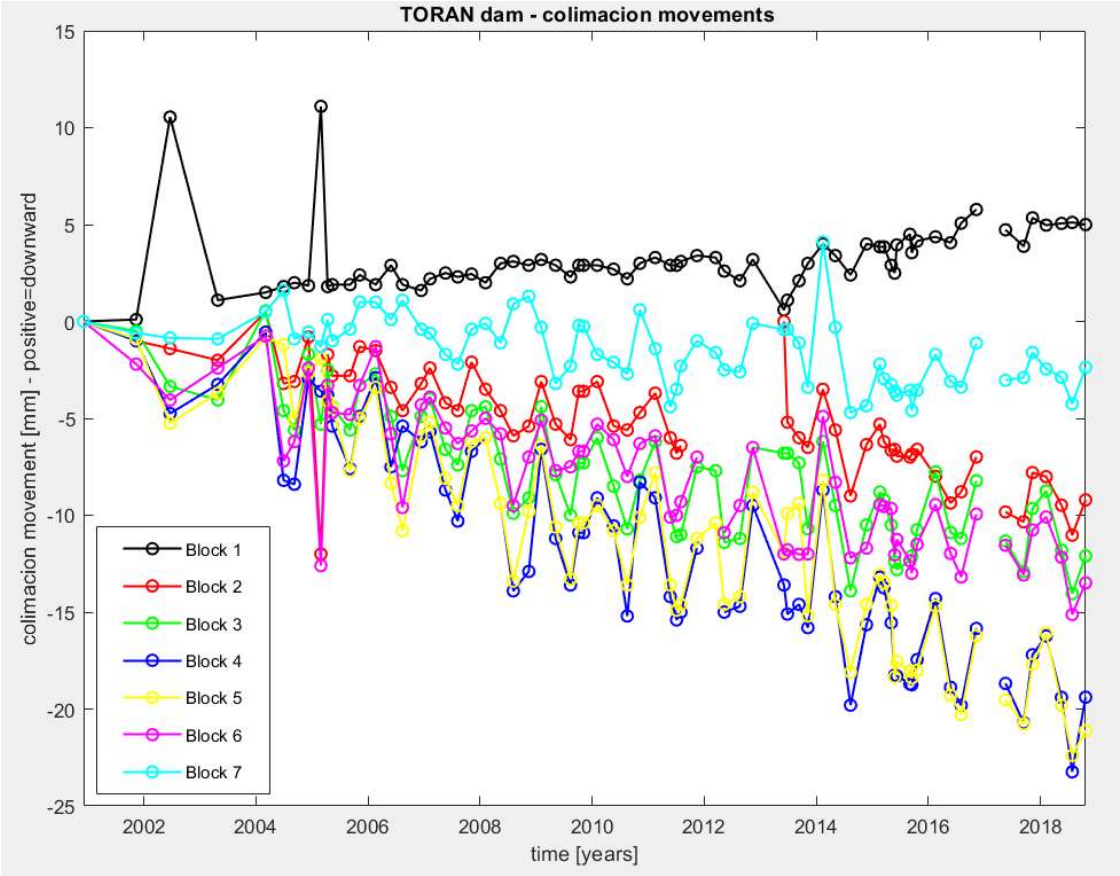

Figure 3.13 - Collimation movements of the 7 measurement stations of the Toràn dam.

The movements of Toràn dam show a clear stabilization trend. Except blocks 4 and 5, whose trends seem to keep on increasing, the other blocks have entered the stabilization part.

One issue that could be liable of influencing the outcome of the displacements is the position of the auscultation system at the top of the dam. Being the top distinguished by a turning movement, as explained before, positioning the auscultation system toward the upstream face or toward the downstream face could have an influence on the results of the measurements, affecting their magnitude. For example, in figure 3.14 representing the Paso Nuevo plan, one can see the positions of the measurements' stations and of the fixed reference measuring bases. For the latter ones' sakes, some stations were installed close to the upstream face (stations 1, 4, 5, 8), others close to the downstream face (2, 3, 6, 7).

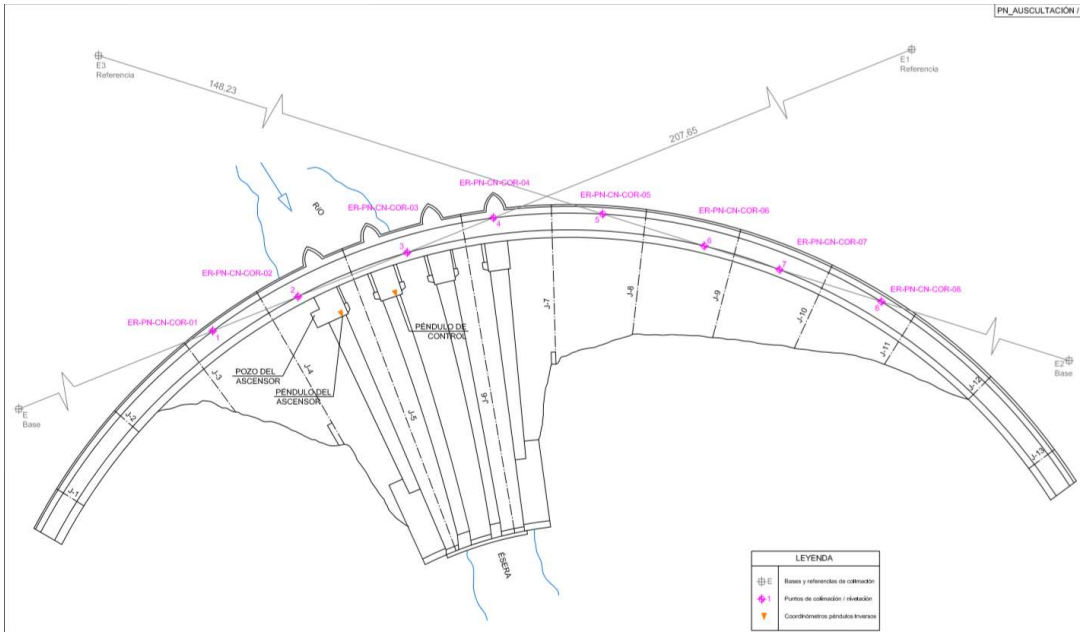

Figure 3.14 - Plan view of the Paso Nuevo dam. positions of the 8 measurements stations and the reference fixed measuring bases. Some of them are close to the upstream face, the others are close to the downstream face.

As many studies have confirmed, the presence of ISA inside the dams produces a differential expansion, concentrated mainly in the superficial portion of the downstream face, that is almost exclusively responsible for the horizontal movements (Campos, 2012, Campos et al., 2016). The sulphate attack gives birth then to significative horizontal movements and much more modest vertical displacements.

3.3.2 Vertical movements

The vertical movements registered at the top were found to be always positive, that means that the movements were always directed upward, in accordance with the expansive character of the inner reactions. Being the base of the dam considered fixed at the foundation level, the top of dam is on the other side less constrained to move, since it is free of move (del Hoyo et al., 2002). The states of stress and strains in the vertical direction

are such that the expansion in this direction is less globally constrained, with respect to the horizontal one (Araúlo, 2008).

ASR is typically more homogeneous when it is up to gravity dams compared to ISA. The deformations depend on where specifically those reactions take place. While the latter ones are known to be more powerful on the downstream face, where the oxidizing agents are more abundant, the former ones are developed in almost all the body of the dam. This trend is confirmed by the measurements of the displacements recorded in the gallery measurements stations (Aguado et al., 2014, 2018, 2020). In the vertical direction small upward displacements are detected, in accordance with the ASR phenomenon. In the horizontal direction instead their entity is much lower, being the oxidizing agents less available and ISA slightly developed. Galleries recorded movements have a recoverable component that is predominant with respect to the non-recoverable one, in contrast to measurements at the top of the dams. The galleries displacements are not reported here.

Whatever the mechanism, the expansions experienced will be translated, for the vertical displacements, in upward movements. The vertical displacements are nevertheless due to both mechanisms, ISA and ASR, being ASR the main contributor (Aguado et al., 2014).

In figure 3.15 the levelling movements of Graus dam are displayed, recorded from 1981 to 2018. A clear tendency to stabilize is not yet met. A similar behaviour is observed in the vertical movements of the Tavascan (figure 3.16) and Paso Nuevo (figure 3.17).

Differently from the trend of the collimation movements, that are manifested since the very first years after the dam commissioning, the vertical ones need many years in order to develop. For the first 10 years, the cyclic component is predominant, after that instead the non-recoverable one gain weight. The reason lays in the fact that ASR reactions, main responsible for the vertical movements (Aguado et al, 2014), take lots of years to develop (Swamy, 1992).

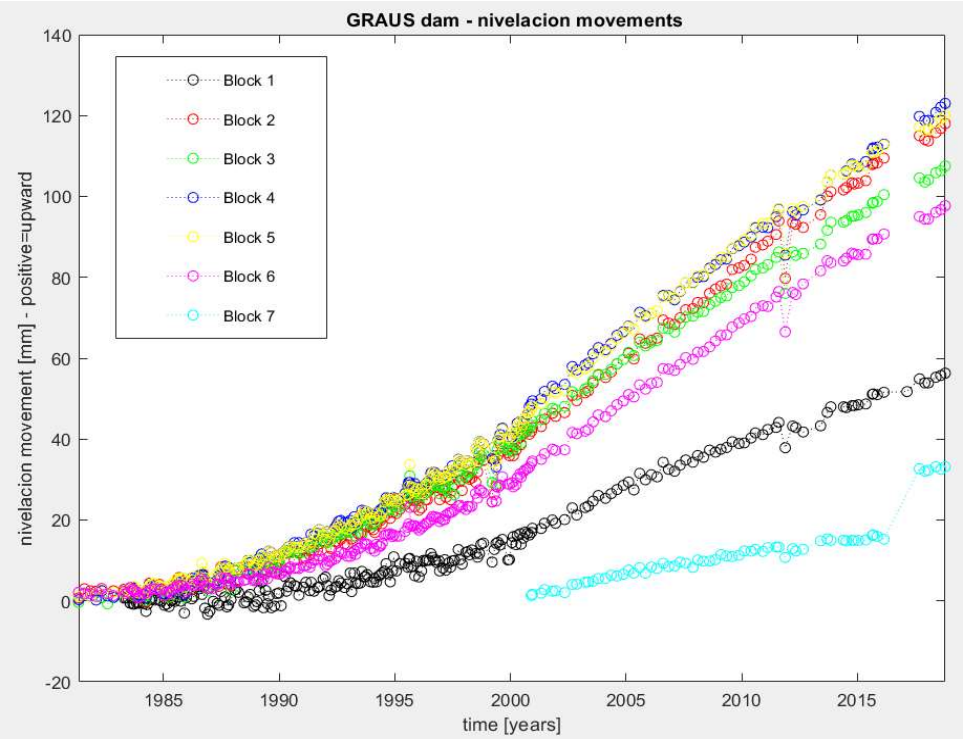

Figure 3.15 - Levelling movements of the 7 blocks of the Graus dam.

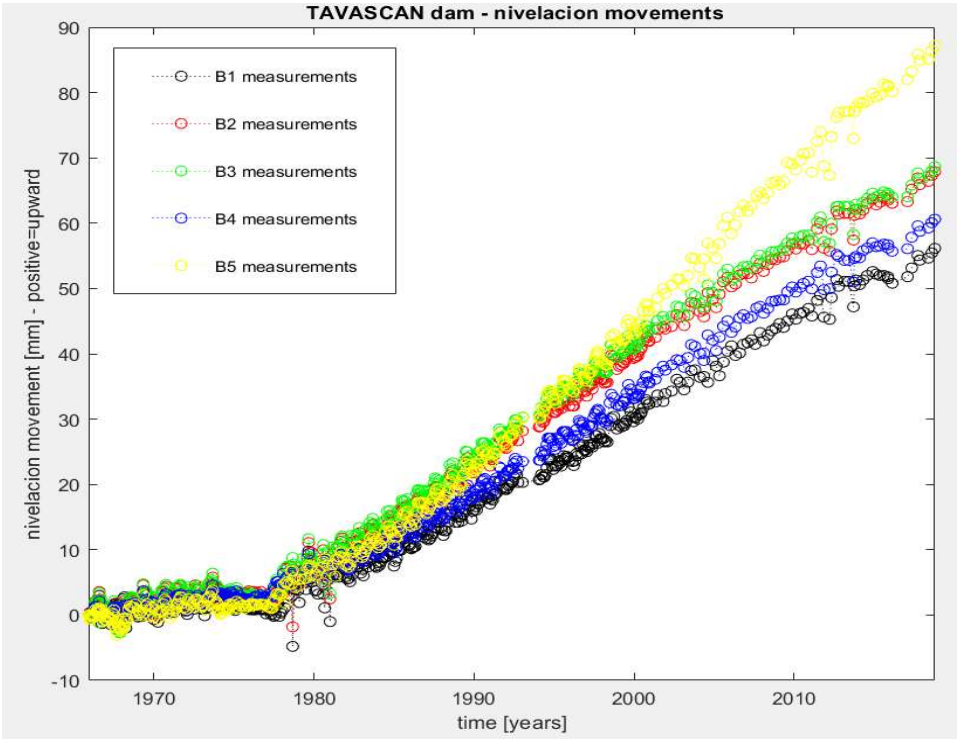

Figure 3.16 - Levelling movements of Tavascan dam.

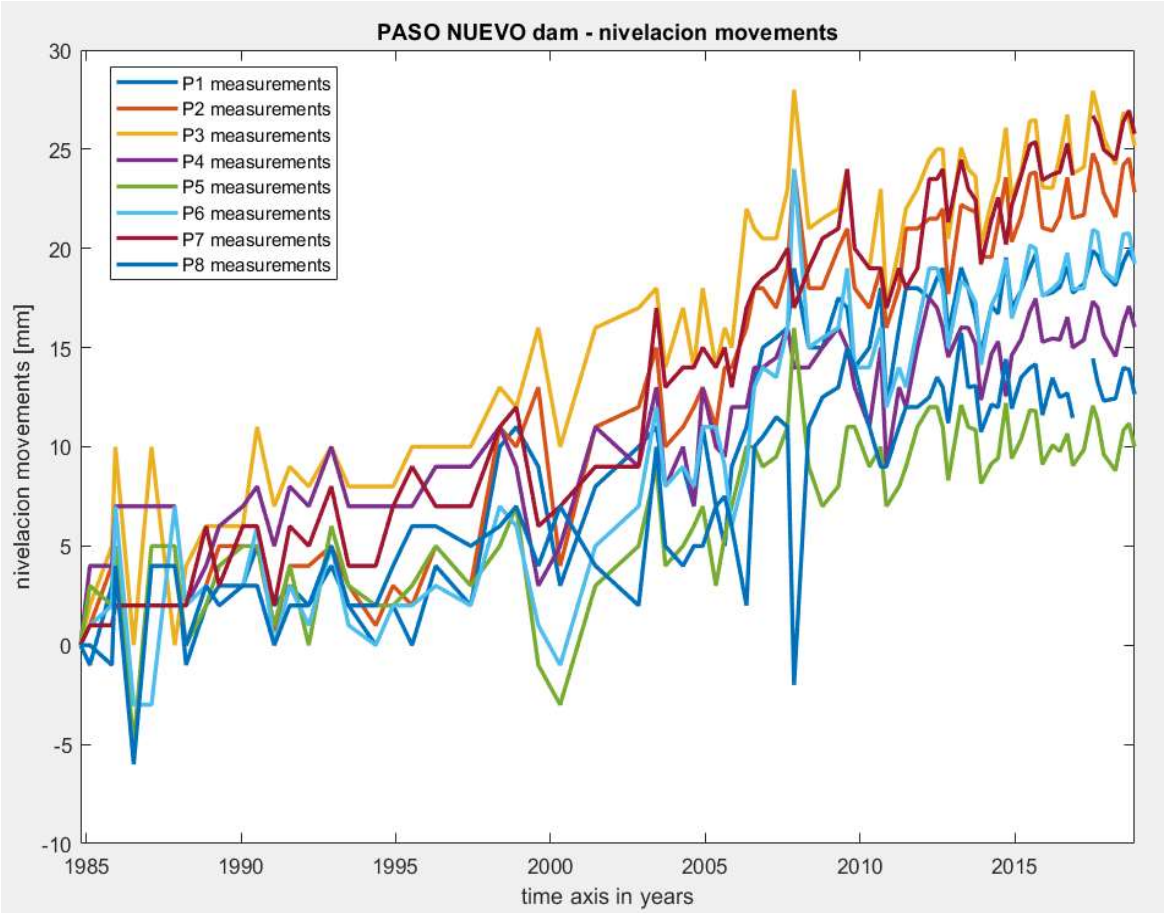

Figure 3.17 - Levelling movements of the 8 measurements stations of Paso Nuevo dam.

The magnitude of the Graus and Tavascan movements is similar, ranging from 50 to 120 mm (except block 7 of Graus dam), in contrary to what happened for the collimation, that showed very different intensities of the movements. The different entity of movements among blocks is again attributed to geometrical features (Aguado et al., 1993). The highest blocks showed larger displacements while the shortest ones were characterized by lower movements. The highest blocks turn out to be the central ones, hence they are also the ones who are less affected by the lateral constraints represented by the abutments presence.

Paso Nuevo vertical movements (figure 3.17) show in most of the cases trends of stabilization. Magnitude and trend of the movements are in opposition to the collimation movements character, regarding the expansive phenomena previously described (Aguado

et al., 2020). They are generally already inside the stabilization phase, in contrast to the collimation ones that show signs of stabilization, despite being characterized by responsible reaction that are, on average, slower in this direction (ASR). Hence from the trend it seems that the future movements to be expected is small, in any case lower than the horizontal one. The opposite happened in Graus and Tavascan dams.

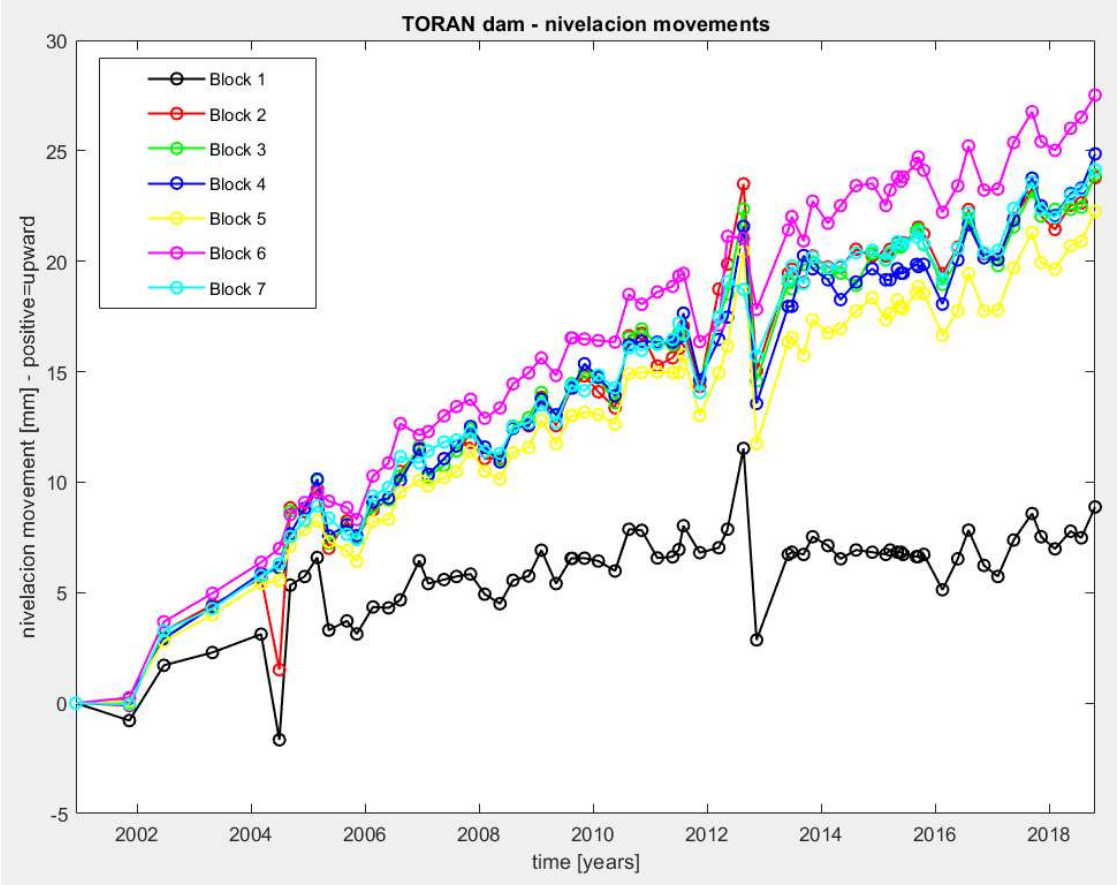

Figure 3.18 - Levelling movements of Toràn dam.

Regarding the Toràn dam movements (figure 3.18), the measurements obtained only cover the period 2000-2018, being the auscultation systems installed many years after the dam commissioning, dated 1964. Here in fact it can be appreciated the stabilization part of the movements, whereas the initiation and the progression parts of the vertical displacements occurred without being measured. As well the magnitude of the displacements is affected by the lack of initial data.

The movements trend of Toràn dam blocks resembles the last part of the levelling movements trend of the Graus dam.

3.3.3 Comparison and general considerations

From a first rough observation of the movements registered in the horizontal and vertical direction, the unequivocal sudden consideration is that the displacements have a non-recoverable component that is order of magnitude higher than the recoverable one, being the latter one imputable to seasonal effects of temperature and water level variations (Aguado et al., 1993).

The trend of movements is similar in the cases of the levelling and collimation movements. They are well described by the three-phase phenomenon of chapter 2, constituted of initiation, development and stabilization phases. All these three phases are identified in the movements of the dams: in the collimation data they are more clear, while in the levelling data the stabilization part in general is just started and so it is difficult to outline it with clarity. In general movements are still increasing in the vertical direction while horizontal ones seem to have on average reached a stabilization. Paso Nuevo movements constitute a little of exception.

In figures are reported, by way of example, the trends of the increment of the horizontal displacement (figure 3.19) and of the vertical displacement (figure 3.20), from Tavascan dam (Convenio CTT:11130, Aguado et al., 2016). Horizontal movements happened considerably sooner than the vertical ones. While collimation displacements increments start to decrease after year 1983-1985, the levelling ones do it around year 2008. This is consistent with the attribution (as causes of the movements) of the ISA (that is faster) to the collimation movements and of the ASR (and in second measure ISA) in the alignments, being ASR mechanism slower to manifest.

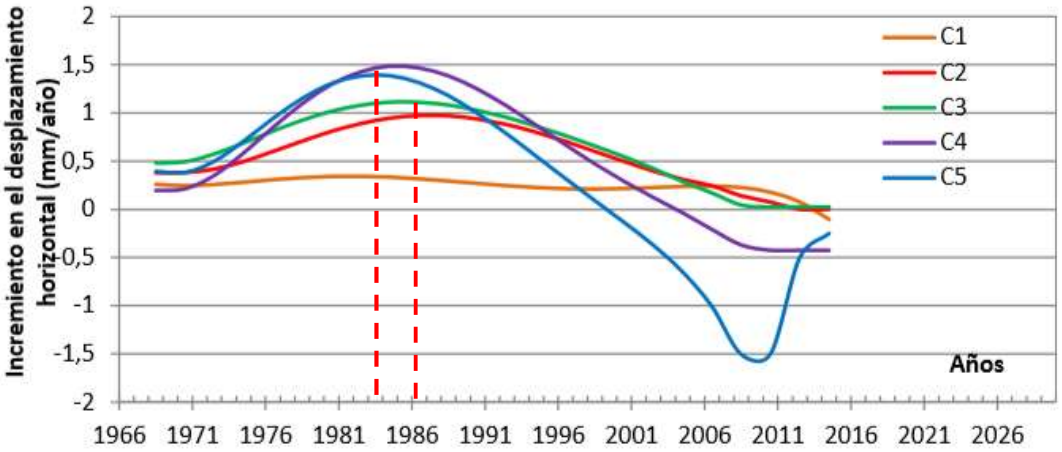

Figure 3.19 - Trends of the horizontal displacements increment of the 5 measurement stations of Tavascan dam (Aguado et al., 2016).

The rate of increment of horizontal displacements is reported (from Convenio CTT:11130, (Aguado et al., 2016). At the beginning the behaviour is similar, then after some years local effects combined with the development of the expansive phenomena pass on each block trend. Stations 4 and 5 have for example a peculiar local behaviour.In figure the vertical movements increment is depicted. At the beginning it is similar to the horizontal rate (same magnitude in mm/years) but after 1983-1986 it keeps increasing.

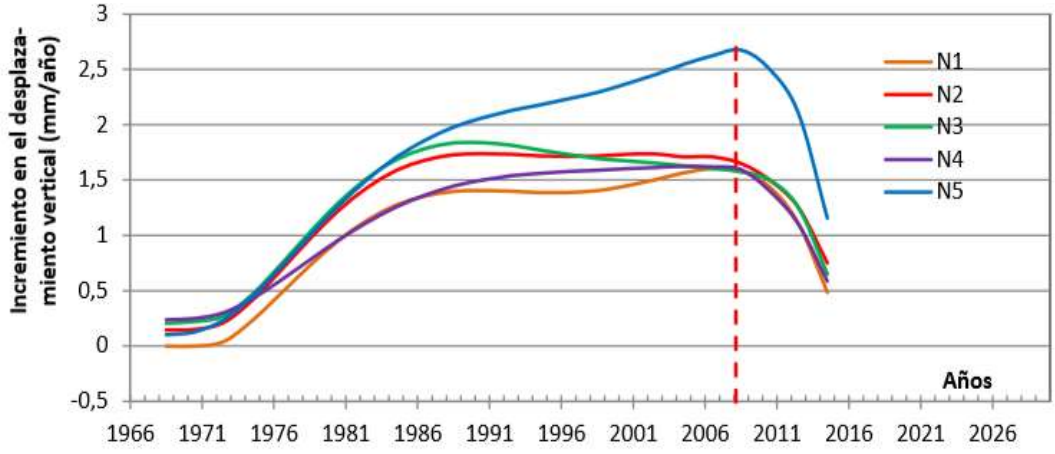

Figure 3.20 - Trends of the vertical displacements increment of the 5 measurement stations of Tavascan dam (Aguado et al., 2016).

In figure 3.21 one can appreciate the superposed effect of the ISA and ASR expansive phenomena, from a qualitative point of view (from Convenio CTT:11130, Aguado et al., 2016). The trend of the horizontal movements' increments could be associated with the ISA mechanism only (orange dashed line in the figure), since these movements are proven to be provoked only by it (Aguado et al., 1998).

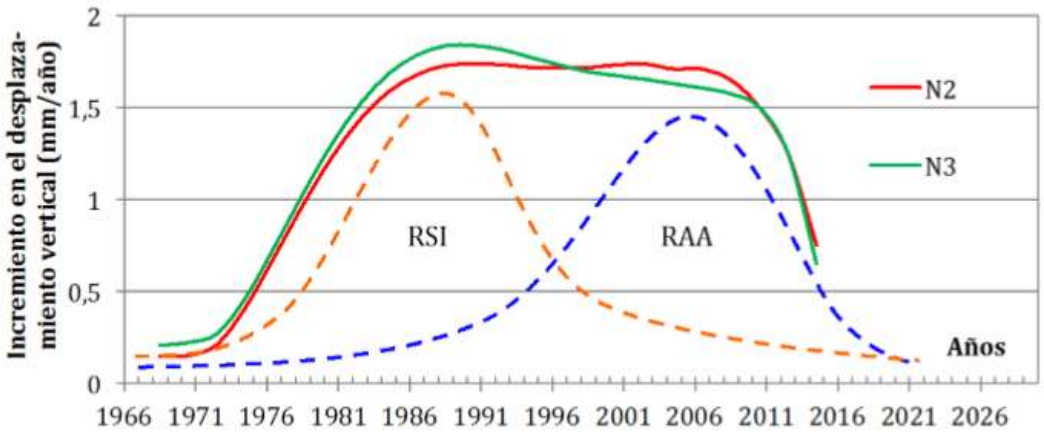

Figure 3.21 – Combined effect of the ISA (or RSI in Spanish, orange dashed line) and ASR (blue dashed line) on the trend of vertical displacements of blocks 2 and 3, of Tavascan dam (Aguado et al., 2016).

Collimation movements in general happen sooner, and they faster than the levelling ones. The main reason could be the nature of the phenomena. As previously mentioned, Paso Nuevo dam seems to be an exception, given that the trends of horizontal and vertical displacements show the opposite: here the vertical movements start to stabilize while the horizontal one seem to not follow that trend yet, as can be seen from figures 3.12 and 3.17.

Tavascan and Graus dams are built more or less in the same period and they are close, so aggragates from the same lithotypes have been used (Aguado et al., 1993). The entity of the levelling movements is similar, being also similar the height of their blocks. Their collimation movements on the other hand is very different, being an order of magnitude higher in the case of Graus dam. Explanations of this behaviour could be found in the position of the auscultation system in the Tavascan dam or in the different development

of the phenomena. ISA acted with two different intensities in the two dams, being markedly more intense in the Graus dam (Aguado et al., 2014).

The Toràn dam, as mentioned, only shows displacements belonging to an advanced phase. They are similar to the last part of the data of Graus for the levelling, and to the last part of the Tavascan and Graus for the collimation. The movements show a stabilization character, more pronounced in the case of the horizontal direction, accordingly to the expansive phenomenon that is known to act in this direction, i.e. ISA. These facts will be the bases for the assumptions regarding the modelling of the Toràn dam movements. Being the data series too short to be fitted, additional assumptions will be made, with the help of the similarity with Graus and Tavascan dams, that instead have been monitored for many years and a huge amount of information belong to them.

CHAPTER 4 – MODELLING OF THE MOVEMENTS

4.1 Introduction

The movements showed peculiar trends of non-recoverable entity, and these trends have been modelled with the model proposed by Aguado (1993):

$$y = A + B \cdot \left(1 - \exp\left(-\left(\frac{t}{C}\right)^{p}\right)\right) \tag{6}$$

that is described in the next chapter. Measurements stations placed on top of the blocks of the dams allowed to obtain ample information on displacements, be them horizontal or vertical, that in turn were able to reflect the specific problematic of each block movement. In this light, as an example, measurements stations placed nearby a vertical joint on two adjacent blocks could reveal the existence of differential movements.

The purposes of fitting and adjusting a mathematical model to the measured data are to be sought in the capability of accurately predicting the future movements that could be reasonably expected, and in the ability of detecting any anomaly during all the phases of measurements. Modelling requires big amount of data and investigation plans that envelope all the aspects that characterize a dam and its behaviour (Gómez Arruche, 1989).

One thoroughly investigated aspect of the model has been its robustness in the fitting of the data. This is done with the help of robust methods that are recalled in the next chapters. Modelling has been carried out entirely in Matlab software.

Each parameter of the model is accurately analysed and described. Specific considerations are made with respect to the parameter A, accounting for its mathematical role and the repercussion that its constraints assume in the modelling of

the movements data. In particular, comparisons are held between setting A equal to 0 and forcing it to be negative.

4.2 Model description, features and implementation

4.2.1 Characteristics of the model

The data collected regarding the displacements of the blocks have been part of a regression analysis. Such aspects of the analysis were highlighted: capability of correctly interpret the data related to the expansive phenomena at the actual time and in the future years, give a physical interpretation to the regression parameters estimated, in order to actually describe the behaviour of the blocks, given their configurations.

As described in chapter 2.3, the model proposed by Aguado (1993) follows an exponential law that is able to properly describe the nature of the development of the expansive phenomena in time (ASR and ISA). The full development of the expansive mechanism can be seen as a sequence of three phases:

4) Activation of the expansions: the expansion phenomena take place. This phase could start immediately or need some time before its beginning, according to many factors, being howsoever the reactions of slow character.

5) Growth/Development: after the first initiation phase, where the gradient of expansion keeps increasing, the gradient here reaches the maximum value. The expansions proceed at the maximum speed, and at the end the phase the speed of reactions starts to decrease.

6) Passivation/Stabilization: after many years, the reactions are almost all consumed and the reactive minerals are nearly all reacted. The movements quite entirely took place and the gradient is approaching to zero.

The curve that manage to represent these three phases, proposed by Aguado, is the following:

$$y = A + B \cdot \left(1 - \exp\left(-\left(\frac{t}{C}\right)^{p}\right)\right) \quad (6)$$

Where: y = movement, be it horizontal of vertical [mm].

A = value of the intercept, ordinate value at the origin.

B = rank of the variation of the ordinate. It represents the total amplitude of the expansion at $t = \infty$.

C = abscissa value of the inflection point [months], when the parameter P is bigger than 1. This value falls where the B parameter has reached a value of about 63% of the total expansion.

P = parameter related to the shape of the curve.

t = time [months]

The physical meaning of these parameters is explained in chapter 5.2. The shape of the model's equation is represented in figure 4.1.

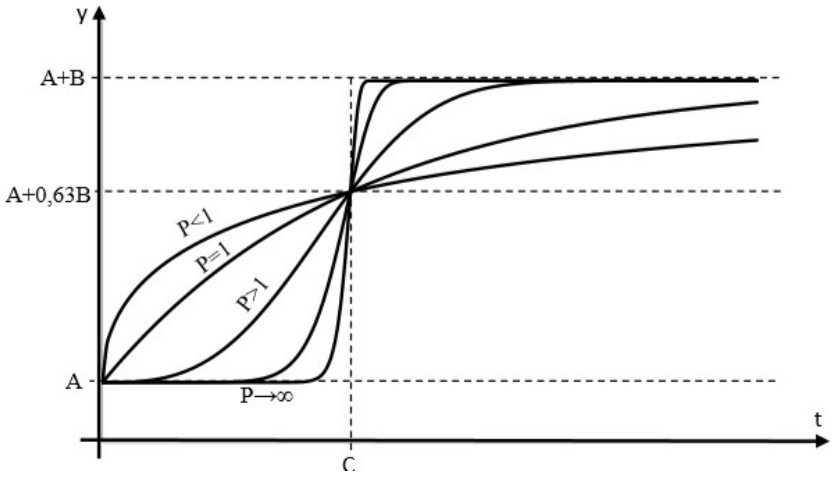

Figure 4.1 - Model that describe the movements caused by the expansion phenomena (Aguado, 1993) and meaning of parameters.

4.2.2 Model implementation

In figure 4.2 the Curve Fitting Tool is displayed, the tool available in the Matlab environment that perform the fitting of a curve given two series of data. Data of the movements and of the dates when they are registered are first imported. Data containing NaN values are automatically not considered. In the figure the data refer to the levelling movements of the Paso Nuevo dam, block 9 (measurements station P-7).

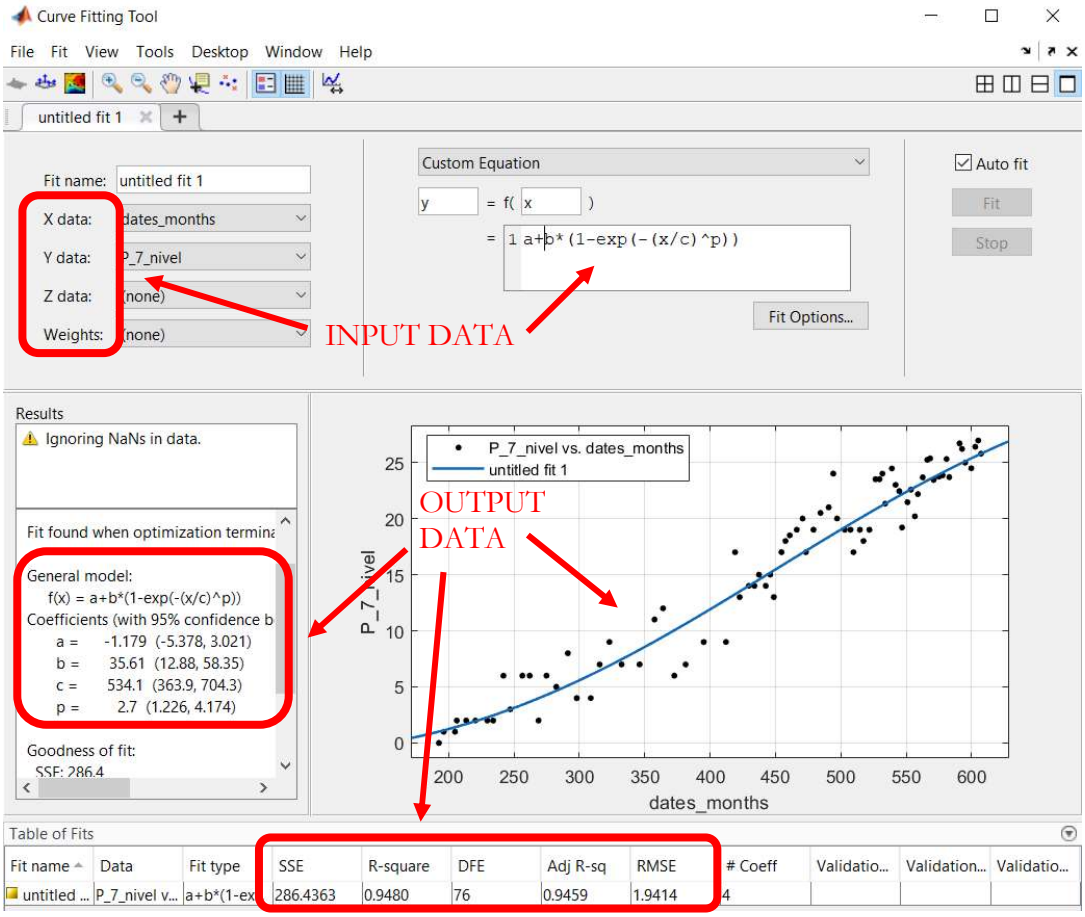

Figure 4.2 – Curve Fitting Tool in Matlab environment, in this picture are reported the input and the output data, the fitting of the P7 station levelling movements of Paso Nuevo dam, and its results.

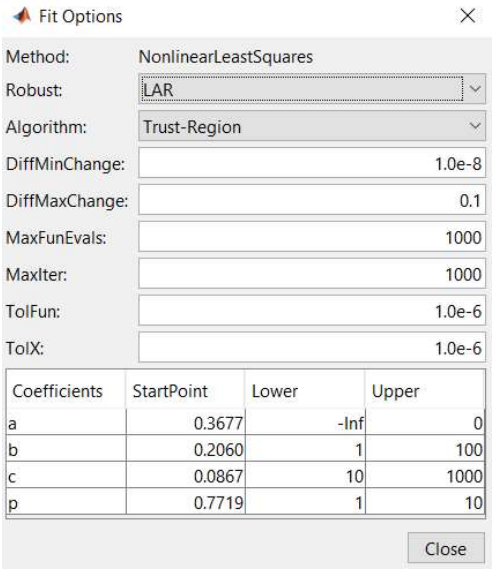

Figure 4.33 – Setting the options for the fitting of the curve in Matlab environment, inside the Curve Fitting Tool.

In figure 4.3 the fitting options are reported. The fitting method is the non-linear least square method. The coefficients are inserted by putting limits to them, in order to reduce the number of iterations that the software will compute (MaxIter = 1000 iterations), for example the C value is set between C = 10 and C =1000, and the A value is set lower than zero or equal to zero. Comments on the setting of the A parameters are remarked in chapter 4.3.1.

The robust methods chosen are commented in chapter 4.4.1.

In figure 4.2 typical fitting results can be seen. They are overviewed in the next chapter. The outputs of the fitting are:

- Parameters A, B, C and P (and 95% confidence bounds values)
- Goodness-of-fit parameters
- Graphical display of the data and of the fit

4.2.3 Matlab fitting outcomes

The results of the fitting operations, mentioned above, express the regression outcomes in terms of parameters of the model, and quality of the fitting obtained. The least-squares fitting estimates the model coefficients minimizing the residuals r_i, defined as the difference between the observed response value y_i and the estimated response value $\hat{y}_i$, considering n data.

$$\sum_{i=1}^{n} r_i^2 = \sum_{i=1}^{n} (y_i^2 - \hat{y}_i^2) = min \tag{7}$$

The parameters A, B, C and P are the ones governed by the least square non-linear method, so they minimize the squared errors, intended as squared vertical distances from the curve. The parameters of the model are estimated by this non-linear method, together with their 95% confidence bounds.

The goodness-of-fitting parameters, computed by equations (7), (8) and (9), express, as the noun says, the goodness of the fitting, in terms of:

- R^2 determination coefficient: values of this parameters close to 1 indicate excellent fitting, values close to 0 mean that the variability is not explained by the model. R^2 indicates the proportionate amount of variation in the response variable (y - movement) explained by the independent variables (t - time).

- $RMSE$ (Root Mean Square Error): It is an estimate of the standard deviation of the random component in the data

$$RMSE = s = \sqrt{MSE} \tag{8}$$

- SSE (Sum of Squares due to Error): this statistic measures the total deviation of the response values from the fit to the response values. A value closer to 0 indicates that the model has a smaller random error component, and that the fit will be more useful for prediction (Matlab). w is a weight function.

$$SSE = \sum_{i=1}^{n} w_i \cdot (y_i - \hat{y})^2 \qquad (9)$$

4.3 Parameters estimation of the modelling of movements

The parameters of the model of equation (6) are evaluated with the methods explained in the previous chapters. The robust method that was used the most is the LAR method, although sometimes the Bisquare method gave results that seemed more reasonable and therefore it was in those cases selected. These methods are described in chapter 4.4.1.

In the tables reported in the following chapters, by way of example, and in the ones attached in the Annex 2, the outcomes of the fitting are reported. The choice of the parameter A is motivated in the next chapter.

4.3.1 Choice of parameter A

Parameter A is the intercept value of the curve in the origin. It corresponds to the displacement observed, from a mathematical point of view, at time t=0. Being the time t=0 the commissioning of the dam, that coincides with the finish of construction works, it would not have any meaning that this parameter would be positive. At the end of construction, the movements of the dam at the top is expected to be zero. From t>0 then they will start to increase. But the character of the expansions, due to the ISA and ASR phenomena, are very slow, hence it is not reasonable to think that at time t=0 the movements already took place.

In the evaluation of the parameters of the model adjusted to the recorded dams' movements, two cases are developed and compared:

- A=0, meaning that at the commissioning of the dam the displacement monitored is forced to be 0. This automatically happens when movements data are available since the dam commissioning data. When movements are available some years later (e.g. in the case of Paso Nuevo dam they are available about 15 years later), this choice could affect the entity of the total movements, as will be seen in the next chapter.

- A<0, meaning that the first part of the movements data is not known, and this parameter tries to evaluate its amplitude. This will be the case of Toràn dam movements analysis. In this case the data are available many years after the dam commissioning (more than 35 years), leading to the capturing of only the last portion of data, i.e. the stabilization part. Here fixing the parameter A equal to 0 would not capture the trend of the movement correctly, as will be explained later.

The comparison of the two cases allowed to choose which case would fit best the data of each dam. In some case it will be appropriate to set the constraint A=0 to the model (in the case of Graus and Tavascan dams especially). In few cases the fitting with A=0 resulted in a too restrictive constraint, bringing to misleading results.

4.3.2 Graus dam

Graus dam behaviour has been deeply investigated. Built in years 1968-1971, since 1981 it has been constantly monitored and inspected. Anomalous behaviour has been detected and thoroughly characterized, by means of visual inspections, thorough characterization of cores extracted from the dam and on each of its construction material, experimental campaigns and numerical and 3-D modelling (Convenio CTT-8400,Aguado et al., 2014).

4.3.2.1 Levelling movements

In tables 4.1, 4.2 and 4.3 the parameters of modelling of the Graus dam levelling movements are reported, for the blocks 1 to 7, in two different conditions: A=0 and A<0. The motivations and comments of these choice are remarked in chapter 4.3.1. Table 4.3 contains the differences of the parameters obtained in the two cases (A=0 and A<0).

A < 0	B1	B2	B3	B4	B5	B6	B7
A	-1.111	-2.36E-14	-1.912	-1.394	-0.1367	-4.16E-14	-70.97
B	60.17	141.3	125.7	146.7	136.2	111.7	98.26
C	446.3	477.1	455.1	467.4	452.1	464.6	270.9
P	4.082	3.397	3.102	3.139	3.347	3.647	1.147
C (years)	2008	2011	2009	2010	2009	2010	1994
R^2	0.9902	0.9998	0.9998	0.9999	0.9999	0.9999	0.9721
SSE	619	50.6	39.33	37.56	30.94	21.51	112.99
RMSE	1.609	0.4535	0.4007	0.3916	0.3554	0.2957	1.3392

Table 4.1 - Parameters of the fitting of the 7 blocks levelling movements of the Graus dam, forcing parameter A < 0.

A = 0	B1	B2	B3	B4	B5	B6	B7
A	0	0	0	0	0	0	0
B	57.06	141.3	118.3	140.5	135.3	111.5	15.66
C	441	477.1	444.7	460.1	450.8	463.9	437.7
P	4.407	3.396	3.332	3.289	3.369	3.654	7.307
C (years)	2008	2011	2008	2009	2009	2010	2007
R^2	0.9895	0.9998	0.9998	0.9999	0.9999	0.9999	0.9695
SSE	668.8	50.64	45.06	40.5	33.78	21.54	123.5
RMSE	1.669	0.4537	0.428	0.4058	0.3706	0.2959	1.3891

Table 4.2 - Parameters of the fitting of the 7 blocks levelling movements of the Graus dam, forcing parameter A = 0.

As can be appreciated in the table 4.3 in most cases the difference is very small (blocks 1, 2, 3, 4, 5 and 6) and parameters B, C and P slightly change, assuring that if A is fixed to 0 the model fits the data with almost equal degree of precision. R^2 stays between 0.99 and 0.9999, confirming the goodness of the model. When fixing A to 0 the errors

SSE and RMSE increase: of a small quantity in blocks 2 and 6 (0.1%), a bit higher in blocks 1, 3, 4 and 5 (3.6%-14.6%). When passing from the parameters obtained with A<0 to the ones obtained with A=0, parameters B and C always decrease of a small quantity (up to 5.9%), the difference by the way is negligible. On the other hand, parameter P tend to increase (up to 7.4%). Hence the curves in the case A=0 are a bit steeper. The curves fitted in this way are plotted in figure 4.4 (in the case A=0).

DIFFERENCES [%]	B1	B2	B3	B4	B5	B6	B7
A	-	-	-	-	-	-	-
B	-5.2	0.0	-5.9	-4.2	-0.7	-0.2	-84.1
C	-1.2	0.0	-2.3	-1.6	-0.3	-0.2	61.6
P	8.0	0.0	7.4	4.8	0.7	0.2	537.1
R^2	-0.1	0.0	0.0	0.0	0.0	0.0	-0.3
SSE	8.0	0.1	14.6	7.8	9.2	0.1	9.3
RMSE	3.7	0.0	6.8	3.6	4.3	0.1	3.7

Table 4.3 – Differences in the parameters of the fitting of the 7 blocks levelling movements of the Graus dam, when passing from A<0 to A=0.

Parameter B seems to depend on each block, everyone having its own magnitude of vertical displacement. Parameters C and P on the other hand are very similar for all the blocks, confirming that the expansions have the same speed and trend on each block. This result corroborates the presence of an expansive phenomenon that is diffused in all the blocks, hitting each block with the same speed but with a different magnitude. C ranges from around 430 to 480, P between 3.1 and 3.6 (only block 1 has a bit bigger values of P). Block 1 and block 7, anyway, being lateral blocks, could be influenced by the abutment presence.

In block 7 instead the difference of the two A conditions is significative: B is reduced of 84.1%, C increases of 61.6% and P increases of more than five times, when passing from the condition A<0 to A=0. However, the errors parameters SSE and RMSE don't change much. The anomalous fitting is assumed to be the case in which A<0, since in this case different values of C and P are found (C=270.9, P=1.147), in discordance with the others (C=430-480, P=3.1-3.6).

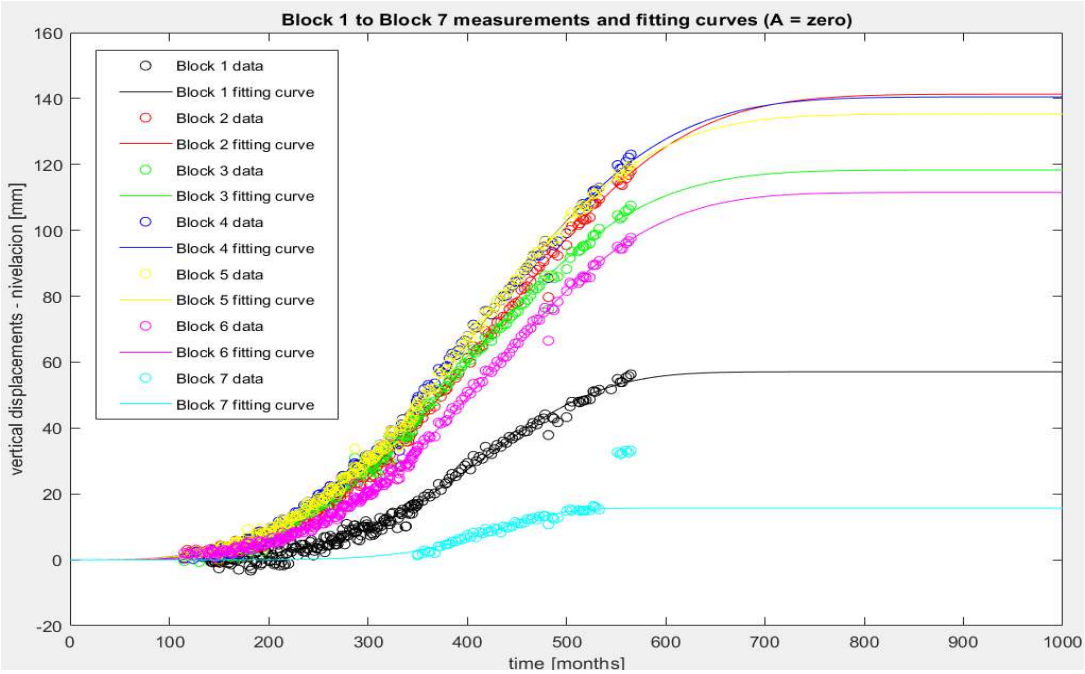

Figure 4.4 – Graus dam levelling movements (blocks 1 to 7) and associated fitting curves (parameter A=0).

Fixing the parameter A to 0 in this case is justified, as results of the modelling confirm.

4.3.2.2 Collimation

The same procedure is repeated for the collimation movements.

A < 0	B1	B2	B3	B4	B5	B6	B7
A	-0.2567	-8.602	-17.69	-15.36	-23.32	-18.92	-7.6E-09
B	15.1	133.4	224.4	270.5	279.8	210.2	19.23
C (months)	375.3	362.5	365.2	357.6	347.6	353.7	329
P	4.023	2.688	2.456	2.67	2.447	2.429	3.978
C (years)	2002	2001	2001	2001	2000	2000	1998

R^2	0.9389	0.9998	0.9999	0.9999	0.9999	0.9998	0.9901
SSE	316.36	69.05	97.33	84.42	109.59	159.49	18.7
RMSE	1.1578	0.5364	0.6368	0.5943	0.6873	0.8186	0.3964

Table 4.4 - Parameters of the fitting of the 7 blocks collimation movements of the Graus dam, forcing parameter A<0.

A = 0	B1	B2	B3	B4	B5	B6	B7
A	0	0	0	0	0	0	0
B	14.61	115.8	192.6	244.7	234.9	183.1	19.23
C	374	353.2	359.3	355	339.1	353.7	329
P	4.28	3.304	3.069	3.099	3.086	3.075	3.98
C (years)	2002	2000	2001	2001	1999	2000	1998
R^2	0.9378	0.9996	0.995	0.997	0.9997	0.9916	0.9902
SSE	322.13	110.77	3770	3787	346.35	5585	15.56
RMSE	1.1659	0.678	3.955	3.9721	1.2192	4.8339	0.3949

Table 4.5 - Parameters of the fitting of the 7 blocks collimation movements of the Graus dam, forcing parameter A=0.

DIFFERENCES [%]	B1	B2	B3	B4	B5	B6	B7
B	-3.2	-13.2	-14.2	-9.5	-16.0	-12.9	0.0
C	-0.3	-2.6	-1.6	-0.7	-2.4	0.0	0.0
P	6.4	22.9	25.0	16.1	26.1	26.6	0.1
R^2	-0.1	0.0	-0.5	-0.3	0.0	-0.8	0.0
SSE	1.8	60.4	3773.4	4385.9	216.0	3401.8	-16.8
RMSE	0.7	26.4	521.1	568.4	77.4	490.5	-0.4

Table 4.6 – Differences of the parameters when passing from A<0 to A=0 in the case of Graus collimation movements.

Similar conclusion to the levelling movements analysis could be outlined in the case of the collimation movements. When passing from the case A<0 to case in which parameter A is fixed to 0, typically parameters B and C decrease a little and parameter P increases.

Regarding the errors' parameters, from A<0 to A=0, R^2 always decreases of a negligible quantity (less than 1%), while the RMSE and SSE grow considerably, especially in stations B3, B4 and B6. This is due in one hand on the fixing the parameter to 0, on the other hand to the large number of data (almost 500 measurements).

In figure 4.5 one can appreciate that the central blocks of the dam have bigger entity of the displacements, while lateral ones are smaller, as can be seen in the values of parameter B. The same happened in the case of the vertical movements.

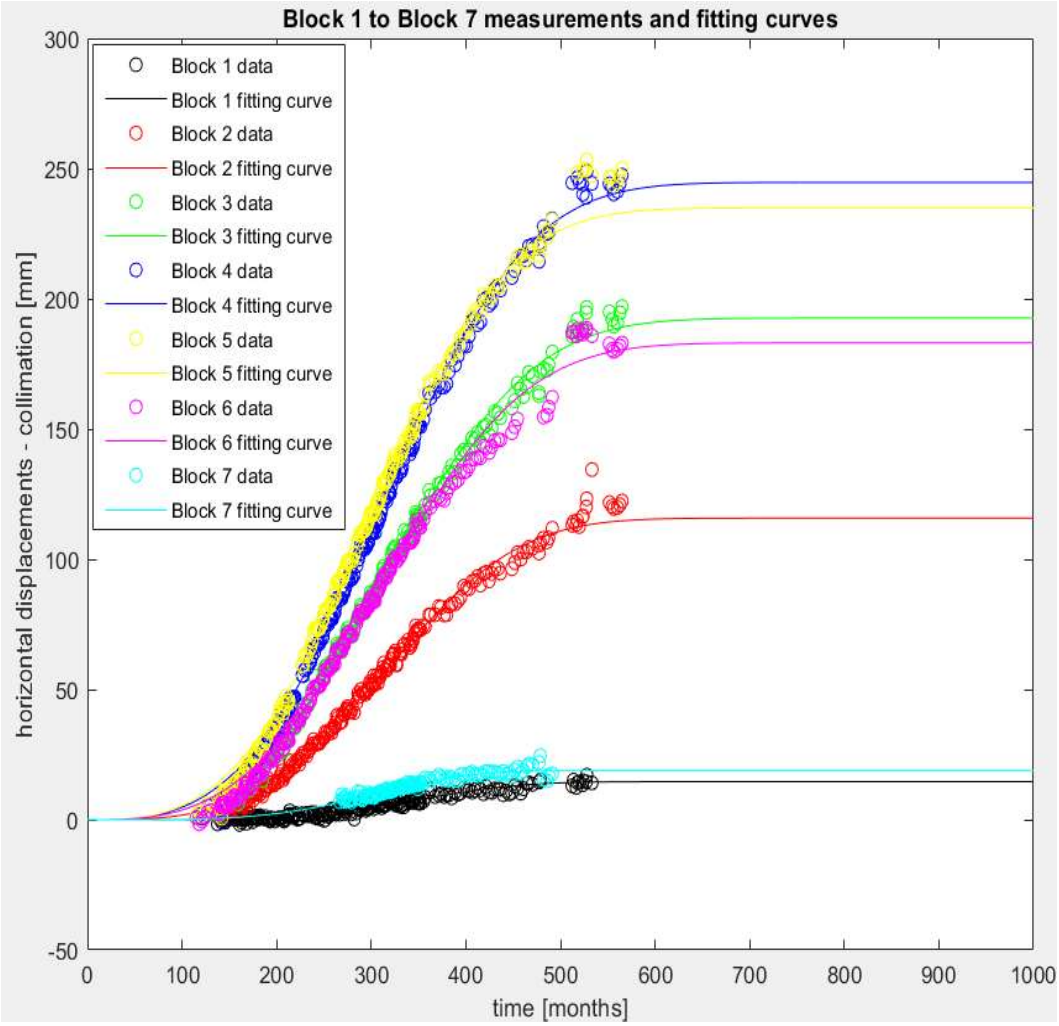

Figure 4.5 - Collimation movements of Graus dam and fitting curves (case A=0).

In figure 4.6 the differences of the collimation movements adjustment of block 5 are plotted. In this case the differences from A<0 and A=0 are mainly in the B and P parameters, being C very similar in the two cases (C= 347 and C=339). The entity of the difference (26.1% in case of parameter P, -16.0% for parameter B) can be explained by the fact that the dam's movements have been first recorded in year 1981, while the dam was commissioned in year 1971, 10 years before. So, when forcing A to 0, the curve is a bit squashed, given the non-linear least-square adjustment.

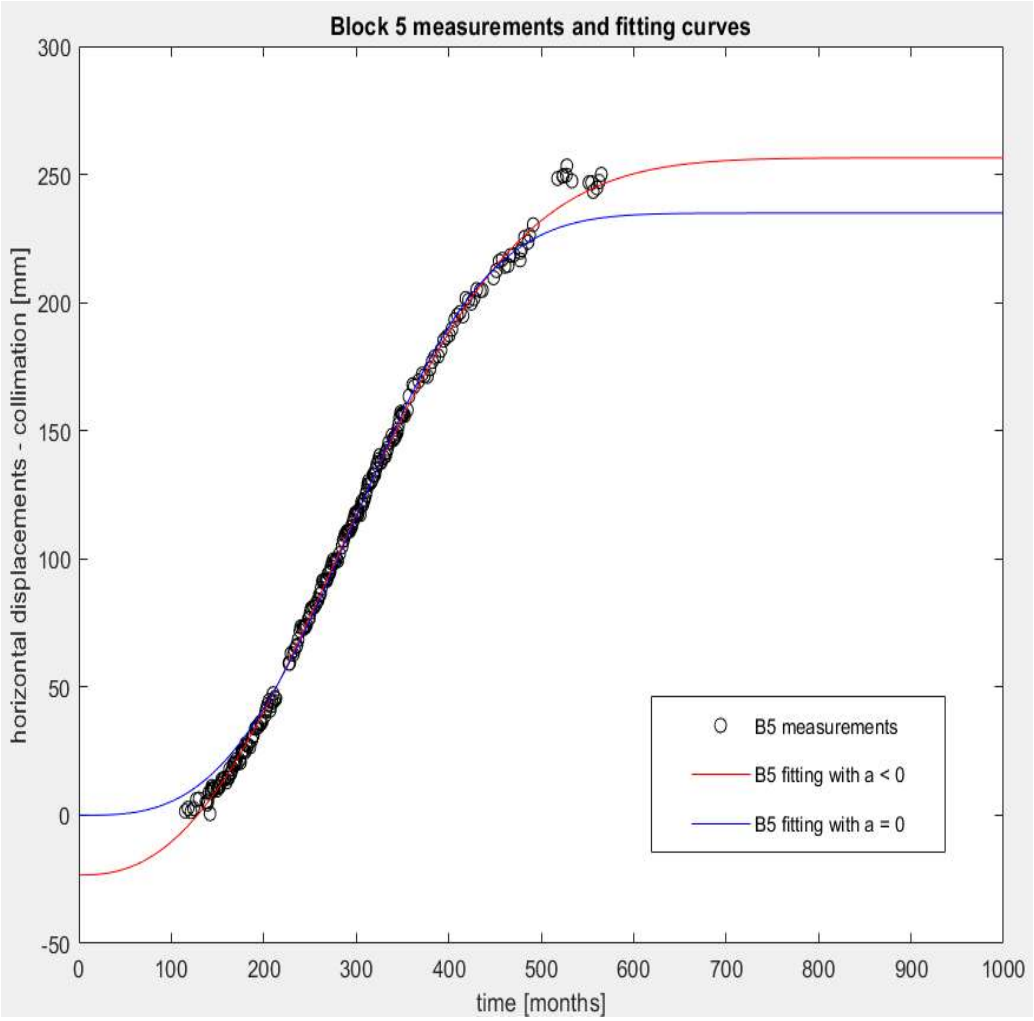

Figure 4.6 – Collimation movements of block 5 of Graus dam. Difference of the fitting with A<0 and A=0.

In the case of the collimation movements as well, the parameter A has been subsequently chosen to be equal to 0, this choice confirming to be adequate.

In figure 4.7 are represented the parameters B of the modelling of the movements of the Graus dam of each block, and the height of the blocks: in this case a good correlation seem to exist between geometry of the blocks and recorded movements (be it horizontal or vertical).

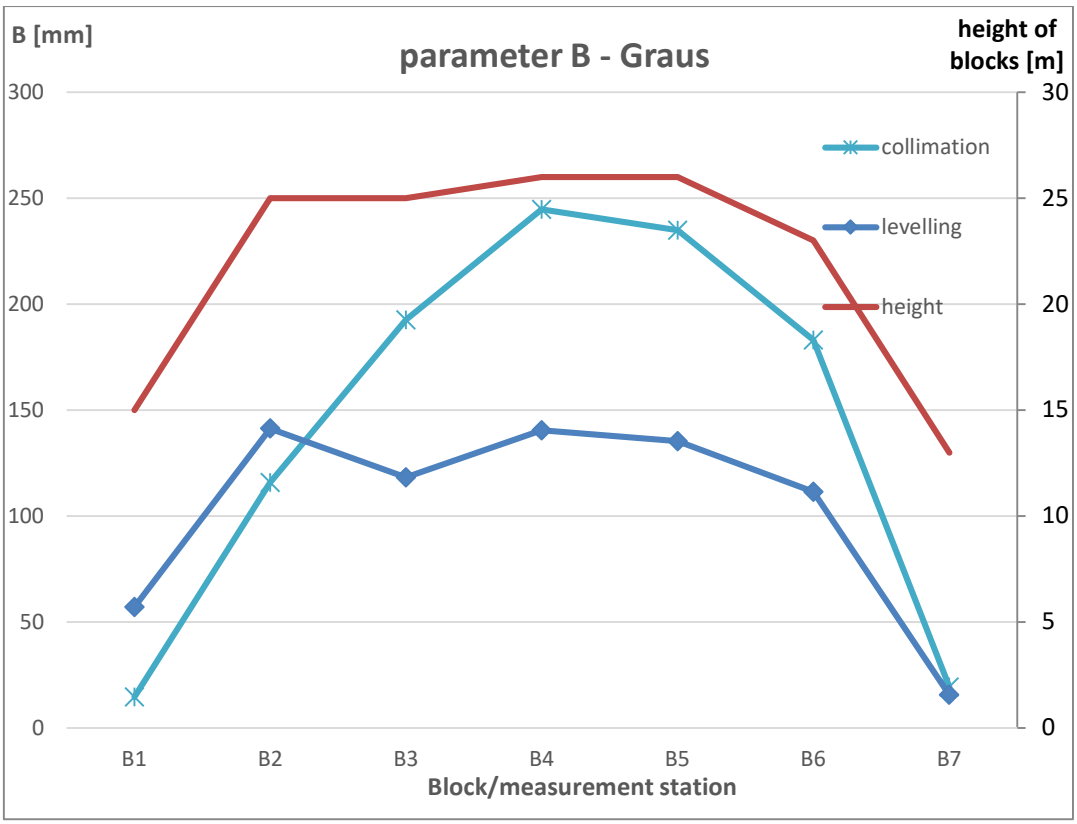

Figure 4.7 - Graus dam. Parameter B of the vertical and horizontal movements model, and height of the blocks.

4.3.3 Tavascan dam

Tavascan dam showed results that are similar to the Graus dam. This could be explained by the vicinity of the two dams (and hence by the similar lithotypes used as aggregates in the concrete), by the analogous geometrical dimensions and type of structure, and by the comparable degradation phenomena that developed in the two dams. As it was done for the Graus dam, more thorough case studies were conducted (e.g. Convenio CTT-10572, Estudio del comportamiento de la presa de Tavascan, Aguado et al., 2018).

4.3.3.1 Levelling

Tables 4.7, 4.8 and 4.9 report the values of the parameters of the model that interpret the vertical movements measured at the top of the dam, and the relative goodness-of-fit statistics.

A < 0	B1	B2	B3	B4	B5
A	-2.3E-14	-2.3E-14	-2.3E-14	-2.27E-14	-0.2513
B	68.33	80.62	80.13	79.41	112.9
C	509.4	486.8	473.2	535.4	541.8
P	2.353	2.151	2.106	2.139	2.407
C (years)	2008	2007	2005	2011	2011
R^2	0.9998	0.9998	0.9999	0.9965	0.9999
SSE	26.78	28.99	28.2	484.37	31.3
RMSE	0.2348	0.244	0.2406	0.9973	0.2538

Table 4.7 – Tavascan parameters of fitting of levelling movements of the 5 stations, A<0.

A = 0	B1	B2	B3	B4	B5
A	0	0	0	0	0
B	68.33	80.62	80.13	79.41	111
C	509.4	486.8	473.2	535.4	536.6
P	2.353	2.151	2.106	2.139	2.438
C (years)	2008	2007	2005	2011	2011
R^2	0.9998	0.9998	0.9999	0.9965	0.9999
SSE	26.78	28.98	28.2	484.37	22.94
RMSE	0.2347	0.244	0.2406	0.9973	0.217

Table 4.8 – Tavascan parameters of fitting of levelling movements of the 5 stations, A=0.

DIFFERENCES [%]	B1	B2	B3	B4	B5
B	0.00	0.00	0.00	0.00	-1.68
C	0.00	0.00	0.00	0.00	-0.96
P	0.00	0.00	0.00	0.00	1.29
R^2	0.00	0.00	0.00	0.00	0.00
SSE	0.00	-0.03	0.00	0.00	-26.71
RMSE	-0.04	0.00	0.00	0.00	-14.50

Table 4.9 – Comparison of the parameters of fitting of the levelling movements in the two cases: A<0 and A=0.

As one can see from the results in the tables above, for stations B1, B2, B3 and B4, no differences are registered in the parameters when passing from A<0 to A=0. In the case of station B5, the difference is slight. This is a confirmation that parameter A can be taken equal to 0, with high accuracy on the prediction if the gap between the commissioning of the dam and the start of measurements recording is short (i.e. Graus dam) or null (i.e. Tavascan dam). As Graus modelling suggests, some small differences arise in the parameters, being bigger in that case since the gap 10 years long.

From the results of the fitting, these conclusions can be drawn:

- Stations B2, B3 and B4 have similar parameter B, and they are placed on central blocks that have similar geometric features (height). station B1 has a small B value, corresponding to smaller total displacements, and this block also has a smaller height. Hence a relation between entity of the movements and height (and in more general, geometry) of the blocks could be outlined. Station B5 instead constitute an exception to this behaviour, registering the highest displacements (and highest B value) despite being placed on a block that has lower height.

- From the results discussed up above, it can be outlined a generalized and diffused phenomenon of expansion, that act on the whole dam (i.e. ISA and ASR). Still, local events halter the generalization, as could be a specific events of station B5.

- Parameter C is similar for all the blocks, ranging from 473 (station B3) months to 541 months (station B5). This is a symptom that all the blocks undergo the same degradation phenomena, hitting each block with a similar but not equal intensity. The same can be said for parameter P, that range from 2.1 to 2.4.

- The fitting showed very high accuracy, being the lowest R^2= 0.996 and the highest R^2= 0.9999. only station B4 error statistics SSE and RMSE are much higher than the others stations' ones.

In figure 4.8 the levelling movements and the fitting curves are plotted.

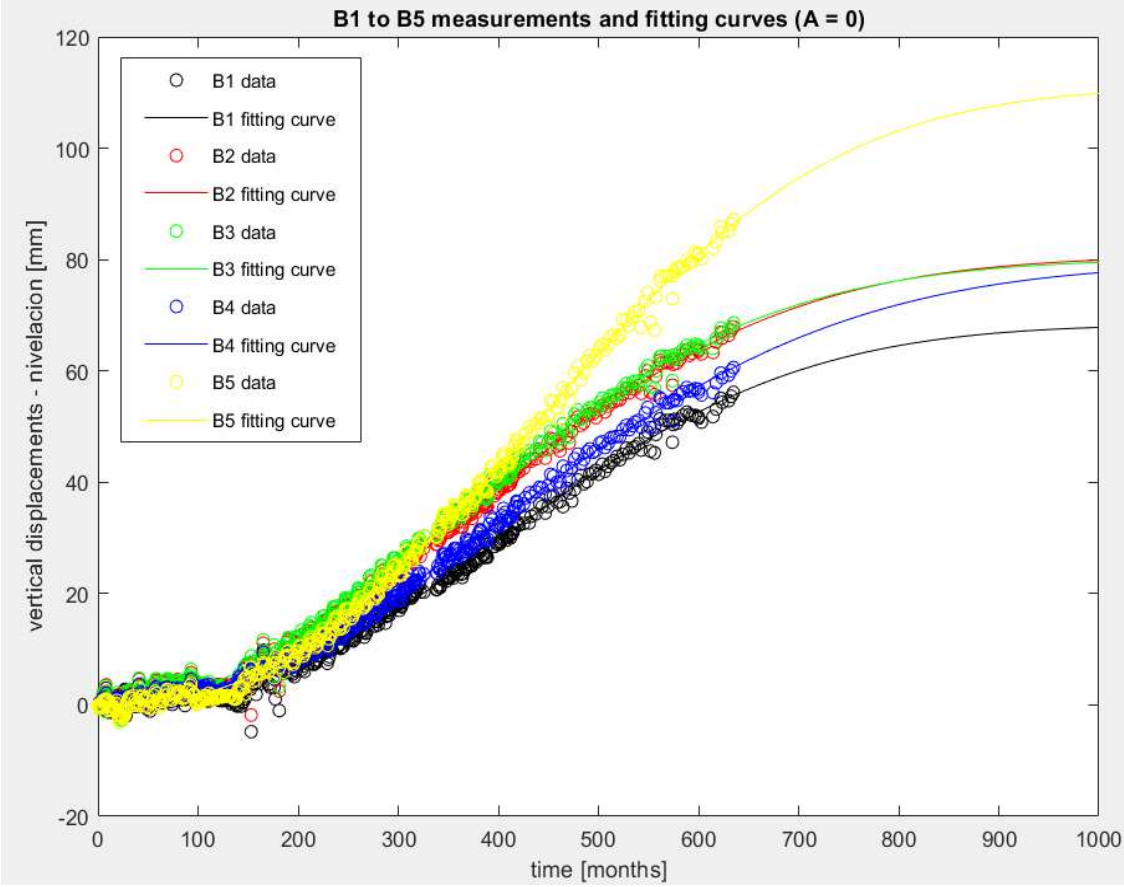

Figure 4.8 - Tavascan levelling movements and fitting curves of stations 1 to 5.

4.3.3.2 Collimation

In the collimation movements of the Tavascan dam the difference between the models with A<0 and A=0, as for the levelling modelling, are negligible. Hence only the case in which A=0 is reported.

In this case, the entity of the horizontal movements is quite lower than the vertical movements and it is much lower than the movements registered for the collimation movements of the Graus dam. This latter fact could be caused by the position of the auscultation system at the top level, that is closer to the upstream face (as explained in the chapter 3.3.1).

A = 0	C1	C2	C3	C4	C5
A	0	0	0	0	0
B	13.38	27.03	31.02	30.23	28.55
C	378.1	310.6	300.1	268.9	247.8
P	1.559	2.225	2.193	2.843	2.429
C (years)	1998	1992	1991	1988	1987
R^2	0.9654	0.987	0.9901	0.9996	0.9884
SSE	255.48	580.45	600.3	24.86	531.97
RMSE	0.7191	1.084	1.1023	0.2246	1.0731

Table 4.10 - Tavascan parameters of fitting of collimation movements of the 5 blocks, A=0.

Station B4 and much more markedly station B5, show decreasing movements in time after years 1999-2000, as can be seen from figure 4.9.

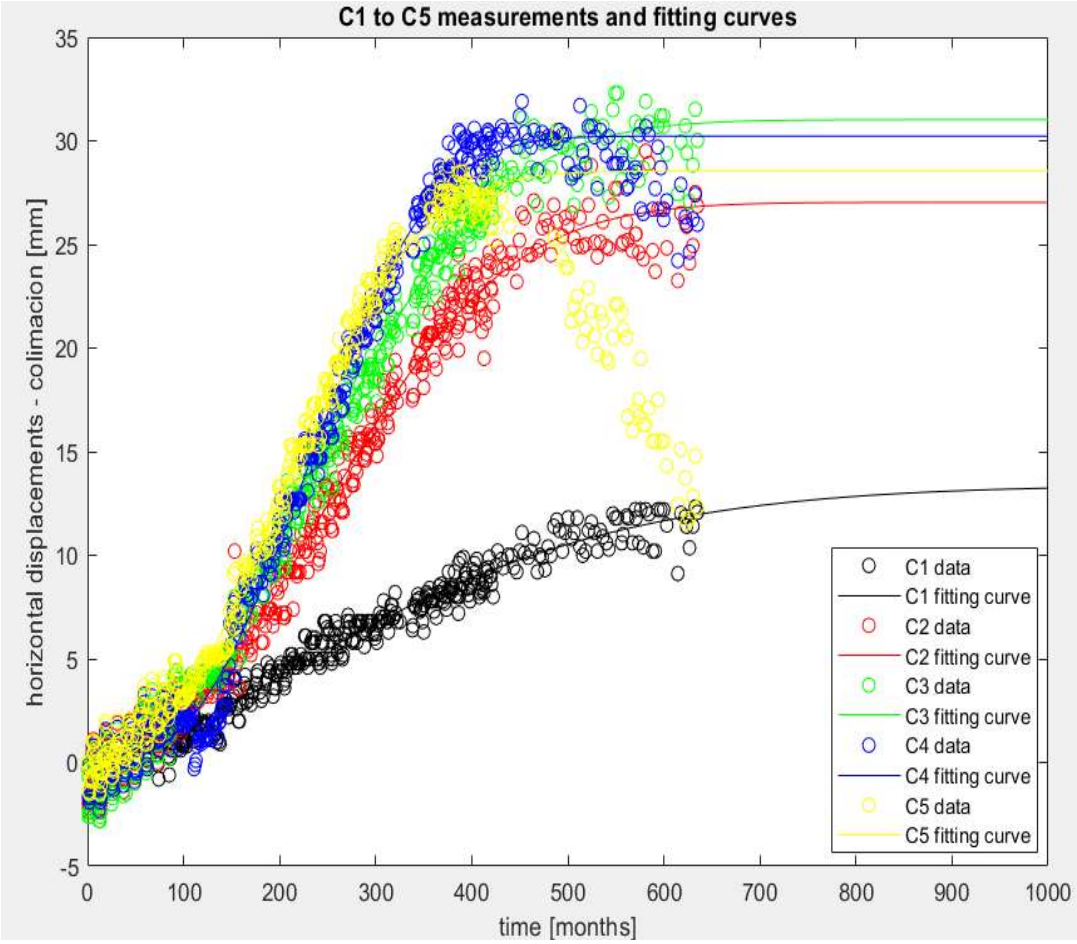

Figure 4.9 - Collimation movements and fitting curves of the 5 stations of the Tavascan dam.

4.3.4 Paso Nuevo dam

Paso Nuevo dam showed a behaviour somehow similar to the Graus and Tavascan dams. Despite being an arch-gravity dam with bigger dimensions of the former two, the construction material used is naturally the same and the expansive phenomena, major responsible for the recorded movements, that have been detected and deeply investigated are in large part the same: sulphate attack and alkali-silica reaction, as confirmed by numerous studies (e.g. Convenio CTT-11130, Re-evaluaciòn del comportamiento de la presa de Paso Nuevo, Aguado et al., 2020).

4.3.4.1 Levelling

The levelling displacements of the Paso Nuevo dam, measured in 8 auscultation stations, showed an increasing non-recoverable component. The data fitted in the two cases A<0 and A=0 resulted in sets of parameters with low variations. In accordance to the procedure followed in the Graus and Tavascan dams, it is considered acceptable to fix parameter A=0. By doing this, generally parameter B and C decrease a little while parameter P increase a little (1-4%, in very few cases more than 7%). The parameters obtained with A=0 are reported in table 4.11, the differences (A=0 vs A<0) in table 4.12.

A = 0	P1	P2	P3	P4	P5	P6	P7	P8
A	0	0	0	0	0	0	0	0
B	19.55	23.68	29.66	21.62	11.93	19.04	30.41	13.81
C	449.3	443.7	454.5	496	451.3	458.7	499	430.1
P	4.887	4.057	2.576	1.711	2.985	6.017	3.222	3.675
C (years)	2006	2006	2007	2010	2007	2007	2011	2005
R^2	0.8859	0.9208	0.9098	0.7888	0.6528	0.8709	0.9493	0.9603
SSE	451.87	424.74	437.01	325.51	459.33	558.65	278.94	81.56
RMSE	2.4069	2.3335	2.367	2.0428	2.4267	2.6762	1.9033	1.0292

Table 4.11 - Fitting parameters of the levelling movements of the Paso Nuevo dam. Stations P1 to P8 corresponding to blocks 3 to 10.

Plot of the movements and of the fitting curves is presented in figure 4.10. From the fitting curves it is easier to evaluate the uniformity of parameter C, that is comprised between 430 and 496 months. It is also easy to identify the much more pronounced variability of the parameter P (that goes from 1.71 to 6.02). According to the models, some blocks have already entered the stabilization parts (stations P1, P2, P5, P6, P8), while blocks P3, P4 and P7 seem to still have to start that phase. The different behaviour of the blocks is attributed to the presence of two types of concretes, the 1st of which contains aggregates far more reactive, and it present in different proportions in each block (Aguado et al., 2020).

DIFFERENCE	B1	B2	B3	B4	B5	B6	B7	B8
B	0.0	0.0	-2.7	-1.2	1.1	0.0	-14.6	-7.6
C	0.0	0.0	-0.5	-1.4	1.1	0.0	-6.6	2.2
P	0.0	0.0	3.5	0.7	-1.6	0.0	19.3	9.3
R^2	0.0	0.0	0.0	-0.1	0.0	0.0	0.1	0.0
SSE	0.0	0.0	0.2	0.2	0.0	0.0	-2.6	0.0
RMSE	0.0	0.0	-0.5	0.1	0.0	0.0	-2.0	-0.6

Table 4.12 – Differences of the parameters of the fitting model of the Paso Nuevo dam levelling movements, expressed in %.

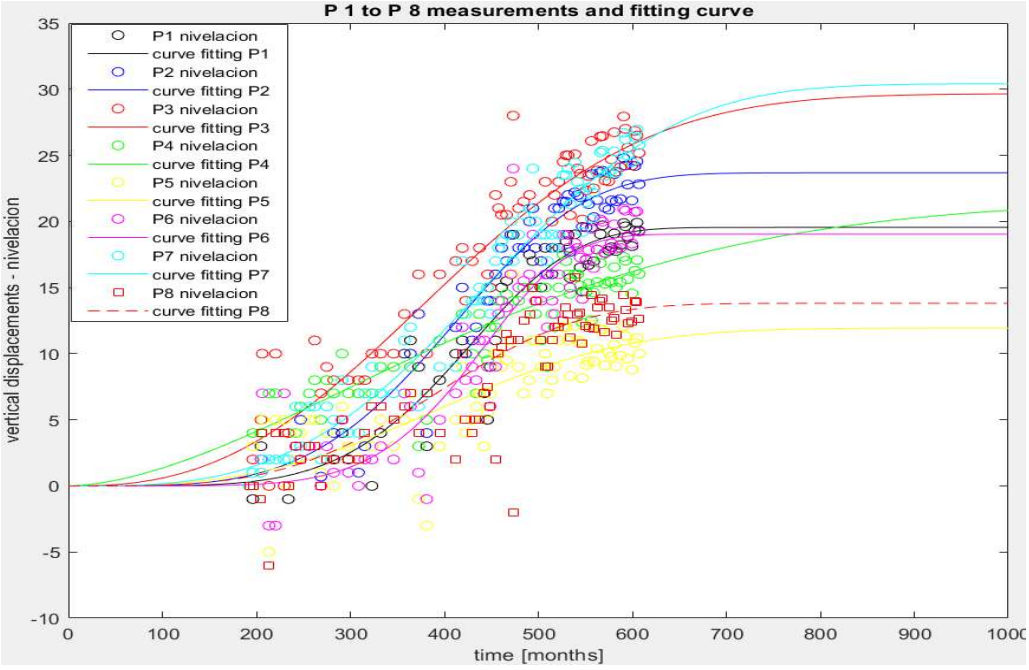

Figure 4.10 - Paso Nuevo dam levelling data and fitting curves of the 8 measurements stations.

4.3.4.2 Collimation

Collimation movements of Paso Nuevo dam are registered with inverted horizontal reference system. Hence in this case the movements towards upstream face have negative sign. Here the conditions A<0 and A=0 lead to a slightly higher difference in the parameters of the fitting. Anyway, the difference is still contained and allow the hypothesis of A=0, and permit to obtain good fitting results, in terms of parameters and error statistics, and goodness-of-fit results.

A = 0	P1	P2	P3	P4	P5	P6	P7	P8
A	0	0	0	0	0	0	0	0
B	93.53	45.08	47.38	61.68	60.22	54.6	62.68	47.83
C	596.9	476.1	484.4	529.6	474.7	456.6	481.6	404.6
P	3.439	3.868	4.066	5.285	3.883	4.341	3.922	5.066
C (years)	2019	2009	2009	2013	2009	2007	2009	2003
R^2	0.987	0.9371	0.9384	0.966	0.9736	0.9721	0.9775	0.9585
SSE	438.43	1114.2	1215.5	1023.9	804.36	831.8	719.3	1032.8
RMSE	2.3708	3.7795	3.9476	3.623	3.2113	3.2656	3.0563	3.6864

Table 4.13 - Parameters of fitting of the collimation movements of Paso Nuevo dam.

DIFFERENCE	B1	B2	B3	B4	B5	B6	B7	B8
B	-9.9	-15.8	-22.9	-3.0	-17.4	-17.1	-23.7	-2.6
C	-4.2	-4.4	-7.6	-0.6	-2.8	-2.2	-6.9	0.8
P	6.5	24.2	33.2	3.4	27.2	31.6	33.9	6.0
R^2	0.0	0.0	-0.2	0.0	-0.4	-0.4	-0.3	0.0
SSE	-0.2	0.2	2.6	1.1	17.2	18.3	16.8	-0.1
RMSE	-0.7	-0.6	0.6	-0.1	7.6	8.1	7.4	-0.7

Table 2.14 - Differences of the parameters of the fitting model of the Paso Nuevo dam collimation movements, expressed in %.

The entity of the movements is quite regular through the blocks, being comprised between 45 mm and 62 mm. Only station P1 seems an exception since its magnitude is considerably higher, despite being a smaller block compared to the central ones.

Parameter C ranges from 456 to 529 months, showing that the phenomenon of expansive reactions is quite generalized through all the dam's body. Exceptions, due to other reasons, are found in P1 and P8 stations, in which C is quite higher in P1 case, and quite lower in P8 case. Parameter P floats in the range 3.4 to 5.2.

Fitting operation is guaranteed to be very reliable by R^2 that in the smallest cases is equal to 0.937. Errors parameters are higher than the ones found for the other dams. This may be partly due to the lower number of measurements available (81 measurements in 35 years), partly by the scatter of data. In figure 4.11 the horizontal movements and the fitting curves are plotted.

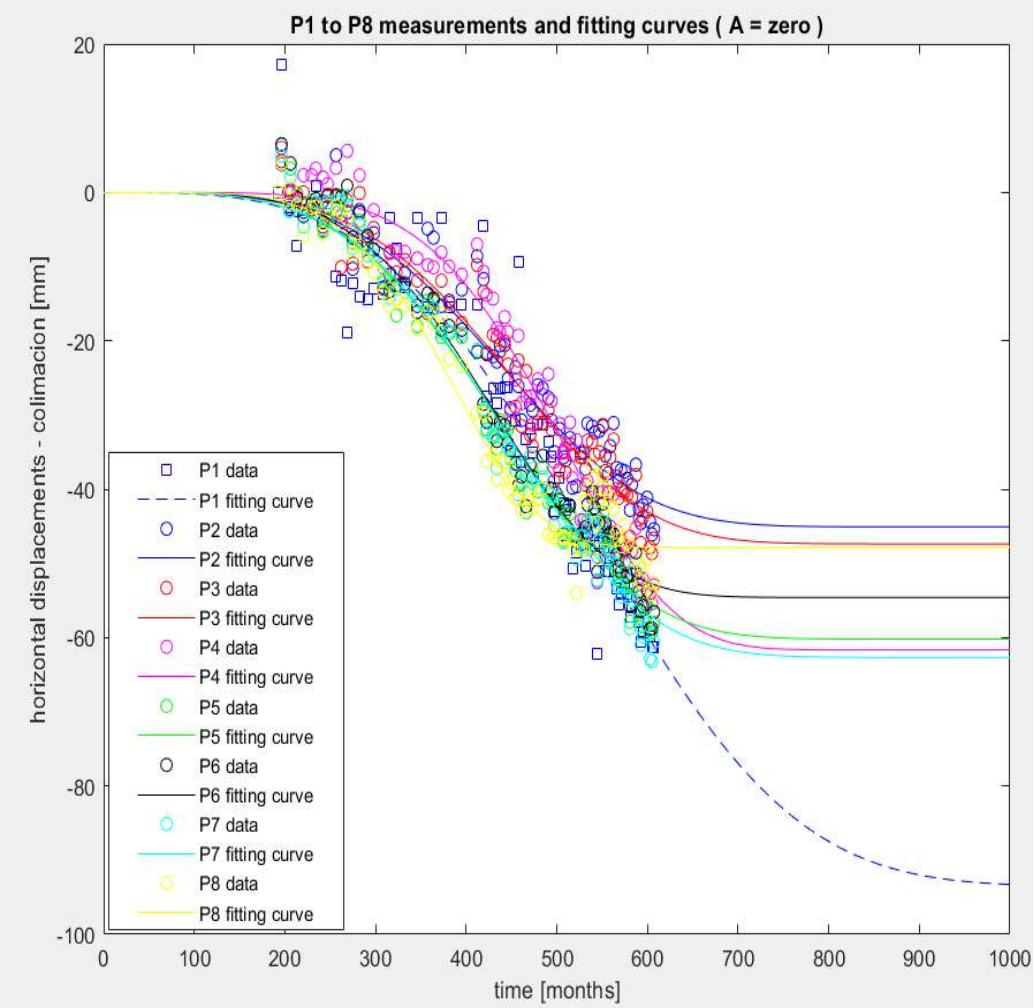

Figure 4.11 - Movements data and fitting curves of the collimation movements of the Paso Nuevo 8 blocks. Negative movements are towards upstream face of the dam.

In the table 4.15 are reported the average differences of the parameters obtained in the two cases, A<0 and A=0, for both the levelling and collimation movements. It is important to remark that when forcing the parameter A=0 we are accepting slightly different results. This choice is translated in acquiring lower values of B (on average 3.1% lower in the case of levelling movements, 14% lower in the collimation case), lower values of C, higher values of P (on average 3.9% higher for the levelling, 20.7% for collimation). In the case of levelling movements, R^2 values on average don't change and error parameters are slightly reduced. The opposite happens in the case of collimation movements, where the case A=0 lead to faintly lower R^2 and higher errors. Generally, when passing from A<0 to A=0, parameters B and C tend to decrease and parameter P increase. This results in fitting curves that reduce the amplitude pf the movements and the time in which the inflection point is manifested, but a steeper curve, i.e. reactions proceed faster and provoke displacements in less time (than in the case A<0).

Passing from A<0 to A=0	Average variations of fitting parameters of LEVELLING movements	Average variations of fitting parameters of COLLIMATION movements
B	-3.1	-14.0
C	-0.6	-3.5
P	3.9	20.7
R^2	0.0	-0.2
SSE	-0.3	7.0
RMSE	-0.4	2.7

Table 4.15 – Average variations of fitting parameters of Paso Nuevo dam, when passing from A<0 constraint to A=0 constraint. Averaged with respect to all the 8 blocks.

In figure 4.12 are reported the parameters B, representative of the maximum displacements, of the Paso nuevo dam, and the height of each block. It is quite clear that no relations seem to exist between the height of the blocks and its vertical or horizontal movements.

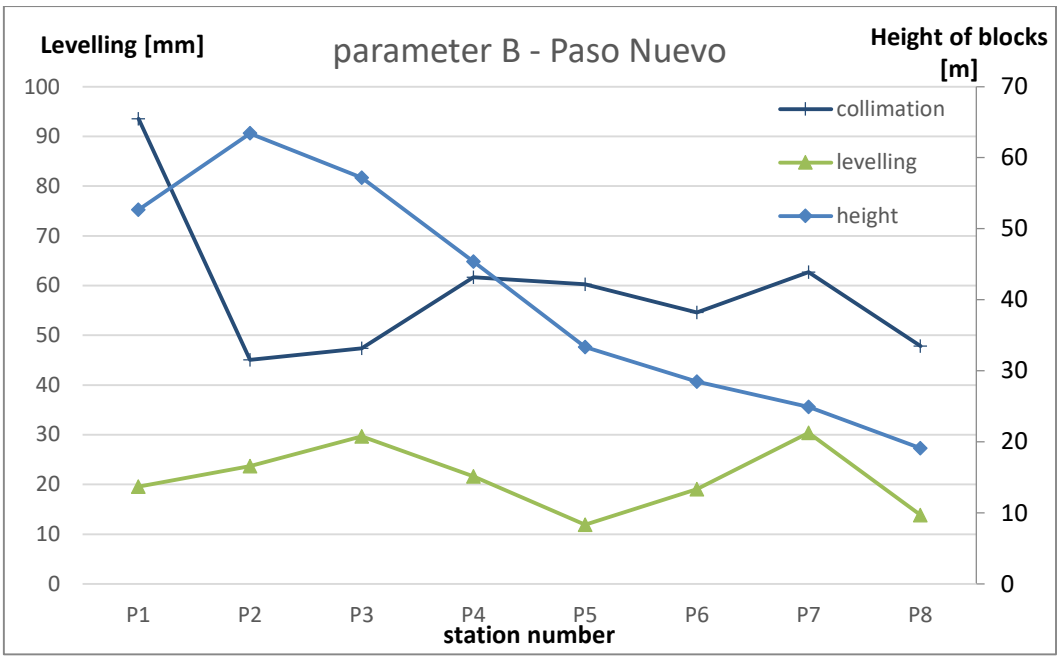

Figure 4.12 – Paso Nuevo dam. Parameter B of the vertical and horizontal movements model, and height of the blocks.

4.4 Robustness analysis

One of the aspects there has been questioned in this master thesis is the robustness of the exponential adjustment proposed by Aguado towards the levelling and collimation movements registered in the four investigated dams. In these two cases, robustness is meant as the capability of the model to extrapolate and infer future movements from the measured ones, even when few measures are available (or only parts of them) or when they show a non-negligible degree of scatter or when outliers are present in significant quantities, and still assuring accurate interpretation and prediction results.

The robustness of the model has been checked by splitting the measurements data, and applying the model to the split portion of data, and comparing if the parameters obtained in this way were still able to appropriately interpret the trends of levelling and collimation movements. The comparison is held between the parameters of the model that fitted all the data sets, and the parameters that fitted portions of them, for

example the central or the last parts. If the two sets of parameters were found to be similar, the robustness of the model would have been further confirmed.

Moreover, if the model accurately describes portions of data, i.e. finds out the same parameters evaluated with the whole set of data, it means that we could use this model with an appreciable degree of certainty also to the situations in which we do not have all the data set, as it turns out to be the case of Toràn dam. This confirmation would have been a great results and could be usefully applied in all the situations similar to Toràn dam.

In addition to this robustness checking procedure, also robust method that are implemented inside Matlab have been used. They are described in the next chapter.

4.4.1 Robust methods

The robust methods that are used, in addition to the splitting of the data in different smaller data sets, are the LAR and the Bisquare methods, both found in the Matlab environment. They are mainly based on the assumptions that the response errors follow a normal distribution (with mean equal to zero) and the extreme values are rare, but still occurring. If the mean of the errors is zero, then the errors are purely random. If the mean is not zero, then it might be that the model is not the right choice for your data, or the errors are not purely random and contain systematic errors (Matlab).

Least square fitting has the disadvantage to be sensitive to outliers, being their squared residual magnified, and these methods work to minimize the influence that outliers bring on to the fitting procedure, which accuracy could be affected.

The LAR method (Least Absolute Residuals) find a curve that minimizes the absolute the absolute difference of the residuals from the curve, instead of the squared one.

The Bisquare method works with the sum of the squares and assigns to them a weight. The weight is given to a datapoint according to its distance from the fitting curve, such

that the farther is the point from the curve, the lesser weight is assigned to it. Therefore, points very far from the bulk of the data gets low or zero weight.

Despite being the Bisquare method generally preferred, in most cases in the fitting operation, the LAR method has been implemented, since that data of the dams' movements used to contain few outliers. Nevertheless, when few data wew available, for example when fitting a portion of data, the Bisquare method was used.

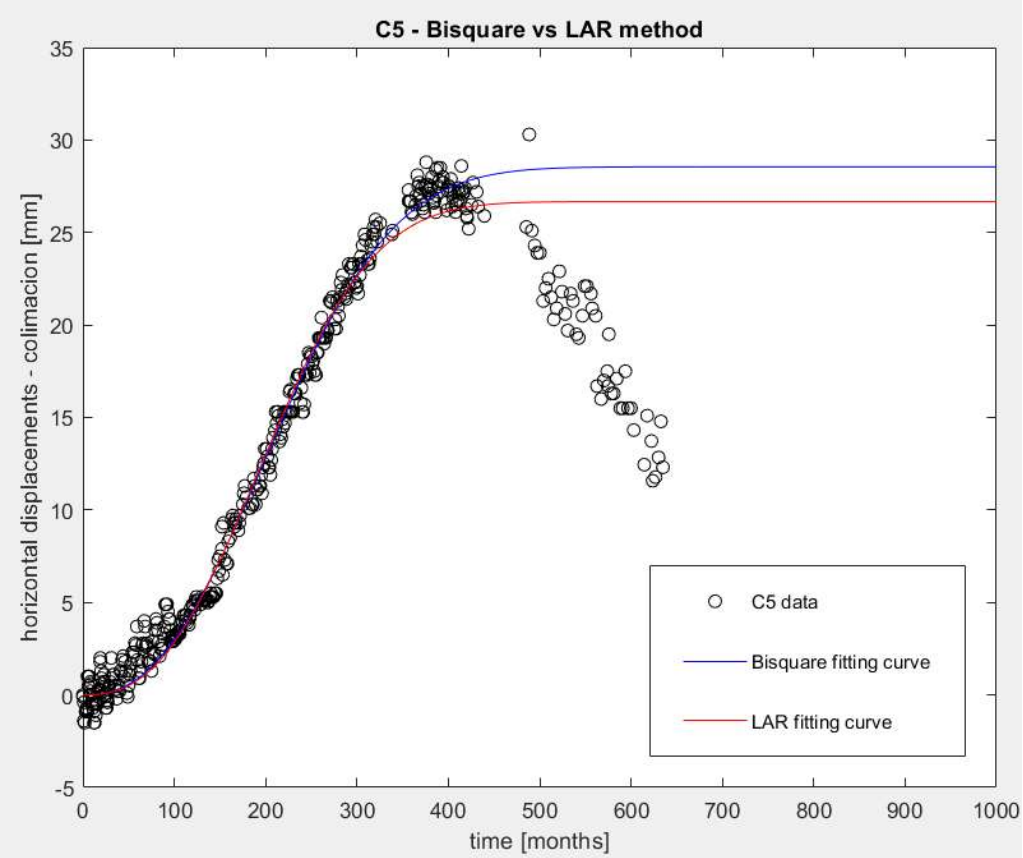

Figure 4.13 - Difference of fitting between the Bisquare and the LAR robust methods.

In picture 4.13 one can appreciate the difference between the two robust methods of fitting of the same data, in this case the collimation movements of station 5 of Tavascan dam. This example shows a significative difference since such data trend of decreasing is observed in only one case. The Bisquare method assigns a lower weight to the data far from the curves and it results is a higher B parameter.

4.4.2 Data splitting and modelling

As mentioned before, the data splitting of the measurements was carried out in order to test the model in the regards of its robustness to prediction errors and misinterpretation of data. Data do not cover all the lifetime of the dam (except the Tavascan case) but only a section of it. In addition, the density of measurements does not have an equal distribution along the time: usually the first years have more measurements per year than the last part.

Data have been split in 4 different ways:

- In 3 parts, each part having the same number of measurements
- In 3 parts, each part covering the same amount of time
- In blocks of measurements spanning a time window of 10 years
- In blocks of measurements spanning a time window of the first 20, 30, 40 years (and 50 years as well when available)

As an example in tables 4.16, 4.17, 4.18, 4.19 are reported the schemes of how the data have been divided, in the case of Paso Nuevo dam (81 measurements), that present the same number of measurements both for levelling and for collimation, for all the 8 measurements stations. The other divisions are attached in the Annex 1 and follow the same rules.

PASO NUEVO dam	number of measurements	years of measurements	years of measurements	measurements/year
blocks 1 to 8	81	1984-2018	35	2.3

Table 4.16 - Paso Nuevo number and years of measurements.

3 PARTS, same number of measurements	number of measurements	years	number of years	measurements/year
block 1 to 8	81	1984-2018	35	
part 1	27	1984-2001	18	1.50
part 2	27	2002-2012	11	2.45
part 3	27	2012-2018	7	3.86
3 PARTS, same number of years				
block 1 to 8	81	1984-2018	35	
part 1	20	1984-1995	12	1.67
part 2	22	1996-2007	12	1.83
part 3	39	2008-2018	11	3.55

Table 4.17 - Data splitting of Paso Nuevo measurements, in 3 parts, in two different ways.

blocks of 10 years	number of measurements	years	number of years	measurements/year
block 1 to 8	81	1984-2018	35	
first 10 years	19	1984-1993	10	1.90
second 10 years	14	1994-2003	10	1.40
third 10 years	32	2004-2013	10	3.20
fourth 10 years	16	2014-2018	5	3.20
blocks of first 20 and 30 years				
block 1 to 8	81	1984-2018	35	
first 20 years	33	1984-2004	20	1.65
first 30 years	65	1984-2014	30	2.17

Table 4.18 - Data splitting of Paso Nuevo measurements, in blocks of 10 years and in blocks of the first 20 and 30 years.

In the case of Paso Nuevo each block of measurements was divided four times, for a total of 12 portions of data to be fitted. Therefore 96 fitting operation were performed for the levelling movements and other 96 for the collimation. In the case of Tavascan dam, even more combinations were realized being longer the data set. All these operations resulted to be quite time-consuming.

The Toràn dam instead was not split, because its monitored movements' data cover yet few data and the first measurement has been recorded 36 years after the dam commissioning. Hence there seemed to be no need to further splitting data for testing the robustness of the model, being the whole recording already a part of the dam lifetime displacements.

Some results of the data splitting are reported here by way of example: in tables are reported the values of the parameters of the fitting of the dam, together with the goodness-of-fit results. In the figures are plotted the recorded movements and the fitting curves, of both the whole data set (yellow squares and curves) and the portions (black circles and curves). Other results are reported in the Annex 2.

	Number of measurements	Years	Number of years	Measurements /year
Block 3 - Tavascan	497	1966-2018	53	
first 10 years	158	1966-1975	10	15.80
second 10 years	105	1976-1985	10	10.50
third 10 years	104	1986-1995	10	10.40
fourth 10 years	78	1996-2005	10	7.80
fifth 10 years	52	2006-2018	13	5.20

Table 4.19 – Splitting of the collimation measurements of station C3 of Tavascan dam, in blocks of 10 years.

In table 4.20 are reported the values of the parameters that fit portions of data: in this case the collimation movements of the C3 station of Tavascan data. Parameter A is fixed to 0.

From results of the fitting and from the plotting of such fits in the figure 4.14, one can conclude that in some cases the fit is poor and have a low R^2 value (e.g. the last portion of data, $R^2 = 0.005$), in other cases the fitting is better (e.g. second part of data, $R^2 = 0.94$).

A = 0	first 10	second 10	third 10	fourth 10	fifth 10
A	0	0	0	0	0
B	4.454	20.84	37.63	32.11	29.79
C	89.87	226.9	355.4	307.5	302.1
P	3.124	2.719	1.927	2.095	3.139
R^2	0.6622	0.9435	0.905	0.6641	0.0051
SSE	214.02	69.13	95.99	78.91	104.54
RMSE	1.1751	0.8232	0.9749	1.0257	1.4607
Robust	LAR	LAR	Bisquare	Bisquare	Off

Table 4.20 – Parameters of fitting of the blocks of 10 years of the collimation measurements of C3 station of Tavascan dam. Plotted in figure 4.14.

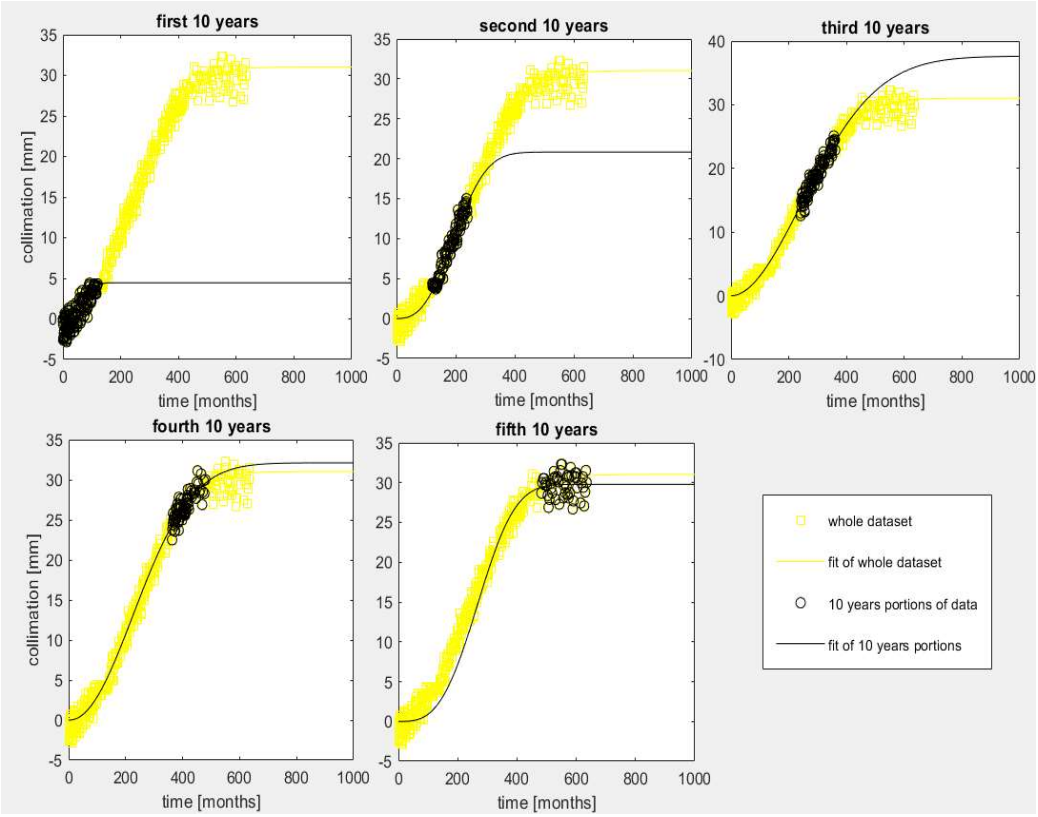

Figure 4.14 - Tavascan dam, collimation movements, block 3. The yellow data are referred to the whole dataset, while the black to the portions of data.

In table 4.21 are reported the differences of the fitting model parameters of portions of movements data (C3 collimation, Tavascan), with respect to the parameters of the model fitting the whole data set (in all cases A=0). The first 10 years of measurements

(1967-1975) clearly are not able to represent the whole data set, in terms of parameters B (85% lower), C (70% lower, and P (42.5% higher), despite having an acceptable R^2=0.66 value.

The second portion of data (1976-1985) shows the highest degree of correlation between monitored data and models (R^2=0.94). Nevertheless, still considerable differences are present between parameter values of this portion and the ones of the whole data set, as can be seen from the table 4.21. Similar considerations can be done for the third portion of data (measurements from 1986-1995). Parameters change in range 12.1%-32.8%.

DIFFERENCE	first 10	second 10	third 10	fourth 10	fifth 10
B	-85.6	-32.8	21.3	3.5	-4.0
C	-70.1	-24.4	18.4	2.5	0.7
P	42.5	24.0	-12.1	-4.5	43.1
R^2	-33.1	-4.7	-8.6	-32.9	-99.5
SSE	-64.3	-88.5	-84.0	-86.9	-82.6
RMSE	6.6	-25.3	-11.6	-6.9	32.5

Table 4.21 - Differences of parameters of the fitting the portions of the data, with respect to the all data set (in both cases A=0).

Instead the last two portions of data, 4th and 5th parts (i.e. measurements in years 1996-2005 and 2006-2018), in spite of showing lower R^2 values (R^2=0.66 and R^2=0.005 respectively), they are able to accurately fit all the measurements. In these two cases parameters B and C and very similar to the ones from the model that fits all the data: maximum 4% of variation is registered. Parameter P instead is similar (-4.5%) in the case of the 4th portion, much less in the 5th portion (+43%) with respect the whole data set. This result is obtained thanks to the constraint of A=0. Without fixing this value of A, these results wouldn't be obtained, since the last part of the data are considerably in the stabilization part (horizontal trend), and quite scattered, as depicted in figure 4.15.

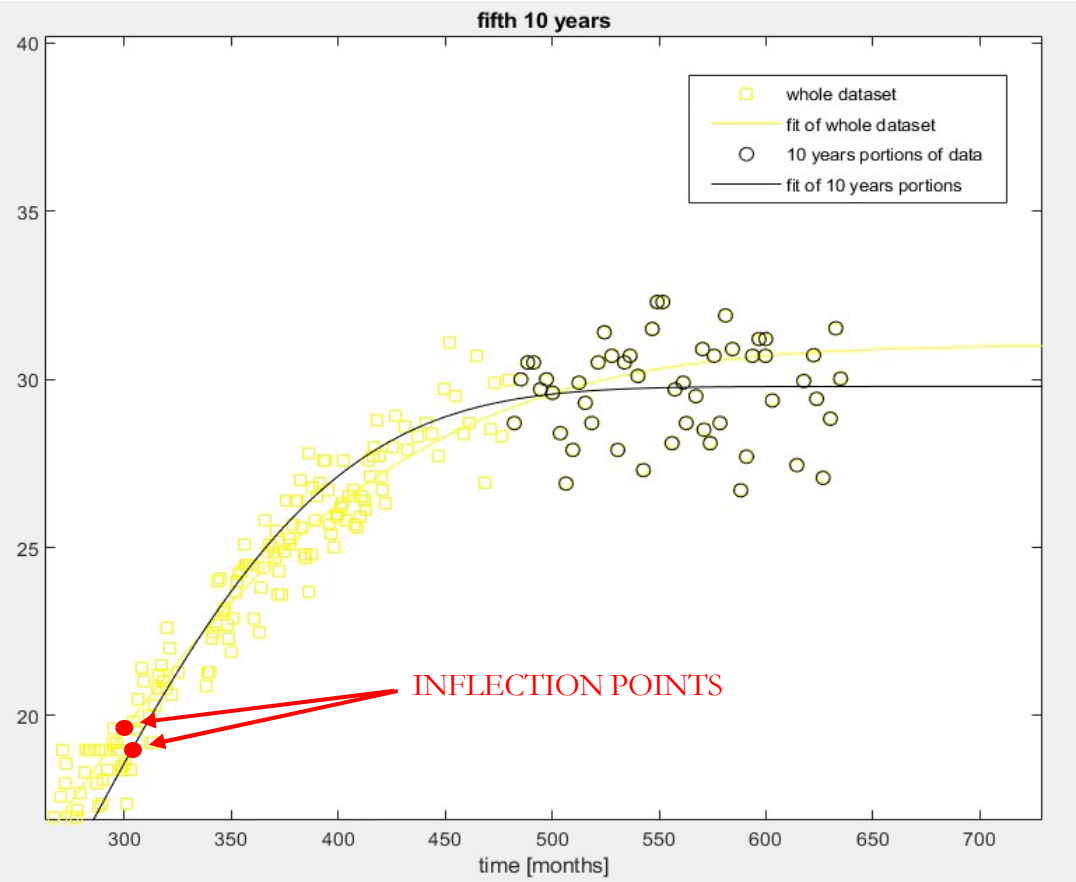

Figure 4.15 - Fitting the last portion of the C3 collimation data of Tavascan movements (years 2006-2018).

Summing up, the results obtained in the splitting of the horizontal movements of the station C3 of Tavascan dam, in blocks of 10 years, can lead to the following conclusions:

- The first 10 years express the initiation of the phenomenon and are not able to identify the trend of the movements as the model does. The parameters obtained are very different from the parameters of the model that fits all the data.

- The central portions (2nd and 3rd parts of data) have the best fitting results in terms of accuracy of the model (R^2=0.944 and R^2=0.905), because this part of the data is in straightforward development. The third block of 10 years of

measurements have been fitted by a model that resemble the whole data set better than the second block, that underestimates the movements. Both blocks (figure 4.14) are parts of the development phase (2nd phase). The third 10 years set of measurements actually contains the inflection point (of the whole data set), that is at 300 months and hence is able to adequately reproduce the fit of the whole data set.

- The last part of the data (figures 4.14 and 4.15) represents the stabilization phase (4th and 5th blocks). Thanks to the setting of the parameter A=0, they are able to satisfactorily fit the data as the model of the whole data. Precision is lower (especially in the very last block R^2=0.005) but B and C parameters are very similar. The best fitting is reproduced by the 4th portion of data, i.e. measurements from 1996 to 2005, where the starting of the stabilization phase is encountered.

- The goodness-of-fitting of the adjustment of portions of data is always lower than in the adjustment of the whole data set (R^2 always decrease). The SSE, being a sum of residuals, always decrease, because the sum is done over less measurements. The RMSE error parameter decreases in the fitting of the central portions (2nd, 3rd and 4th parts), increases in the fitting of the starting and in the ending portions (1st and 5th parts).

- In order to reconstruct the behaviour of the movements trend in the first years, and so to evaluate the amplitude (parameter B) and the inversion of trend (inflection point – parameter C) of the whole movements, it is acceptable to adjust only the last part of the movements data and to fix the parameter A=0. In this way parameter B and C can be estimated with accurate results, parameter B with slightly different results. This procedure will be used in the case of Toràn dam, where only the last part of the measurements, corresponding to the stabilization phase, is available.

The same procedure is repeated for the all measurements stations, for all the dams, in order to understand if the interpretation provided by modelling the movements of the station C3 of Tavascan (collimation data) could be extended to all the other cases, and hence the robustness of the method can be confirmed. By way of example, levelling measurements of block B3 of the Graus dam are split in 3 parts, fitted and compared.

In table 4.22 are reported the splitting operations of the block B3 movements in 3 parts having the same number of years, and then in 3 parts having the same number of measurements. As can be seen the last measurements data (3rd part) are less dense.

GRAUS – BLOCK 3	number of measurements	years	number of years	measurements/year
Same number of years	252	1981-2018	38	
part 1	111	1981-1993	13	8.54
part 2	97	1994-2006	13	7.46
part 3	48	2007-2018	12	4.00
Same number of measurements	252	1981-2018	38	
part 1	84	1981-1990	10	8.40
part 2	84	1991-1999	9	9.33
part 3	84	1999-2018	20	4.20

Table 4.22 – Block 3 of Graus dam: split data set in 3 parts in two different ways.

In tables 4.23 are reported the parameters of the fitting of the three parts of the data. Parameter A, as done previously, has been set to 0, in accordance to the results obtained until now. Parameters B, C and P and statistics of the goodness-of-fitting are reported. Then in tables 4.24 are reported the differences of the parameters of the fitting of portions of data, compared to the fitting of the whole data set.

Same number of measurements	B3 - part 1	B3 - part 2	B3 - part 3
A	0	0	0
B	673.2	48.14	125.5
C	584.5	310.2	461.3
P	4.268	4.044	3.104
R^2	0.8956	0.9882	0.9992
SSE	118.73	41.12	31.67
RMSE	1.2107	0.7125	0.6372
Robust method	LAR	LAR	LAR

Same number of years	B3 - part 1	B3 - part 2	B3 - part 3
A	0	0	0
B	37.5	149.6	136.7
C	281.6	495.1	486.3
P	4.622	3.132	2.809
R^2	0.9624	0.9873	0.9958
SSE	148.52	214.52	30.24
RMSE	1.1727	1.5107	0.8485
Robust method	LAR	Bisquare	LAR

Table 4.23 - Parameters of fitting of the 3 parts of the Graus B3 station levelling movements. Parameters obtained with same number of measurements on the left, same number of years on the right. Plotted in figure 4.16.

Same number of measurements	B3 - part 1	B3 - part 2	B3 - part 3
B	469.1	-59.3	6.1
C	31.4	-30.2	3.7
P	28.1	21.4	-6.8
R^2	-10.4	-1.2	-0.1
SSE	163.5	-8.7	-29.7
RMSE	182.9	66.5	48.9

Same number of years	B3 - part 1	B3 - part 2	B3 - part 3
B	-68.3	26.5	15.6
C	-36.7	11.3	9.4
P	38.7	-6.0	-15.7
R^2	-3.7	-1.3	-0.4
SSE	229.6	376.1	-32.9
RMSE	174.0	253.0	98.2

Table 4.24 - Differences of the parameters of fitting of the 3 parts of B3 (Graus levelling) with respect to the whole data set. The smallest variation is observed for the third part, in terms of parameters and in terms of goodness-of-fit results (errors).

The two different way of splitting the data in 3 parts lead to quite diverse results between them. One reason of this is the fact that data are not homogeneously distributed in time. While in the first years of measurements a lot of movements were recorded (8-9 measurements per year), in the last years, i.e. from around year 2000, less measurements were taken (3-4 measurements per year). Hence, except the last part of data, when in one case a parameter is overestimated, in the other case it is underestimated. The split data models are plotted in figure 4.16.

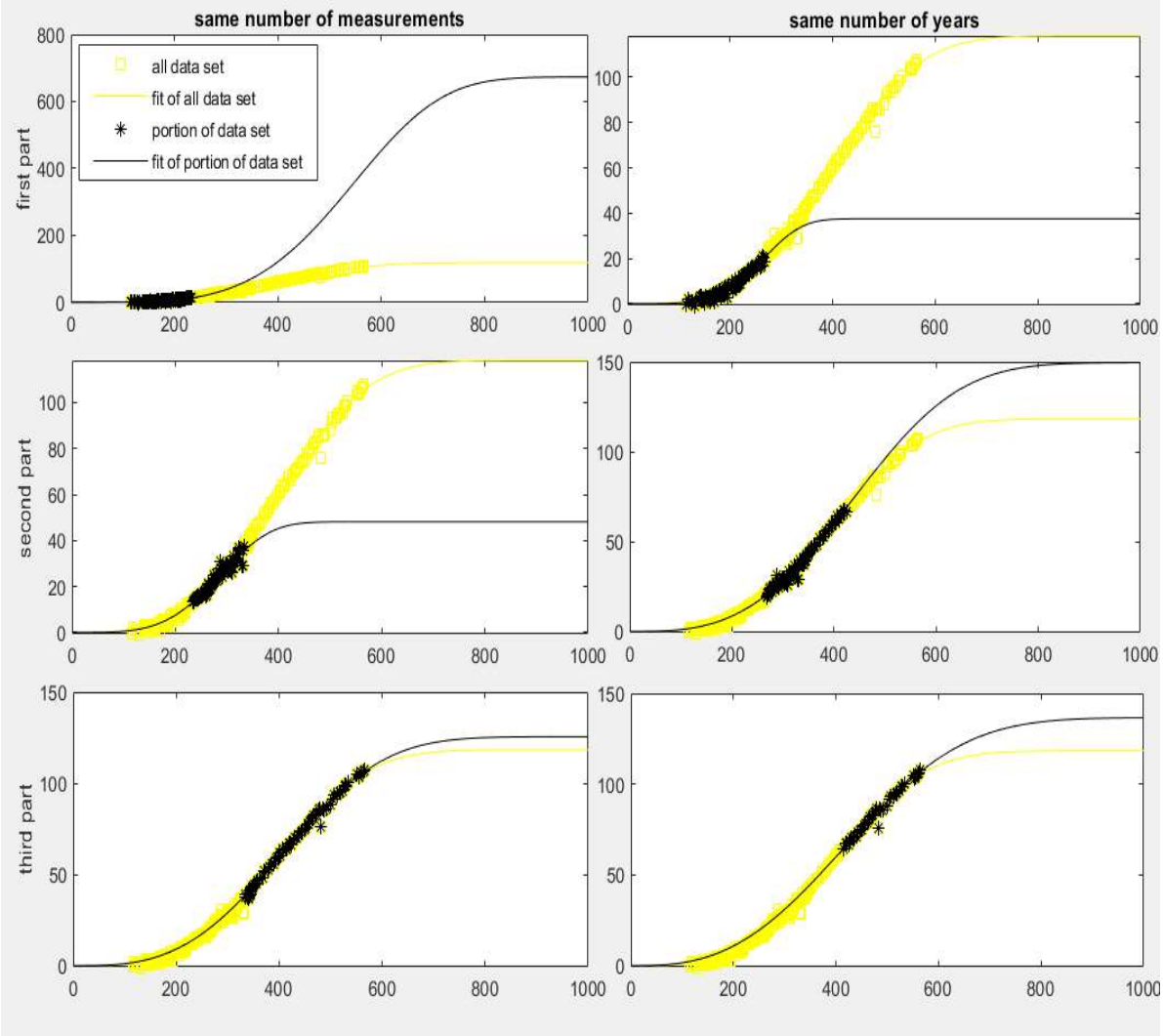

Figure 4.16 – Graus dam, levelling movements, block 3. The yellow data are referred to the whole dataset, while the black to the portions of data. In the left column the data are divided in 3 parts having the same number of measurements (84), while in the left column each part of the data covers the same amount of time (13 years).

These conclusions can be drawn from the results of the parameters of fitting in the two cases and their differences, and from the plots reported in figure 4.16:

- The models that fit the first part of data are not able, as happened in the case of Graus dam, to satisfactorily represent the whole data trend. In the case with same number of measurements (1981-1990, left column), it clearly overestimates parameter B (469% higher) and parameter C and P (31% and

28% higher), as can be seen in figure 4.16 as well. In the case of the same number of years splitting (1981-1993, right column), the parameters are underestimated, except parameter P, with respect to the parameters of the model of the whole data. This initial phase in fact has no information on the degree of development that the measurements will assume in time, as happened in Tavascan case.

- The models that fit the central portion of data show slightly better results compared to the whole data set fitting. The case with the same number of years (1994-2006, right column) is closer to the whole data set fitting than the case with same number of measurements (1991-1999, left column). The former case in fact contain a bigger amount of data (97 against 84) and it is closer to the inflection point of the whole data set (C=444 months, year 2008), leading to a better fit.

- The models that fit the last portion of data are the best fit in terms of similarity with the fit of the whole data set. This is due to the fixing of parameter A to 0. The case with same number of measurements (left column) this time shows better results, being the fit very close to the whole dataset one: here more measurements are available (84 against 48) and longer time interval is covered (1999-2018 against 2007-2018). Parameters B and C increase slightly (6.1% and 3.7%) while P decreases (-6.8%), with respect to the model of the whole dataset.

- Adjusting the last part of data (3rd parts) with the same model lead to the confirmation of the correctness of fixing A=0. By doing so, also the previous measurements are correctly estimated. This procedure can be applied to the Toràn dam to hypothesise the trend of the movements that have not been recorder, based on the last part (that has been recorded, and to fixing A=0). In addition to this, other assumptions have to be made, and they will be done in the regards of other parameters of the model, as will be done in next chapter.

- Regarding the goodness-of -fit parameters, R^2 is higher when fitting the first part of data, lower when fitting the last one. Similarly, errors SSE and RMSE are bigger in the fitting of the first part. Moreover, in general when fitting a portion of data, when when parameter B and C increase, then parameter P decrease, and viceversa when B and C decrease, P increases.

The results of splitting the data in blocks of measurements spanning a time window of the first 20, 30, 40 years lead to an additional confirmation that the more data is available, the better the goodness-of fit results and statistics are. In these cases, the parameters of the fitting models obtained are even more similar to the parameters of the whole data set fitting. Other data obtained in this part is reported in Annex 2.

As a result of this splitting operation, the major goal reached is the ability of the model to accurately interpret and estimate the trend of the movements data when only the last part of the data is used, by setting appropriately the parameters (e.g. A=0). This fact can be of great help in all the circumstances where only tardive measurements are monitored, coinciding with the stabilization part of the curve, as could be the case of Toràn dam, where for the first 35 years measurements of movements where not recorded.

4.5 Toràn dam

The parameters obtained fitting the movements data of the Toràn dam are acquired using the available data, that cover a range of time that is quite short. Being the dam built in 1964, the registered movements covering the years 2000-2018, are liable of not being sufficient for a decent fitting operation. The parameters that would result could be highly misleading, and no measure of accuracy could be performed. It is therefore necessary to formulate additional hypothesis on the dam whole behaviour.

Observing the Graus dam movements, it is clear to see that some blocks show magnitude of displacements considerably higher than others, despite having a trend

of movements that is quite common for all the blocks. This fact can be as well depicted by the values of the fitting parameters: while C and P parameters assume values that are slightly varying and fall inside a small region of variability (as can be seen from figures 4.17 and 4.18), the same can't be said for the parameter B, as one can see in figures 4.4 and 4.5.

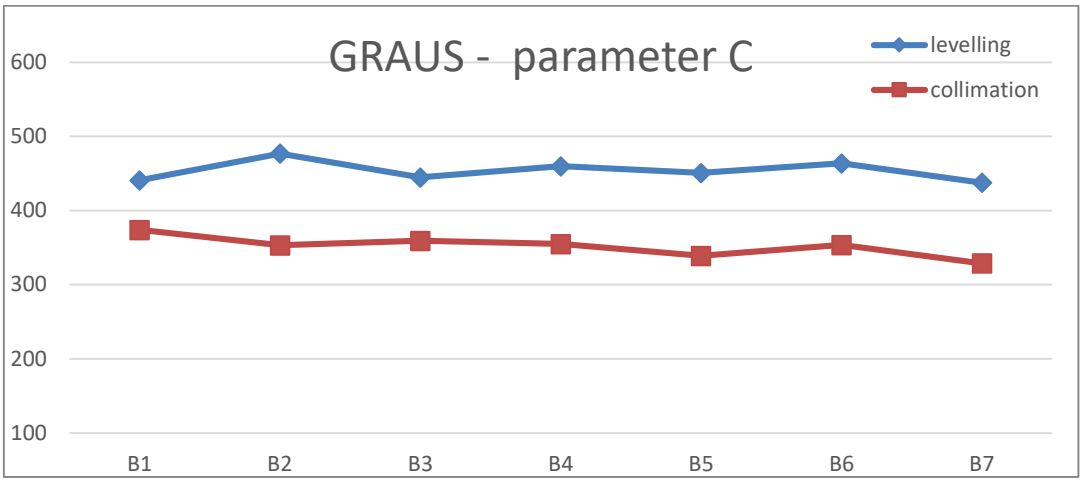

Figure 4.17 - Parameters C of the 7 blocks measurements stations of the Graus dam. Both levelling (blue) and collimation (red).

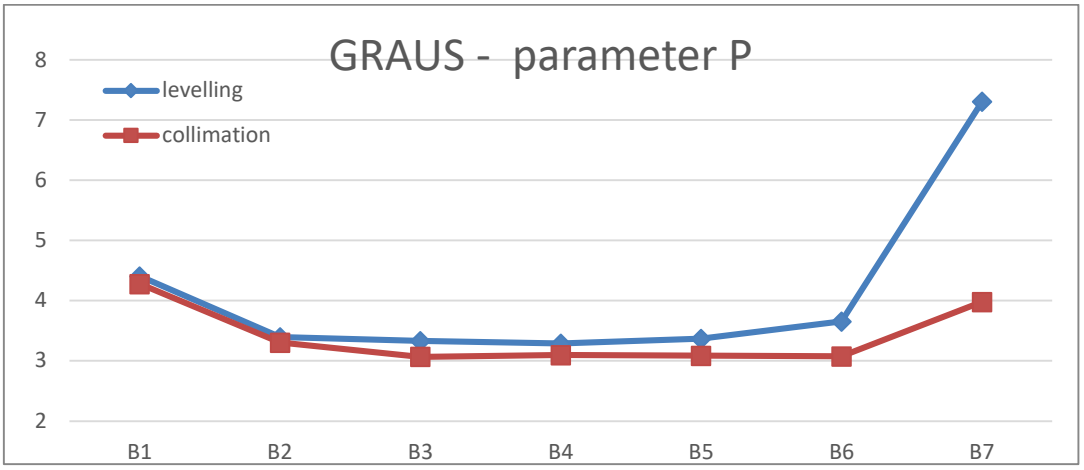

Figure 4.18 - Parameters P of the 7 blocks measurements stations of the Graus dam. Both levelling (blue) and collimation (red).

All these parameters have been obtained fixing the parameter A = 0. Parameter C ranges from 430 to 480 in the case of levelling movements, and from 330 to 370 in

the case of collimation movements. It is immediate to see the more quickly development of the collimation movements. This is underlined as well by the parameter P, that runs between 3.2 and 3.6 in the case of the levelling and between 3.1 and 3.3 for the collimation, with some exception in the cases of the lateral blocks' movements. In fact, in these lateral blocks, the presence of abutments and their geometric features could constitute a sort of constraints in the movements. The displacements of marginal blocks 1 and 7 result to be much lower than the others, nevertheless their C and P parameters didn't differ significatively, sign that the same expansive phenomena are going on.

These data could lead to think that the expansive phenomena that hit the dam are generalized phenomena, with the existence of local specificities, that could be thought as non-homogeneously distributed in the whole body of the dam. Same speed of reactions and expansions development (similar C and P) means same phenomenon inside different blocks. Different B parameters (total entity of displacement) could mean that each block experience same phenomenon but with different amplitude, due to the geometry of the block or to other reasons, e.g. local concentrations of reactive aggregates and oxidizing agents.

Now, observing the last part of the Toràn dam, one can see that their trend is very similar to the last part of the Graus dam movements, that were analysed in the robustness section (chapter 4.3). Given the mature of the expansive phenomena and the characteristics the influence them, and given the similarity between the two structures (they are made with the same material -concrete- and with the same structural scheme -gravity dam-), and being the two structures also similar in dimensions (also comparing the blocks that compose the dams), one could extend the parameters (or some of them) of the Graus dam, that are well established, to the Toràn dam, that instead could not be otherwise be estimated.

Parameters P and C are chosen to be extended from the Graus dam to the Toràn dam, to able to estimate the remaining parameters A and B, that catch the entity of the movements. This fact is justified if one thinks that C and P parameters are related to

the speed of the movement development, that in turn may be related to the speed of the ISA and ASR expansive reactions. These parameters could be in common since the expansive phenomena have been reported in both dams. On the other hand, the parameters A and B are representative of the amplitude of the movements and they are more related to the geometry of the blocks, so being this characteristic dam-dependent, so are these parameters.

In the next chapter, such argument is applied to the Toràn dam, in order to be able to estimate the development of the evolution of its displacements in the whole lifetime.

4.5.1 Parameters estimation

The main assumptions for the estimation of the trend of the Toràn dam displacements, both in the horizontal and vertical direction, are the following:

- The degradation phenomena are identified to be the Internal Sulphate Attack and the Alkali-Silica Reaction, and they produce expansions that could be seized at the macroscopic level as levelling and collimation movements.

- The available measured displacements are the ones taken during the years 2000-2018, and being insufficient for a regression analysis, other hypothesis has to be formulated.

- The available displacements, being measured quite lately with respect to the dam commissioning (1964), are representative of the stabilization part of the expansive movement trend. This is evident in both direction of the movements.

- The similarity of the last part of the Graus movements with the Toràn movements, and the other similarities explained in the previous chapter, led to formulate as hypothesis of behaviour that the speed of reactions is similar for the whole blocks, being the deterioration mechanism a generalized and

diffused mechanism. This will be translated in the adoption, foe the Toràn dam, of the same parameters C and P or the Graus dam. Parameters are chosen (table 4.25):

	Levelling	Collimation
C	450	350
P	3.4	3.1

Table 4.25 - Chosen parameters for the estimation of the Toràn dam movements fitting curve.

Parameters are estimated with the Curve Fitting Tool in the Matlab environment, and are here reported in tables 4.26 and 4.27.

LEVELLING	B1	B2	B3	B4	B5	B6	B7
A	-8.426	-44.73	-42.94	-37.42	-35.36	-47.67	-40.9
B	16.49	69.14	66.99	60.25	56.45	75.05	64.92
C	450	450	450	450	450	450	450
P	3.4	3.4	3.4	3.4	3.4	3.4	3.4
R^2	0.9260	0.9908	0.9930	0.9915	0.9682	0.9743	0.9733
SSE	24.00	24.90	17.44	20.46	62.84	85.13	67.81
RMSE	0.5855	0.5964	0.4992	0.5407	0.9475	1.1028	0.9842

Table 4.26 - Parameters of fitting of levelling movements (Toràn dam).

COLLIMATION	B1	B2	B3	B4	B5	B6	B7
A	-27.66	65.36	79.35	194.6	204.6	96.58	31.65
B	31.24	-72.15	-89.23	-210.9	-220.4	-106.8	-34.13
C	350	350	350	350	350	350	350
P	3.1	3.1	3.1	3.1	3.1	3.1	3.1
R^2	0.8249	0.8914	0.6326	0.6518	0.6068	0.5400	0.2044
SSE	38.99	56.36	302.70	771.16	906.54	409.41	169.10
RMSE	0.7517	0.9384	2.0946	3.3676	3.6247	2.4537	1.5657

Table 4.27 - Parameters of fitting of collimation movements (Toràn dam).

As can be seen from the values of R^2 coefficient, in the case of the levelling movement, the hypothesis of the similar behaviour of Graus dam was quite confirmed. The correlation coefficients have very high values ranging from 0.926 to 0.993. The errors

parameters (RMSE and SSE) have acceptable values, a bit higher in the case of blocks 5, 6 and 7.

In the case of the collimation movements, the obtained results don't possess the same accuracy of the levelling movements. The R^2coefficient ranges from 0.54 to 0.65, being higher only for blocks 1 and 2 (R^2=0.82 and 0.89) and much lower for block 7 R^2=0.20. This trend is confirmed by the error coefficients, being them quite higher when the $R^2$was lower.

The movements in the vertical direction have lower variations with respect to each other than the horizontal ones, similarly as it happened in Graus dam. This may be reflected by the fact that the parameters C and P are taken from that dam and applied to another one, i.e. Toràn dam.

In the figure 4.19 is reported the plots of the levelling data and of the fitting curves thus obtained. Differently from Graus dam, the blocks that seem experiencing the highest movements in time are blocks 2, 3 and 6. Instead blocks 4 and 5 have slightly lower values of expected movements, as can be seen from parameters A and B.

Parameter B ranges from 56 to 75 mm (except for block 1), while the Graus parameters were in the range 111 to 141 mm (excluded lateral blocks). A similar range of variation is found, reasonably. The difference with respect to the Graus dam lays in the fact that central blocks, that are the highest, don't experience the biggest displacements, according to the model, as instead happened in Graus dam.

A reason may be found in the too restrictive assumptions of the modelling, regarding parameter C and P, or in the presence of local effects, as could be the spillway in the central blocks that alter the developments of the reactions and then of the displacements.

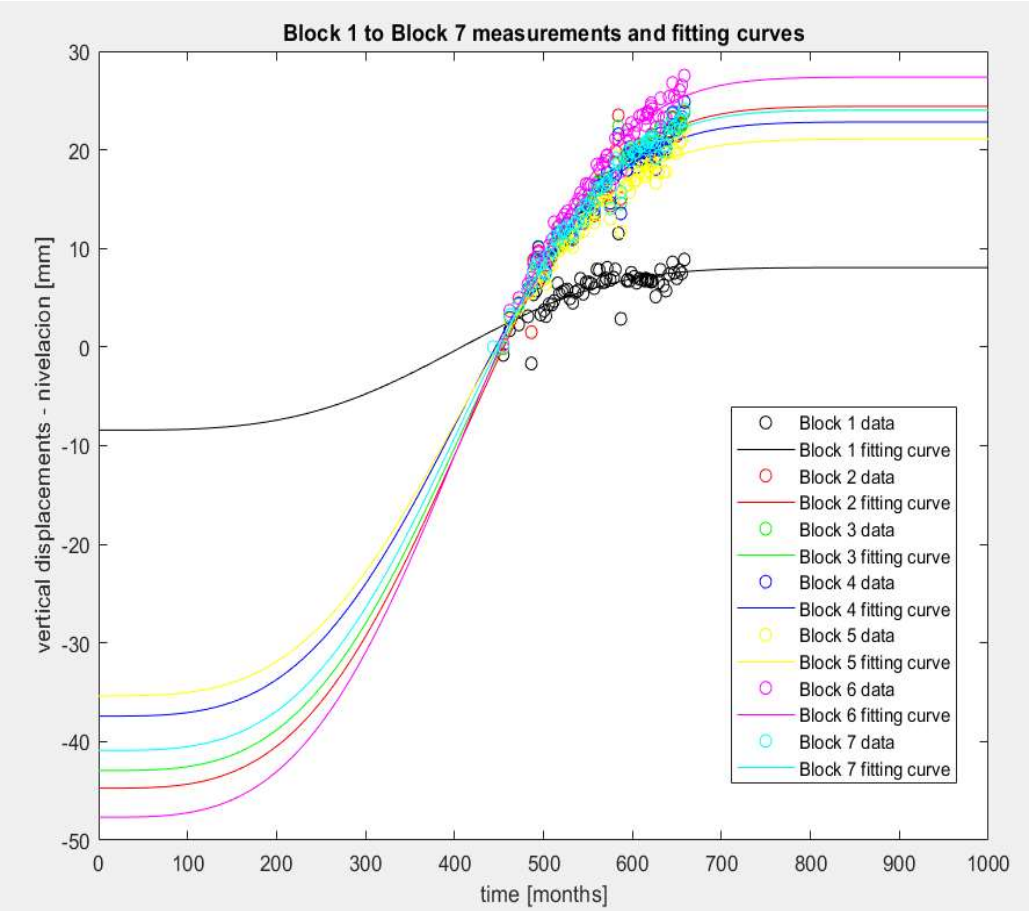

Figure 4.19 - Toràn levelling movements and fitting curves, obtained with C and P parameters drawn from Graus fitting analysis.

In figure 4.20 the collimation movements and their fittings are plotted. From the fitting operations, blocks 4 and 5 have here much bigger collimation movements toward upstream face, while blocks 2, 3 and 6 have horizontal displacements that are about the half of them. The same degree of variation of the movements is found in the Graus dam, and such degree of variation could be caused by the choice of the parameters of the Graus dam to infer the parameters of Toràn dam. Central blocks here register the highest movements, as happened in most of the monitored cases of dams expansions.

Nevertheless, the obtained results are very nicely related to the geometry characteristics of the dam, i.e. geometry of the blocks, as will be explained in next chapter.

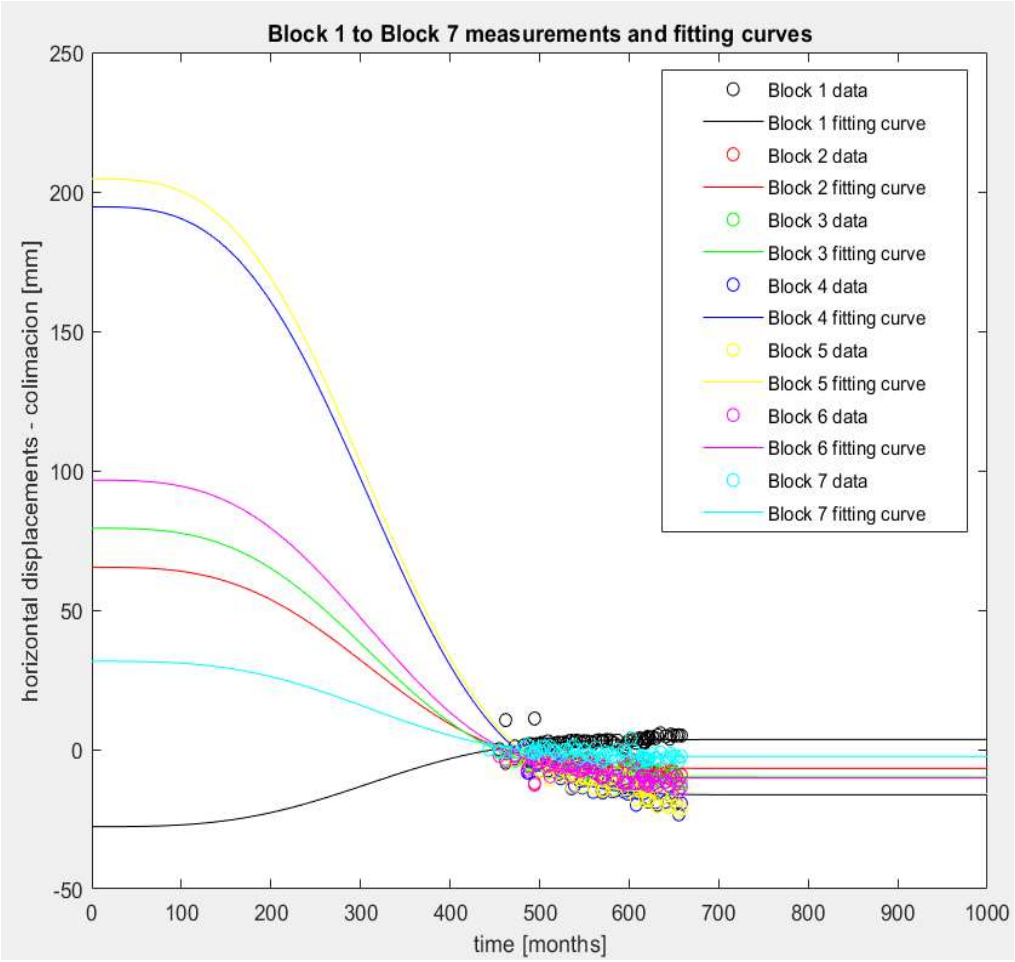

Figure 4.20 - Toràn collimation movements and fitting curves.

CHAPTER 5 – PHYSICAL MODELLING OF THE PARAMETERS

5.1 Introduction

The last part of the work of the master thesis was focused on the physical interpretation of the parameters of the fitting curves, that inasmuch being parameters of a mathematical model, appear to be related to physical issues. In the case of the model proposed by Aguado, that describes the trends of the horizontal or vertical movements at the top level of dams, reported in the following equation:

$$y = A + B \cdot \left(1 - \exp\left(-\left(\frac{t}{C}\right)^{p}\right)\right) \tag{6}$$

the parameters A, B, C and P seem very much linked to physical features of the two degradation mechanisms (ISA and ASR), and more specifically with the expansions of the concrete body of the investigated dams.

The modelling of the parameters considers their role inside the mathematical model. The goal of this stage seeks to correlate the analytical aspect of the model to the physical-chemical aspects that characterize the deterioration phenomena dealt hereby. The two deterioration mechanisms that were addressed to be responsible for non-recoverable movements, are also accountable for the diffused cracking, in form of map or oriented cracking, and for the formation and deposit of reaction products in precise locations, i.e. in the cement matrix or inside aggregates, where reactions take place, in forms of gel or powder according to what reaction has developed in more abundance.

The difficulties arisen in this phase were the complexity of the two degradation phenomena from a chemical-physical point of view, the elevated number of parameters that influence the deterioration mechanisms, the massive size of the dams and quantities of concrete that yield a vast amount of data to be analysed and always troublesome passage from laboratory data to the unique specificity of the field

conditions (as could be the ones of the dams), together with the difficulty of reproducing the iron-sulphide degradation mechanisms in the laboratory (Schmidt et al, 2011).

5.2 Physical meanings of the parameters and relation with the deterioration phenomena

Despite the previously mentioned difficulties that could arise in this stage, the parameters of the model described in equation (6) can be related to physical characteristics of the deterioration phenomena, at least at a conceptual level. The main differentiation is done with respect the two main evidences of anomalous behaviour: the levelling and the collimation movements. In the following, a physical interpretation of the parameters is given.

Parameter A represents the value of the ordinate intercept. As discussed in chapter 4.3.1, this value is usually fixed to 0, meaning that at time t=0 the measured movements are null, coherently with the behaviour of a concrete dam. When movements data are available after a certain distance of time, i.e. the first portion of data have not been recorded, this parameter could be useful to understand the entity of the movements happened in that missing portion of time. The intercept A, anyway, is constrained to assume only values lower than 0, since positive values, representing values of displacements bigger than 0 at the moment of the dam commissioning, don't have physical sense.

Parameter B depicts the total amplitude of the ordinate variation, i.e. the rank of variation of the movements, be it horizontal or vertical. It is the total displacement at $t=\infty$, and it can be correlated with the amount of reactive species that are found in the concrete, in particular in the aggregates. Attempts were done in past studies to correlate the potential expansion to the geometry of the blocks, linking it to the height or to the slenderness of the blocks, with established good experimental results (Martínez et al., 1991, Aguado et al. 1998, 2014). In this master thesis' optic, having

detected the Internal Sulphate Attack and the Alkali-Silica Reaction as the deterioration phenomena responsible for the movements (Aguado et al.), effort was put in order to relate contents of reactive minerals to the entity of the total expected movements, represented by parameter B. As a general rule, the higher the content of reactive aggregates or components (iron-sulphides bearing aggregates in case of ISA, cement alkali content and siliceous character of the aggregates in case of ASR), the higher the amplitude of expected displacement, i.e. parameter B.

In figures 5.1 and 5.2, comparing non-recoverable movements with the plan view of the Graus dam (Aguado et al.,) one can appreciate that higher/bigger blocks also register larger collimation movements, and this can be related to the issue that higher blocks have a wider quantity of concrete and therefore more reactive aggregates. Block number 3 constitute a little of exception, having similar height but smaller displacement. This could be due to the presence of the spillway in that block.

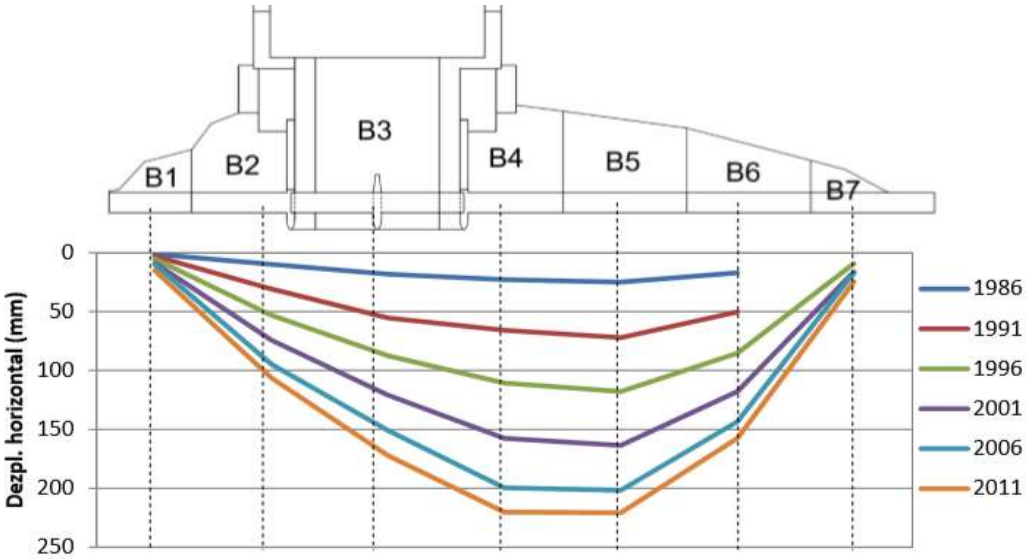

Figure 5.1 - Plan view of the Graus dam and collimation movements of blocks, measured every 5 years (Aguado et al., 2014).

Collimation movements are near exclusively due to the ISA reactions, as confirmed by large number of studies (Araúlo, 2008, Campos, 2012, Aguado et al., 2014, Gobbi,

2019). Hence parameters B of the collimation are attempted to be related to reactive component in the regards of the ISA, i.e. iron-sulphide bearing aggregates.

On the other hand the levelling movements are mainly attributed to the ASR development, so the parameters B of the levelling are related to the ASR reactive components, i.e. alkali of the cements (and of the aggregates, Berubè et al., 2002), despite also the sulphate attack mechanism could have a non-negligible role in the development of the vertical expansion considering long enough times. In figure 5.2 are reported the vertical displacements of the Graus dam, each 5 years (Aguado et al., 2014). The difference of the movements seems to be related to the geometry/height of the blocks, in the light of considering the Alkali-Silica Reaction a generalized phenomenon.

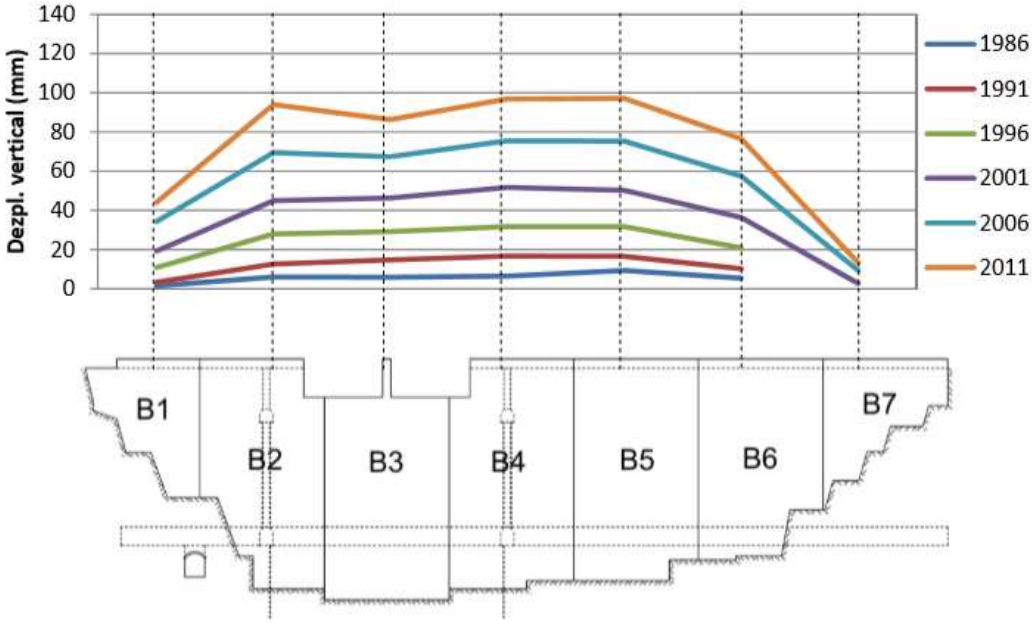

Figure 5.2 – Front view and vertical displacements of the blocks of Graus dam, with a time step of 5 years (Aguado et al., 2014).

Parameter C is identified as the inflection point of the curve. Expressed in months, it is the time after which the trend of the movements, i.e. its gradient, stops to increase and starts to decrease, therefore represent the point of maximum gradient of movements (the latter one could be expressed in mm/years for example). Form an

analytical point of view it is found to represent the time at which the total movements (parameter B) have reached about the 63% of their amplitude. When all the blocks of a dam that have been monitored are fitted with such an exponential curve, and a very similar value of parameter C (as it happens in Graus and Tavascan dams) is obtained, this can be a sign of a phenomenon that is enough uniformly diffused through the blocks, as could be ISA and ASR.

Parameter P describes the shape of the curve and it is representative of the speed of the expansion. Values of P lower than 1 lead to a curve without an inflection point and without a first slow initiation phase typical of the studied deterioration phenomena as ISA, so generally they are disregarded. High values of P indicate that the expansions (and so the reactions) happen in a short amount of time. Similarly to parameter C, a value of P that is more or less constant for all the blocks of the dams could mean that the reactions happen at about the same speed in all the blocks, and so the phenomenon could be generalized to the whole body of concrete.

The speed of reactions could be related to the availability and the possibility of access of the oxidizing agents involved in the ISA and ASR reactions. These aspects, depending on a number of factors, as oxygen and water concentration on the upstream and downstream faces, or degree of cracking of the concrete at superficial level, are tried to be modelled together with parameter P.

Experimental campaigns that were conducted on each dam, at different years (Aguado et al., 2014, 2018, 2020), allowed to monitor the state of the dams and the specific problematic that were detected. In the locations where the dams are built, and where the aggregates then are extracted for their use in the concrete, the major geological rock types were identified and characterized. With the help of petrographic examination and microscopy analysis, a lot of studies allowed to identify the reactive components in the rocks that were responsible for the expansive phenomena, such as pyrite and pyrrhotite iron-sulphides.

5.3 Conceptual modelling of the parameters

During the experimental campaigns conducted in each dam the extraction of cores allowed, in different years, to perform mechanical, hydraulic/permeability, and chemical tests in addition to microstructural characterization (e.g. XRD, X-rays efflorescence). In all the four dams that were the object of the study, evidences of sulphate attack and alkali-silica reaction have been detected.

Amongst all the available physical characteristics of the aggregates, cement and concrete that have been employed in the dams' construction, an attempt was carried out to correlate the parameters of the model to:

- Quantity of reactive aggregates/cement components: in particular iron-sulphide bearing aggregates as pyrite and pyrrhotite and sulphur content ($\%\ SO_3$) for the ISA, and alkali content of cement for ASR ($\%\ Na_2O$ and $\%\ K_2O$)

- Kinetics of the reaction mechanisms

- Potential expansivity of the concrete

- Access and availability of oxidizing agents (O_2 and H_2O concentration and diffusion) to the places where reactions are likely to be more developed (i.e. the downstream face for the ISA, the whole body for the ASR).

5.3.1 Parameter B

In the work of Oliveira (2011) and Oliveira et al. (2012), a methodology is proposed to correlate the potential expansions caused by the presence of iron-sulphide bearing aggregates and their effective contents in the aggregate to the non-recoverable movements observed in dams. In this work a volumetric expansion of a unit meter of concrete could be defined, given input data as $\%\ SO_3$ and $\%gypsum$ in weight,

porosity of concrete φ [%], masses of cement and aggregates used (in a unit cubic meter of concrete), based on the amount of pyrrhotite in aggregates and its molar volume increase $[\frac{m^3}{mol}]$. The relation can be written like this, where the volumetric total expansion is due to the sum of the primary expansion (pyrrhotite oxidation) and secondary one (ettringite formation):

$$\Delta V_t = \Delta V_{prim} + \Delta V_{secon} = 7.5 \cdot 10^{-5} \cdot M_A \cdot \%SO_3 + 1.44 \cdot 10^{-3} \cdot M_c \cdot \%gypsu \quad (10)$$

From the total volumetric expansion, considering also a damping parameter $\alpha = e^{-(0.24 \cdot \varphi)}$ in function of the concrete porosity, the volumetric strain can be obtained, and from it the linear strain in one direction. If the strain is supposed to be isotropic, it can be expressed:

$$\varepsilon_{linear} = \sqrt[3]{\varepsilon_{volumetric}} \quad (11)$$

The volume variation $\Delta V_{t,real}$ is a function of the % of the reacted pyrrhotite, that depends on many parameters, as explained in the work of Oliveira et al., amongst them lay time and distance from the downstream face. Here in this section, the parameter B is related to the maximum amplitude of the movements, that happen when all the reactive agents are oxidized and reacted. Therefore, the time evolution of the reaction and its kinetic were not taken into account (at least in the superficial layer), and only the final maximum value is considered, i.e. at time $t = \infty$, when $\%R = 100\%$.

From the linear strain ε_{linear} $[\frac{mm}{m}]$ one can evaluate the displacement, taking in consideration the geometry of the blocks of the dam.

This approach should be differentiated when applied to the dams, according to the character of the expansive behaviour. In the cases of Graus, Tavascan and Toràn dam, the expansive character due to the presence of reactive aggregates is diffused to the whole body of the dam, then the expansion should be applied to the entire body. In

the case of Paso Nuevo dam, from past studies and investigations of the available construction documents (Espinós et al. 2008, Aguado et al., 2020), two types of concrete that compose the dam are outlined. The first concrete (1st phase concrete) that was poured contained aggregates coming from a local quarry that was lately found to be rich in iron-sulphides minerals (in particular pyrite FeS_2 and pyrrhotite $Fe_{(1-x)}S$). In a second stage this quarry was abandoned since the aggregates are known to be harmfully reactive in concrete, and a second local quarry has been used (2nd phase concrete). The change of aggregate types (still containing iron-sulphides, but in lower quantities) lead to the use of two different concretes in the dam whose expansive behaviours are different in magnitude: the concrete with aggregates form the first quarry is more contaminated of iron-sulphides and therefore more lead to higher expansions. Hence the blocks of the Paso Nuevo dam are not considered homogeneously affected by ISA: the 2nd phase concrete is the contaminated one and blocks that have more of this concrete in proportions experienced the biggest expansions (Espinós et al. 2008, Aguado et al., 2020).

Two procedures are outlined for the modelling of parameter B with physical issues: the vertical movements modelling, due to ASR (mainly) and to ISA, and the horizontal movements modelling, due almost exclusively to ISA.

5.3.1.1 Vertical movements

Parameter B corresponds to the displacements happened when all the reactive minerals have reacted and generated expansive products, hence the kinetic and the time-evolving aspects aren't taken in consideration in the modelling of B.

In the case of vertical movements, ISA and ASR should both be considered. In the work of Oliveira et al. (2012), the methodology briefly exposed in chapter 5.3.1 is applied to the Graus dam and levelling displacements are evaluated, with good degree of precision in comparison to the actual measured movements, considering only ISA. The scheme in figure 5.3 is a rough resume of the levelling movements estimation

from the data concerning the content of pyrrhotite, expressed in term of % in weight of SO_3, considering the geometry of the blocks of the dam. The unit expansions used for the computation of the total volumetric expansion are: expansion due to oxidation of a mol of pyrrhotite to produce sulphuric acid and iron hydroxides (primary expansion, that is equal to $6.04 \cdot 10^{-6}\ m^3$), and expansion due to formation of one mol of ettringite (secondary expansion, equal to $2.48 \cdot 10^{-4}\ m^3$), (Oliveira et al., 2012).

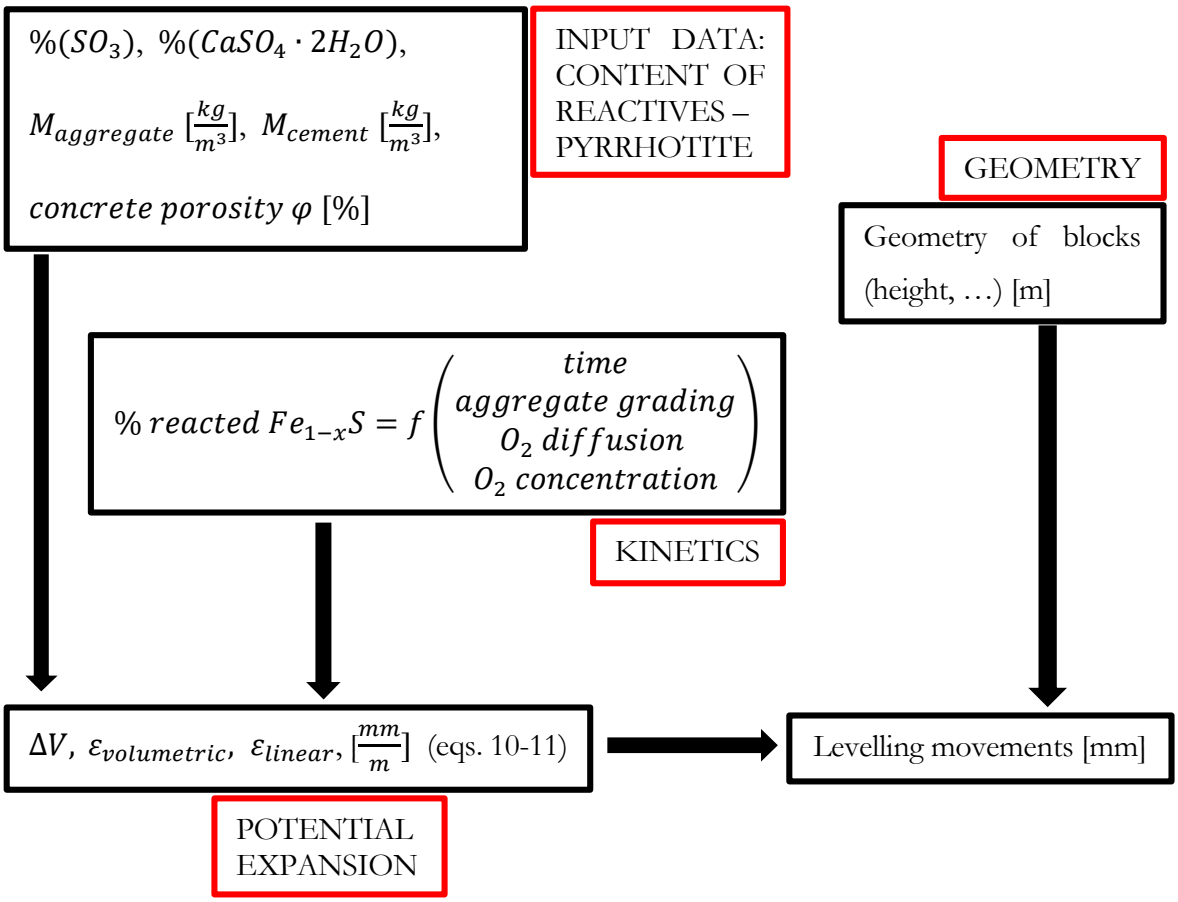

Figure 5.3 – Conceptual scheme for the estimation of the potential expansion and of the vertical movements, given quantities of reactive minerals, geometry of the blocks and kinetic model for the reaction (Oliveira, 2012).

A similar approach could be outlined for the ASR contribution, considering the reactive materials quantities as input data (e.g. $\%(Na_20_{equivalent})$ in a cubic meter of concrete) and the potential expansion produced by an equivalent mol reaction, or

by water absorption by the alkali-silica gel.. Once evaluated $\varepsilon_{volumetric}$ and ε_{linear}, through the geometry of the blocks, levelling movements could be estimated and compared to the experimental monitored movements data. A model that could be used in this direction is the thermo-chemo-mechanical model for the ASR expansion derived by Ulm et al. (2000).

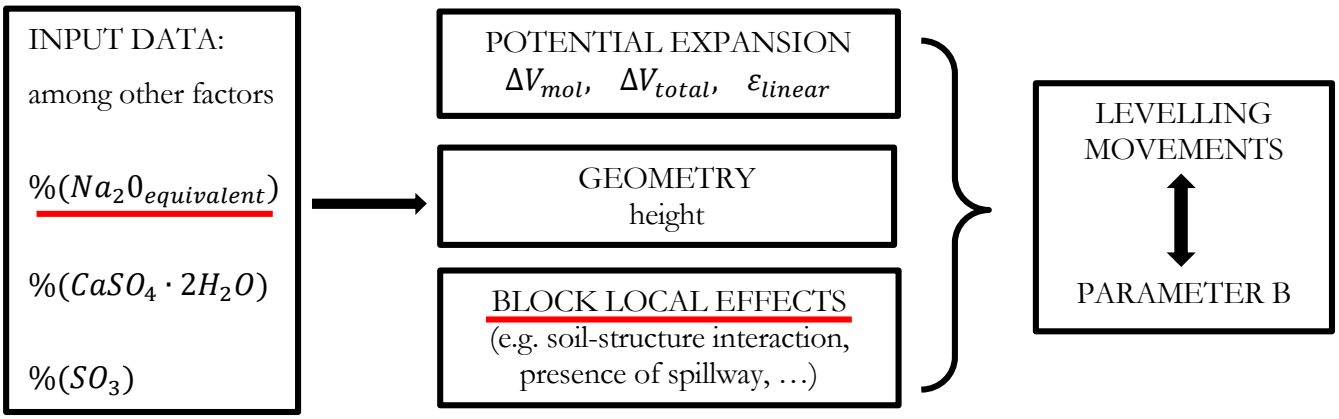

Figure 5.4 – Conceptual scheme for the estimation of potential expansions and levelling movements (Oliveira, 2012), with additional input data to consider ASR, and local effects consideration.

$$B \leftrightarrow \left(\varepsilon_{linear} \cdot f_V(geometry)\right) \cdot g \qquad (12)$$

$$[mm] \leftrightarrow \left(\left[\frac{mm}{m}\right] \cdot [m]\right) \cdot [-]$$

$$B \leftrightarrow \left(strain \cdot f_V(geometry)\right) \cdot g(local\ effects, position)$$

In equation (12) B is related to the linear strain (that is mainly a function of the quantity of reactive aggregates (Oliveira et al., 2012) and the molar volumetric expansion), to a geometric factor $f_V(x)$, for example the height of the blocks (subscript V stands for vertical movements), and to a further adimensional parameter g, function of local effects (e.g. influence of the position of the auscultation system of a block in the dam).

The linear strain ε_{linear}, once evaluated the molar volumetric expansions and the number of moles of reactive components in a unit cubic meter of concrete, can be

considered the sum of the two components: the ISA and the ASR ones, as in equation (13):

$$\varepsilon_{linear} = \varepsilon_{linear}(ISA) + \varepsilon_{linear}(ASR) \quad (13)$$

$\varepsilon_{linear}(ISA)$ can be computed with the method proposed by Oliveira et al. (2012). $\varepsilon_{linear}(ASR)$ with the method of Ulm et al (2000), for example.

A strain distribution like the one in figure 5.5 could be considered (Aguado at al., 2014), where the strain ε_B is due to the ISA and it's localized in the superficial layer that is exposed to the atmospheric air (of width δ). The strain ε_A is of much lower intensity and is generalized to the whole dam body, and it is linked to the ASR.

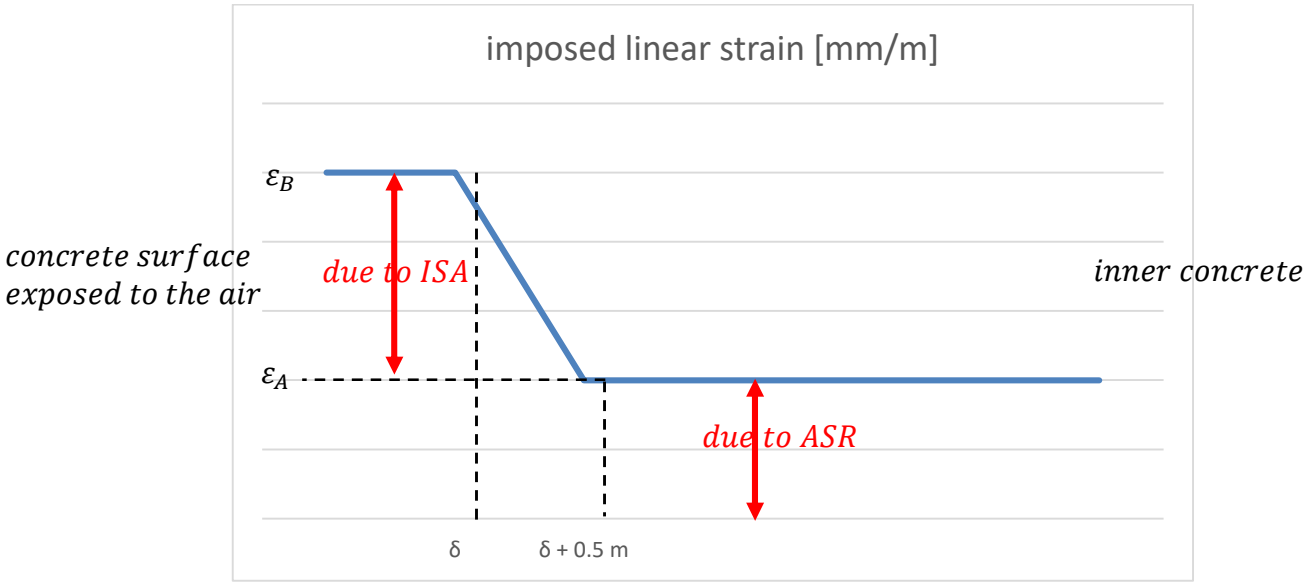

Figure 5.5 - Distribution of imposed strain due to ISA (ε_B) and ASR (ε_A) on the concrete dam transversal cross-section.

Different values of δ and ε_A and ε_B have been used by the Authors Aguado et al. (for example: $\varepsilon_A = 1.62\ \frac{mm}{m}, \varepsilon_B = 5\ \frac{mm}{m}, \delta = 0.5 - 1.5\ m$). They generate displacements that properly match with the measured movements at the top of the dam.

These expansions could be applied to the entire height of the blocks, since all the concrete mass is supposed to contain the same amount of reactive aggregates and cement (as in the case of Graus, Tavascan and Toràn dam).

In the case of Paso Nuevo, as mentioned earlier, a differentiation should be set between the two different aggregates types used in the concrete, that generate expansions of different character and magnitude. As a consequence, the expansions generated by the ISA phenomenon is more localized than in the other three dams.

The good degree of correlation between the Graus and Tavascan displacements and the height of the blocks (Martínez et al., 1991) has been already commented. In the case of Paso Nuevo, together with the height of the blocks it must be considered the portion of concrete that contains the contaminated aggregates from the first quarry (1st phase concrete). In table 5.1 are qualitatively reported the proportions [%] of contaminated concrete, the blocks heights [m] and their product. Their product seems to have a good correlation with the parameter B of the levelling movements, as can be seen from figure 5.6. The relation was not found when correlating movements (parameter B) with height of the blocks instead (Aguado et al., 2020).

PASO NUEVO levelling	parameter B [mm]	Block height [m]	Contaminated concrete [%]	height · %contaminated
P1 (block 3)	19.55	52.68	0.10	5.27
P2 (block 4)	23.68	63.43	0.25	15.86
P3 (block 5)	29.66	57.17	0.30	17.15
P4 (block 6)	21.62	45.36	0.20	9.07
P5 (block 7)	11.93	33.36	0.05	1.67
P6 (block 8)	19.04	28.46	0.40	11.38
P7 (block 9)	30.41	24.91	0.60	14.95
P8 (block 10)	13.81	19.12	0.55	10.52

Table 5.1 – Paso Nuevo dam: parameters B, height of the blocks, percentage of contaminated concrete and product of the last two parameters.

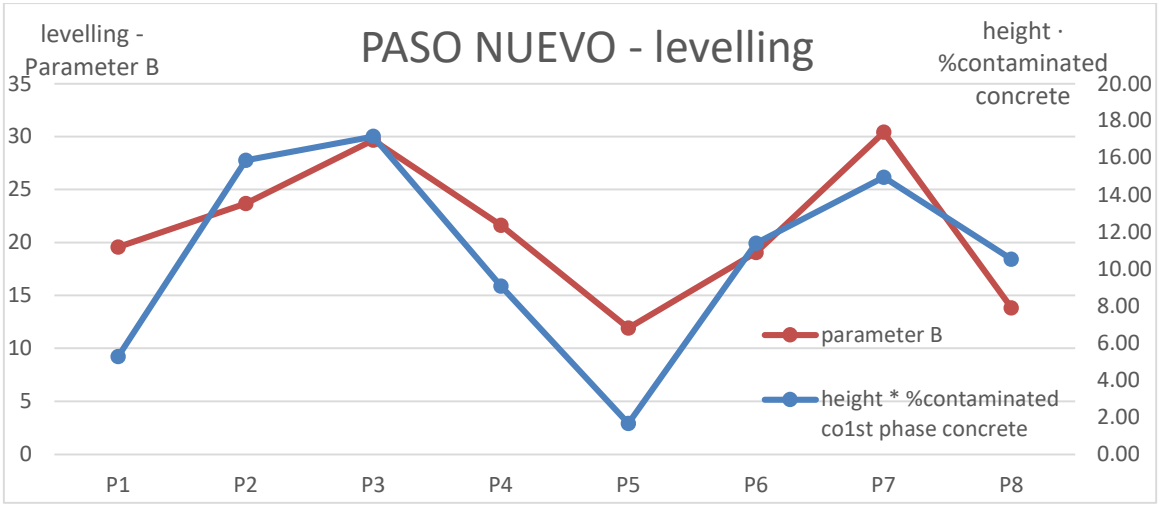

Figure 5.6 – Relation between parameters B of the levelling movements model and product of block height and % contaminated concrete.

Then, together with the geometry modelled by $f_V(x)$, that for simplicity's sake can be defined as the height of the blocks at an initial stage, also local effects should be taken into account. In the case of Paso Nuevo dam a rough estimation of the % of contaminated concrete with the more reactive aggregates (coming from the 1st quarry) lead to a good modelling of the movements (parameter B) with physical issues. Here the function g introduced before coincides with the product of height of the block and % of 1st phase concrete, i.e. the iron-sulphides contaminated one.

$$B \leftrightarrow \left(\varepsilon_{linear} \cdot f_V(geometry)\right) \cdot g \qquad (12)$$

$$g \leftrightarrow quantity\ of\ contaminated\ concrete\ [\%] \qquad (14)$$

Local effects could include the consideration of soil-structure interaction, presence of spillway, presence of lateral abutments with specific stiffness characteristics or steepness, position of the auscultation systems at the top of the dam, and other reasonable causes. All these effects on the total movements could be condensed in the function g.

Regarding the other three dams, there is good correlation between height of the blocks and entity of the displacements in the case of Graus dam (Martínez et al., 1991), and

the function g that accounts for any local issues is bound to have less influence on the parameter B (total displacement), as can be seen in figures . while it is more evident in the case of the Graus dam, it is less for the Tavascan and Toràn dams, whose correlation with the geometry seem poorer. In the Tavascan dam other effects should be considered, i.e. environmental effects, presence of local disturbances (e.g. advanced-stage fissures and cracking in some blocks, Aguado et al., 2018). In the Toràn dam, that showed very similar behaviour with the Graus dam and, the reason may be the lack of measurements data, that lead to the strong constraining of the model (i.e. fixing C and P parameters after the Graus modelling results). In Toràn dam, central blocks movements could have been underestimated, or lateral ones overestimated.

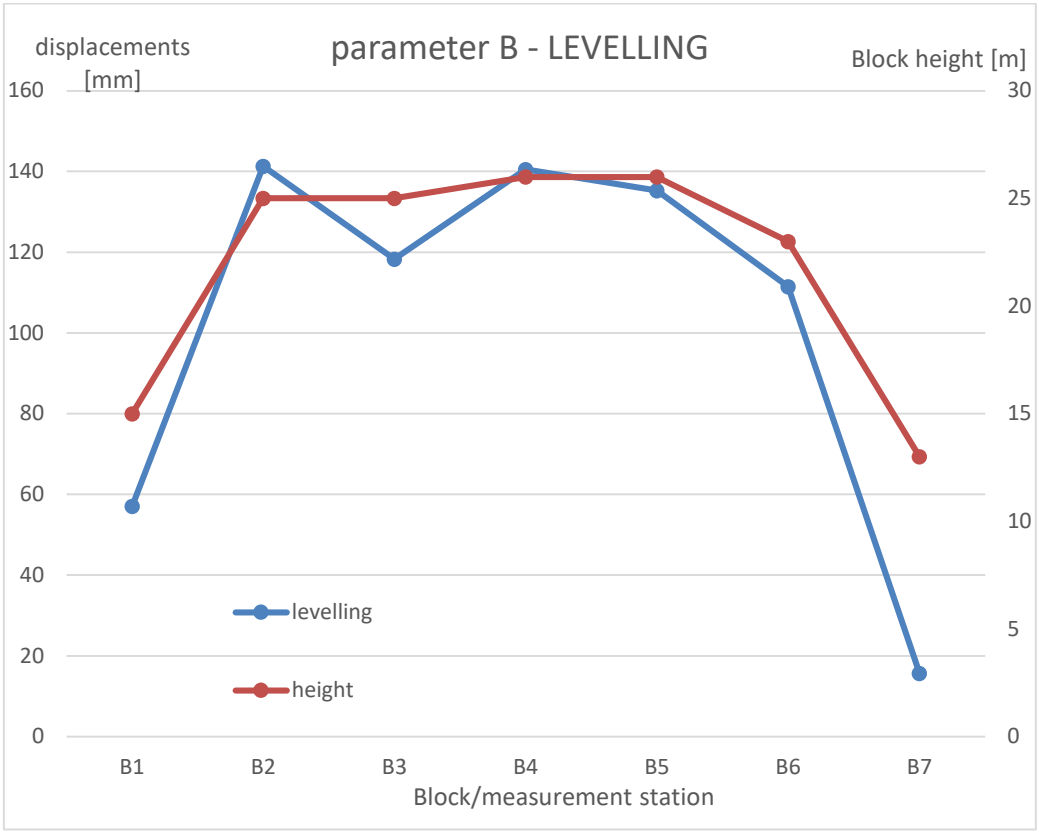

Figure 5.7 – Relation between parameter B of the levelling movements of Graus dam and the height of the blocks.

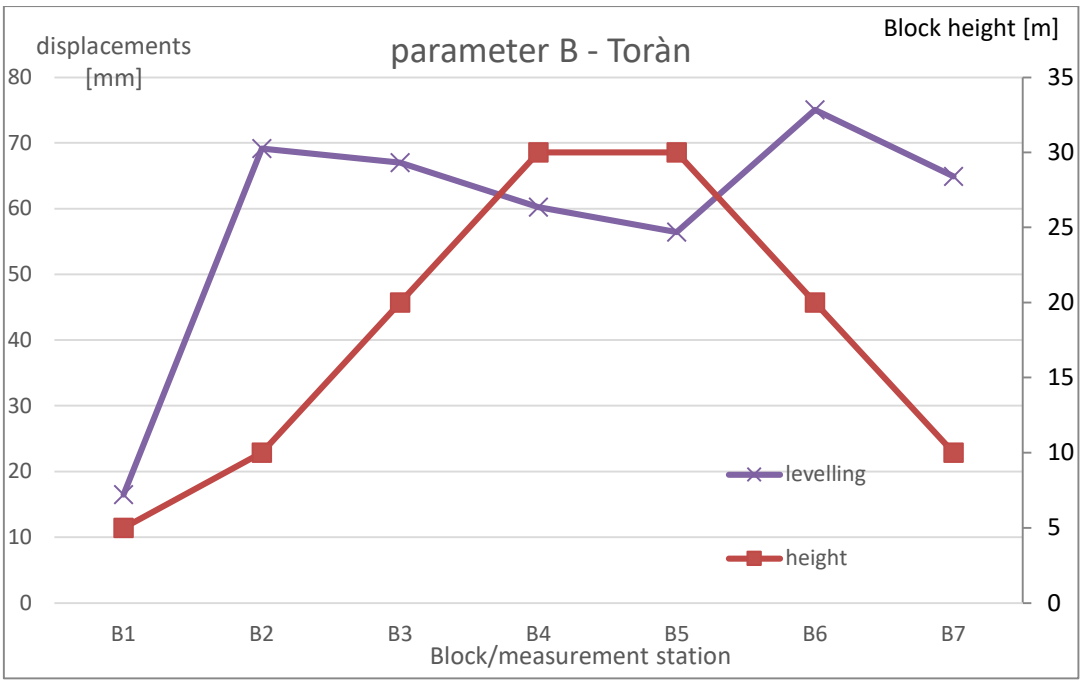

Figure 5.8 - Relation between parameter B of the levelling movements of Toràn dam and the height of the blocks.

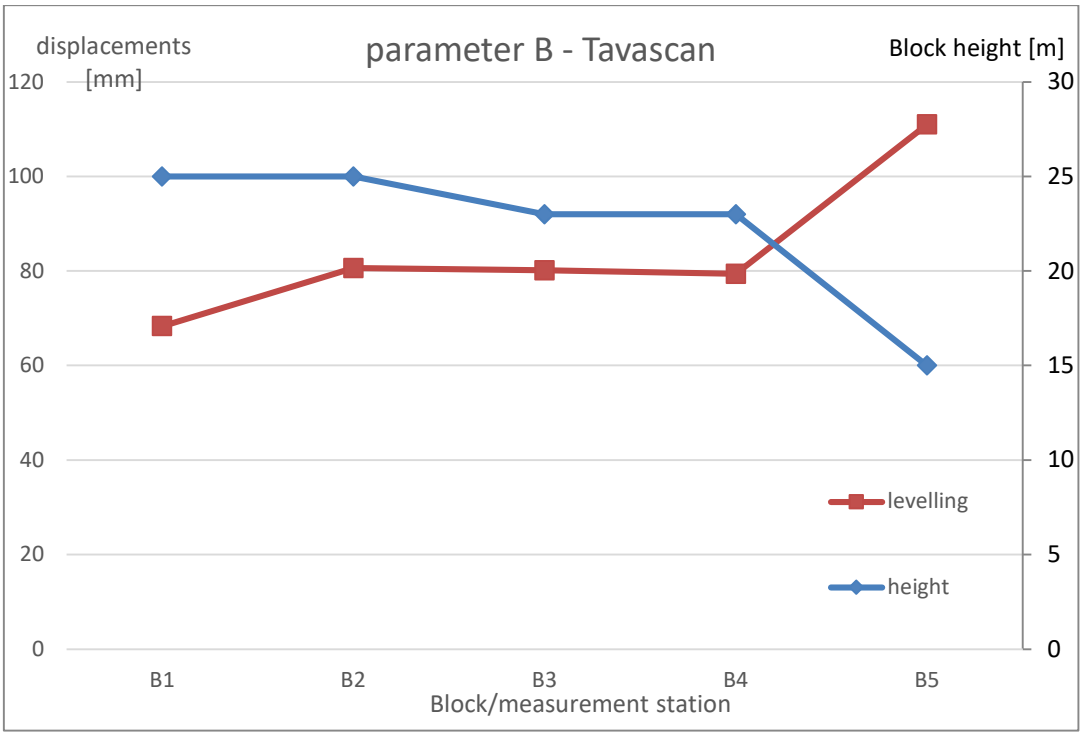

Figure 5.9 - Relation between parameter B of the levelling movements of Tavascan dam and the height of the blocks.

In Tavascan dam, station B5 (located in block 1) may be regarded as an anomalous behaviour, since it is monitored with highest movements although it is the shortest block. Environmental effects and excessive cracking could have played a major role in this block behaviour, leading to an increased expansion (Aguado et al., 2018).

5.3.1.2 Horizontal movements

In the case of the horizontal movements, the first hypothesis made is that they are caused only by the internal sulphate attack, while negligible contribution comes from the ASR, that could be disregarded as cause of collimation displacements. In the case of the vertical ones their occurrence has been attributed to both phenomena, despite being ASR in major proportions. Hence, only ISA is considered in the collimation movements.

Figure 5.10 - Typical cross-section of a gravity dam. In dark colour are highlighted the zones where the ISA reactions take place with higher intensities.

Approach of Oliveira et al. (2012) can be followed and adapted, since geometry must considered in a different way, i.e. the linear expansion ε_{linear} must not be applied to

all the height of a block but only to the portion of concrete affected by ISA in the horizontal direction, that typically is restricted to some meters of depth of the downstream face, and the upper portion of the upstream face, above the water level of the basin, as highlighted in figure 5.10.

The difficult geometry interpretation (trickier than in the case of vertical movements), the turning movement that is generated by the differential expansion, in combination with local and peculiar aspects of each block, lead to think that the potential expansion could be more accurately evaluated by means of numerical modelling, for example finite element analysis (for example Campos, 2012, Aguado et al., 2014), once the strain provoked by the ISA mechanism is sufficiently well known.

The scheme that could be used, anyway, for the modelling of the parameter B, may be the same of figures 5.3 and 5.4.

The same considerations could be advanced for the dams. Graus, Tavascan and Toràn dam show ISA effects of similar intensity on the whole concrete mass. For Paso nuevo dam instead the use of different reactive aggregates must be considered (in parameter g).

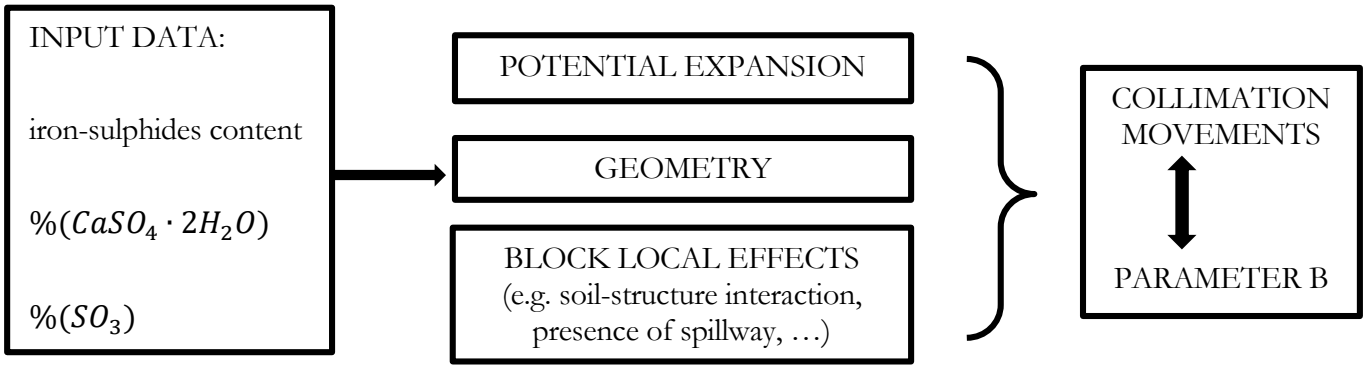

Figure 5.11 – Scheme for the horizontal movements.

The difference for the horizontal movements would be in a different consideration of the geometry through the function $f_H(x)$ (subscript H=horizontal).

$$B \leftrightarrow \left(\varepsilon_{linear} \cdot f_H(geometry)\right) \cdot g \tag{15}$$

$$[mm] \leftrightarrow \left(\left[\frac{mm}{m}\right] \cdot [m]\right) \cdot [-]$$

$$B \leftrightarrow \left(strain \cdot f_H(geometry)\right) \cdot f(local\ effects, position)$$

The strain ε_{linear} would account for the quantity of reactive aggregates and the volume variation of a mol of reactive substance $[\frac{m^3}{mol}]$. The function $f_H(x)$ that envelope the effects of the geometry should account for the differential strains highlighted in figure 5.10, and local effects of each block inside the function g, regarding the same issues that have been suggested in the case of the vertical movements.

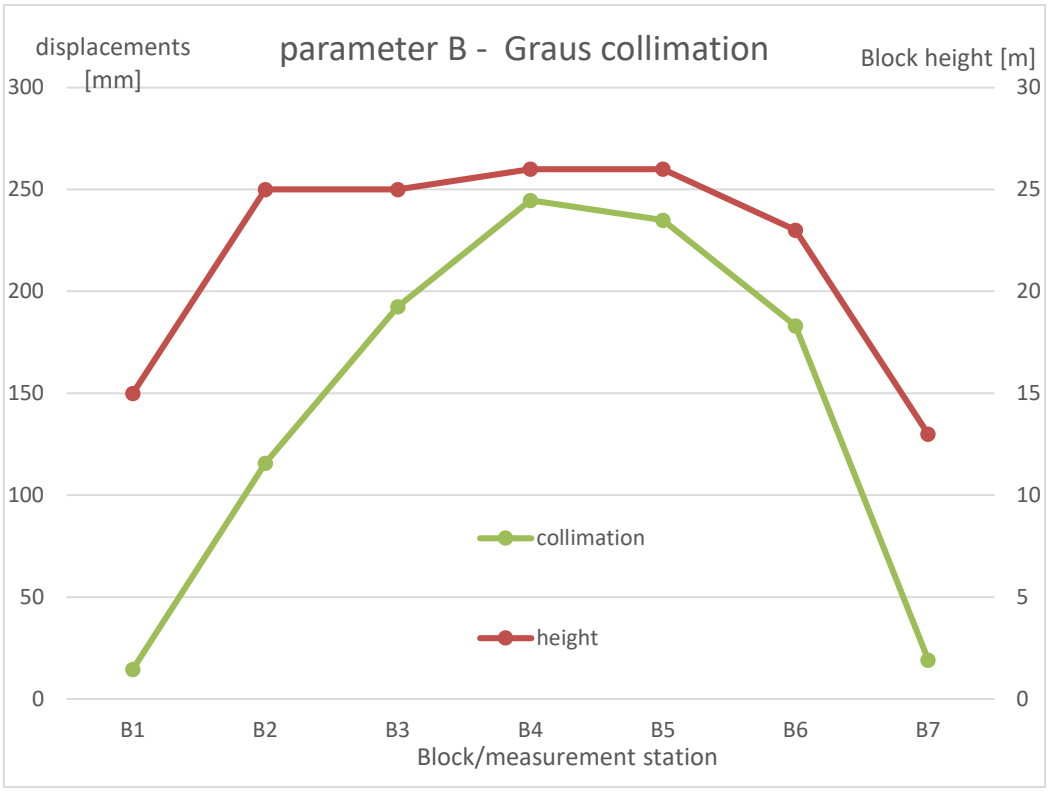

Figure 5.12 – Relation between parameter B of collimation movements of Graus dam and the height of the blocks.

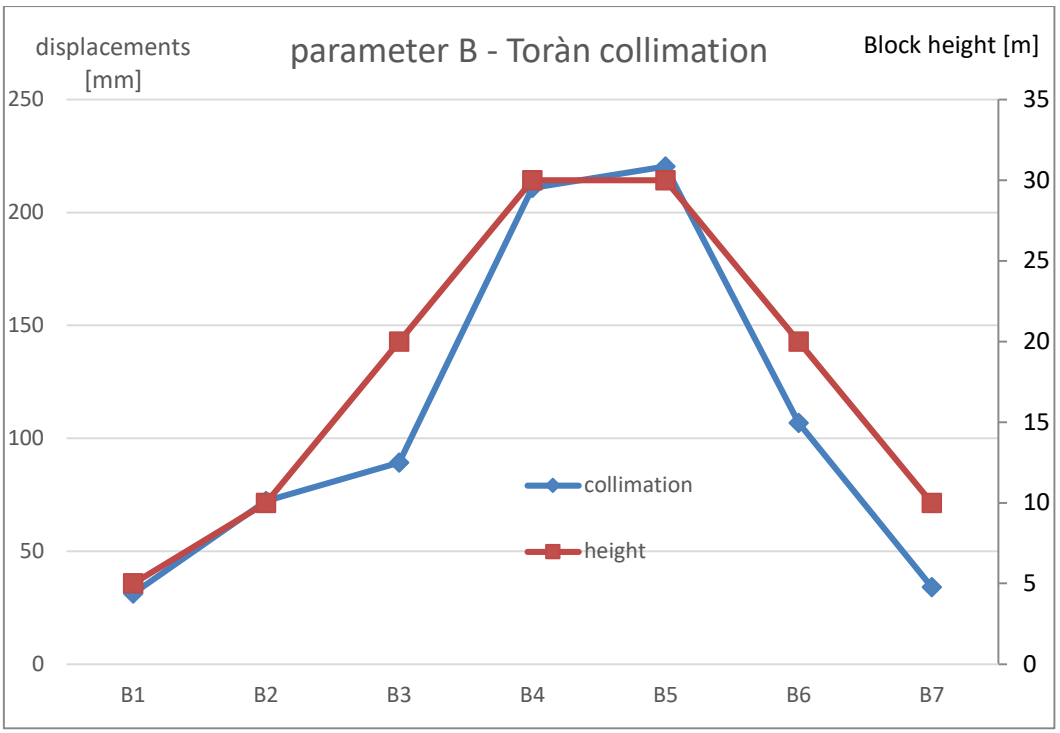

Figure 5.13 - Relation between parameter B of the collimation movements of Toràn dam and the height of the blocks.

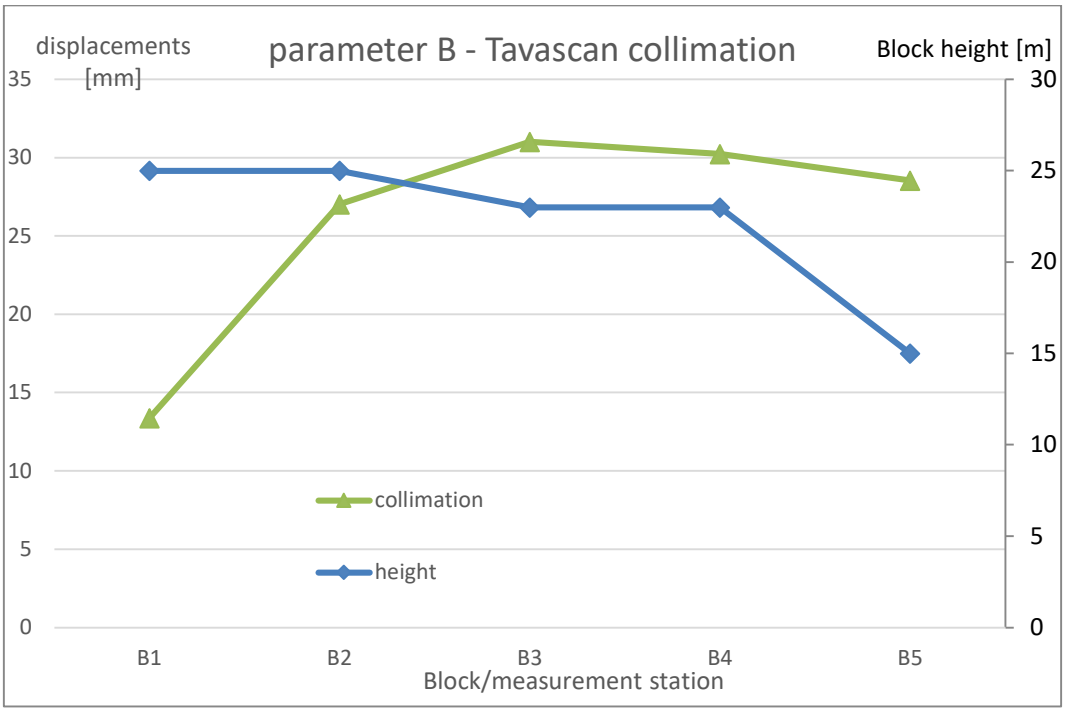

Figure 5.145 – Relation between parameter B of the collimation movements of Tavascan dam and the height of the blocks.

As one can appreciate in the figure 5.12, for the Graus dam similar considerations to the levelling movements can be drawn. The parameter B, expressing the total displacements, is related to the geometry of the block, in this case the height (Martínez et al., 1991). Hence there should not be the need of introducing the function g to account for local effects. The same can be said for the Toràn dam (figure 5.13). Despite its movements have been modelled with the parameters of the Graus dam (P and C), the parameter B estimated from the stabilization part of the measurements seem very much correlated with the geometry (height of the blocks). The same did not happen when considering the vertical movements.

The Tavascan dam instead shows values of the movements that do not relate to the height of the blocks (figure 5.14). In this case the use of a function g to envelope the possible local effects should lead to a correlation between entity of displacements (parameter B) and content of reactive aggregates, accounting for local effects of each block.

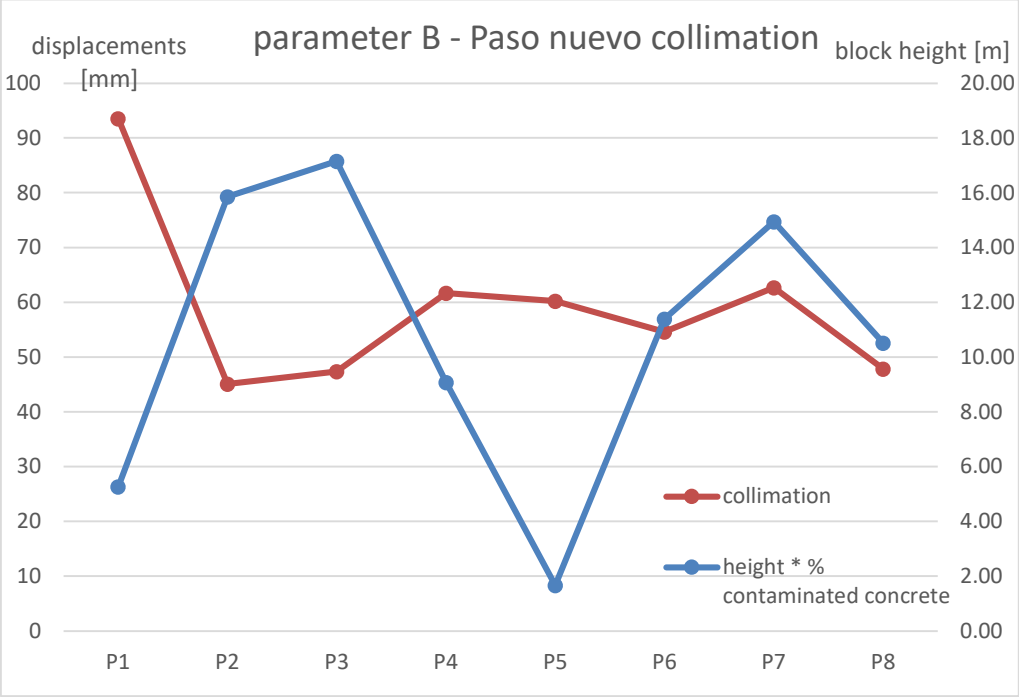

Figure 5.15 - Relation between parameter B of the collimation movements of Paso Nuevo dam and the product between the height of the blocks and the percentage of contaminated concrete (same quantities used in the levelling relation).

In the case of Paso Nuevo dam the same correlation that was found in the case of the vertical movements is proposed for the horizontal ones, but in this case no relation is found (figure 5.15). While for the levelling the entity of displacements correlates with the product of height and proportion of contaminated aggregate, for the collimation it doesn't. Another correlation must be sought and included in the function g, different from equation (14).

5.3.2 Parameter P

Parameter P of the mathematical model is related to the 'speed' of the movements' development. The ISA phenomenon has proven to be more rapid in its development (with respect to ASR), due to the nature of its chemical reactions, and therefore the expansions it provokes and the related non-recoverable movements are manifested more rapidly. On the contrary, ASR is slower by character and it shows its effects on a larger time interval. The values that parameter P assume reflect this fact, and according to its relative intensities the prevailing reactions (ISA or ASR or both) could be determined.

In the figure 5.16 are reported the values of parameter P for the levelling movements. In the case of the Toràn dam, they are chosen after the Graus dam (P=3.4). Except for the lateral blocks, that in general have higher P values, the central blocks show similar values, that lead to confirm that the blocks experience the same expansion phenomena.

In the case of Paso Nuevo dam the values assumed by parameter P are more variable with respect to Graus and Tavascan dams. One could think that each block has its own 'speed' of movement developments, hence expansive phenomena are developing with different speed in each block and could be associated to inhomogeneous behaviour of these expansive phenomena in each block.

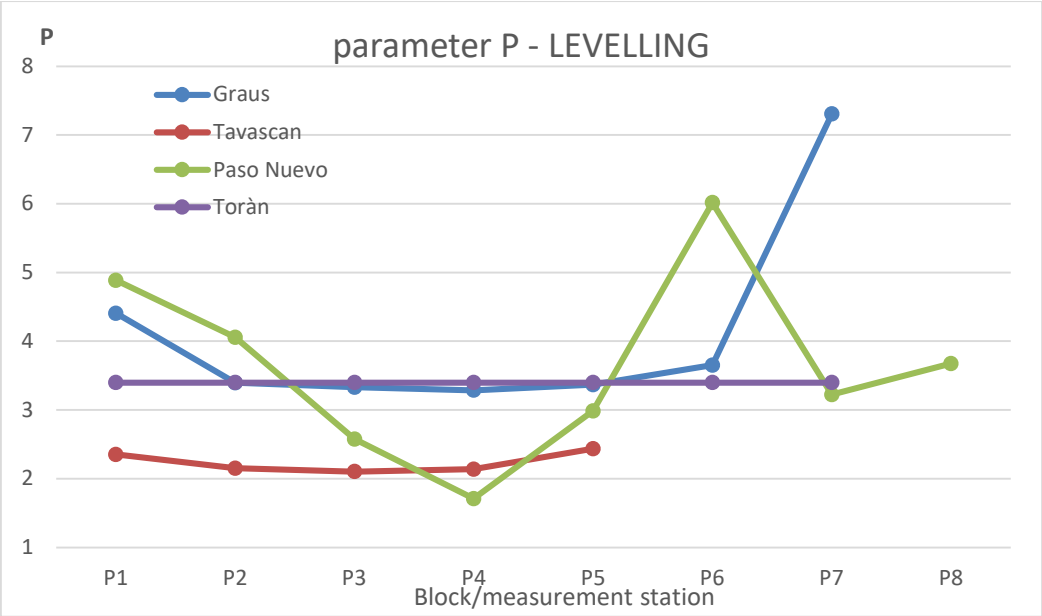

Figure 5.16 – Values of parameter P for the modelling of the levelling movements of the four dams.

Similar considerations are found in the case of the parameters P of the modelling of the collimation movements (figure 5.17). Parameter P values of Toràn are fixed at 3.1, from the similarity with Graus. Paso nuevo has values of P that vary more, from block to block, than Graus and Tavascan ones, that are more uniform.

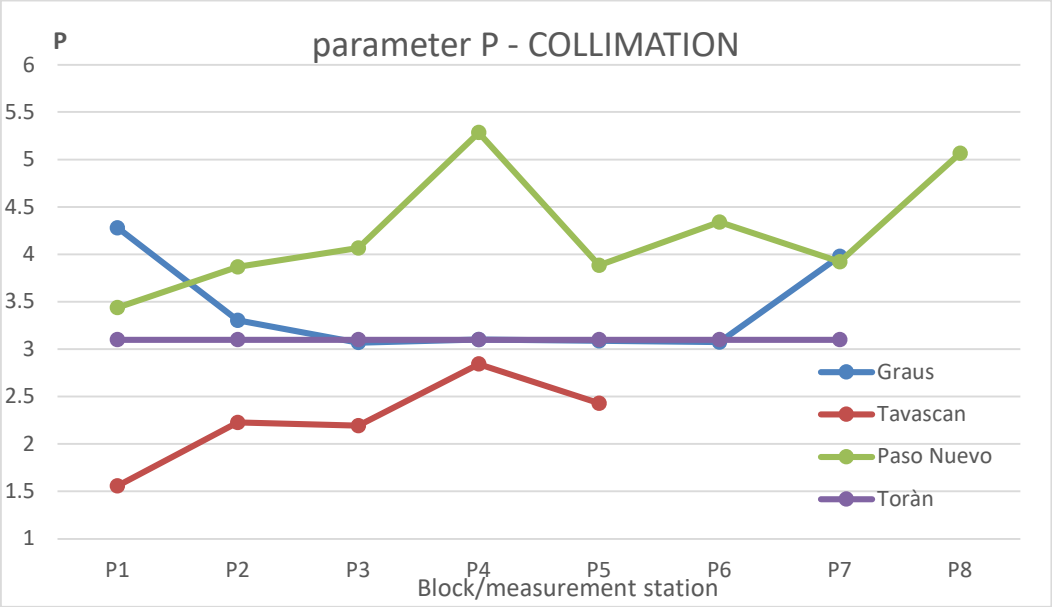

Figure 5.17 - Values of parameter P for the modelling of the collimation movements of the four dams.

From the comparison of the two figures 5.16 and 5.17: Graus parameters P values are lower in the case of collimation than levelling, consistent with the fact the ISA, responsible for the collimation, is faster and increases the 'speed' of movements happening. In the case of Tavascan dam, the values of the P values are similar, because the same degradation phenomenon is going on.

In the case of parameter P of the Paso Nuevo dam, it takes values that vary from block to block, and it seems that when parameter P of the levelling model is higher for a block, its value its lower for the collimation model.

Parameter P, expressing the 'speed' of the development of the movements, could be related to the availability of oxidizing agents, that constitute primary elements in the trigger of the deterioration mechanisms and the start of the expansive phenomena.

As a general rule it can be stated that ISA degradation mechanism is faster and lead to higher values of the parameter P of the movements modelling, while on the other hand ASR mechanism is slower and results in lower values of parameter P. Despite this, the kinetics of the degradation phenomena have a major impact on the development of the expansions. Values of parameter P could be representative of the kinetics of the expansive reactions.

ISA depends on the availability of O_2, being around 9.37 $\frac{mol}{m^3}$ in the dry air, and around 0.26 $\frac{mol}{m^3}$ in the water (Oliveira et al, 2012). Its diffusion inside concrete can be described by Fick's second law of gas diffusion through solids:

$$\frac{dC_x}{dt} = \frac{d}{dx}\left(D_m \cdot \frac{dC_x}{dx}\right) - \left(\frac{dC}{dt}\right)_{reaction} \quad (16)$$

Where C_x is the concentration of oxygen in the horizontal direction X, D_m is the mortar diffusion coefficient, dependent and the humidity conditions, and $\left(\frac{dC}{dt}\right)_{reaction}$ is the trend of oxygen consumption by the oxidation of the pyrrhotite. Its numerical solution in time and in space can allow the quantification of the oxygen

concentration $[\frac{mol}{m^3}]$ inside the concrete in the horizontal direction X, in a generic time instant. This relation is necessary to estimate the trend of oxygen concentration inside the concrete and so the quantity of the oxidized pyrrhotite (Oliveira et al, 2012).

The higher the concentration of oxygen, the higher the pyrrhotite oxidation. Therefore, if the oxygen diffuses quickly, the ISA will be faster and expansions and non-recoverable movements as well. Oxygen diffusion and pyrrhotite oxidation are dependent on aggregate grading curve and oxygen diffusion coefficient $[\frac{m^2}{s}]$, among other factors.

Hence, P parameter of the modelling of the top dam movements can be related to these parameters: oxygen concentration C (spatial and temporal variations), oxygen diffusion coefficient D (depends on the material in which it diffuses and its porosity, for example it diffuses more quickly in concrete than in pyrrhotite), quantity of pyrrhotite and kinetics of its oxidation.

Another factor that could have an influence is the degree of fracturing of the concrete superficial layer in direct contact with air. High degree of fracturing could alter Fick's second law results.

$$P_{horizonta} = P_{ISA} \leftrightarrow f(C, D, pyrrhotite\ content, degree\ of\ fracturing) \quad (17)$$

Where P depends on: oxygen concentration C=f(time, space, material), the oxygen diffusion coefficient D=f(material, porosity), the pyrrhotite content depends on the aggregate used and can been evaluated by means of laboratory testing, e.g. XR-efflorescence, degree of fracturing is a function of % of reacted pyrrhotite, environmental effects.

ASR

ASR instead depends on the water absorption of the alkali-silica gel reaction product, so depend on the water content and availability inside the concrete mass, that depend

on many factors, such as infiltration paths and magnitude, drainage systems, environmental conditions, and other factors.

Regarding the water availability, in the case of concrete dams an acceptable assumption is that all the concrete is saturated. This is clearly reasonable near the upstream face, that is in close contact with basin water, while it must be considered partially saturated in the case of the downstream face, that is in contact with atmosphere. The partially saturated zone has an extension of some meters as order of magnitude (Bazant and Wittman, 1982).

The degree of saturation of the concrete near the downstream face can be expressed, according to (Campos et al., 2012), in this way:

$$\theta(x) = \theta(x=0) + \left(1 - \theta(x=0)\right) \cdot (1 - e^{-\alpha \cdot x}) \qquad (18)$$

Where $\theta(x)$ is the content of water of the concrete in the downstream face at a distance x from the surface in contact with air and α is a shape parameter.

In the case of ASR phenomena, parameter P could be modelled with the water content inside the concrete mass, expressed by the equation (18), and the abovementioned oxygen availability C (equation (16)).

$$P_{ASR} \leftrightarrow \theta(x,t), alkali\ oxides\ content, degree\ of\ fracturing \qquad (19)$$

The P parameter of the vertical direction movements could embrace both the phenomena, as parameter B did. In this case a weight function w could be added, according to what phenomenon mainly occur: if in the vertical movements only the ASR is considered responsible: $w_{ASR} \cong 1$ and $w_{ISA} \cong 0$. Instead w_{ISA} increase if the ISA expansive phenomena act also in this direction.

$$P_{vertical} = w_{ISA} \cdot P_{ISA} + w_{ASR} \cdot P_{ASR} \qquad (20)$$

5.3.3 Parameter C

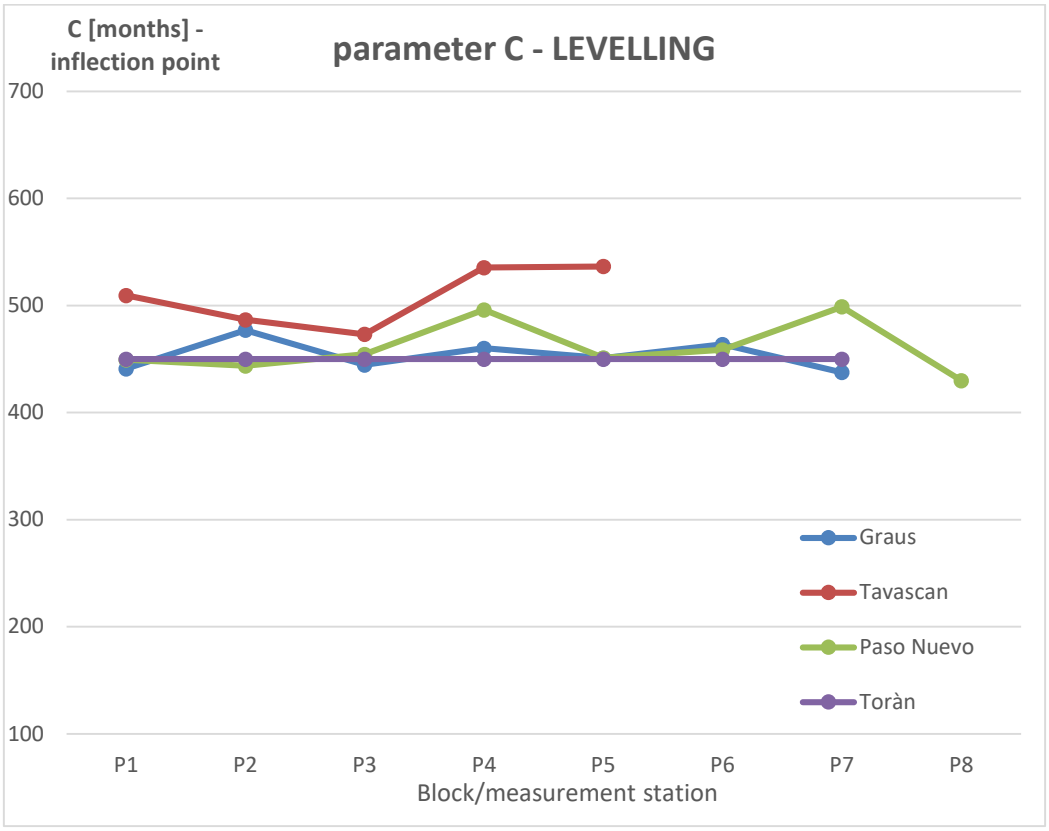

Figure 5.18 - Values of the parameter C of the model describing the levelling movements, for the four dams.

Parameter C show values that are similar among the dams. Clue that the reactions developed are of similar nature and take on average an analogous amount of time to assess. Slightly higher values in the case of Tavascan dam. Toràn dam values have been fixed to 450 months in the case of levelling, and to 350 months in the case of collimation, as mentioned in chapter 4.5.

The collimation movements fitting instead show values of the parameter C typically lower. While C of the levelling movements is almost always bigger than 450 months, the collimation ones are always lower than 400. The only exceptions are represented by the Paso Nuevo dam movements. In the latter dam, the levelling movements have bigger parameters, meaning that these movements stabilize later the levelling, in opposition to what happened in the other dams.

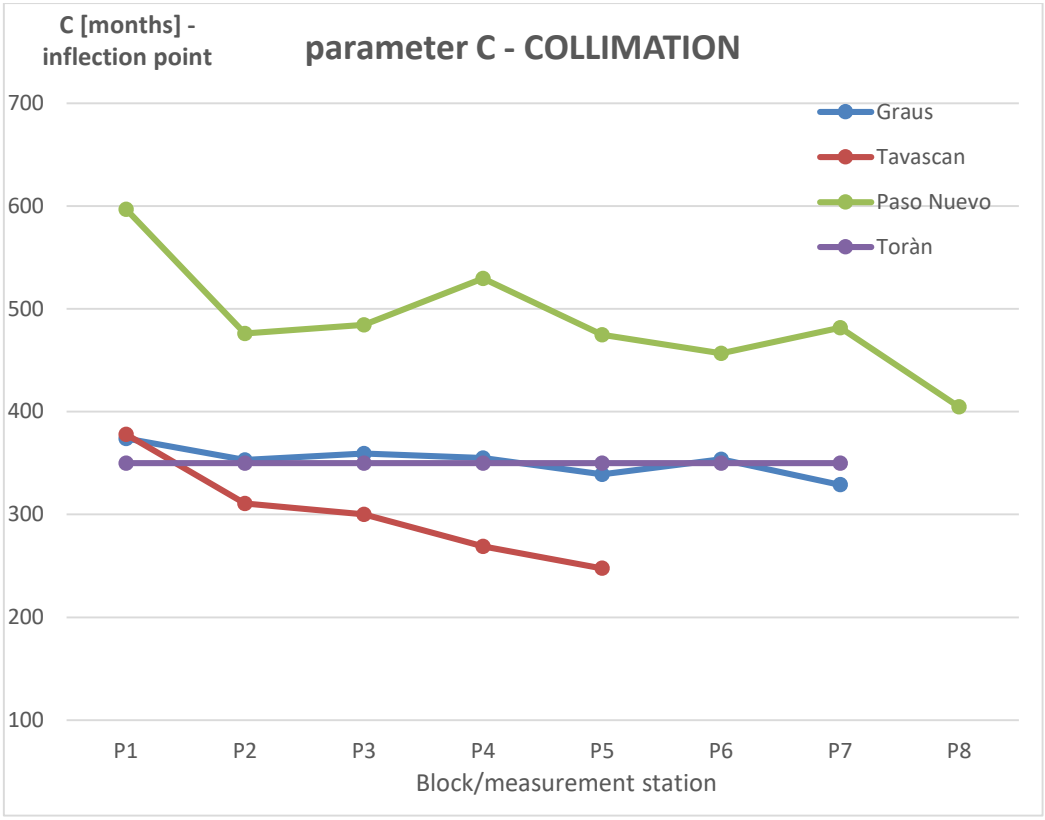

Figure 5.19 - Values of the parameter C of the model describing the collimation movements, for the four dams.

Parameter C could be modelled relating it to parameter B, since from the analytical point of view it corresponds to about the 63% of the total displacements, i.e. 63% of the value of parameter B. Hence it can be correlated to the same features which parameter B is linked to.

CHAPTER 6 – CONCLUSIONS

6.1 Conclusions

Movements in concrete dams happen and it's fundamental to understand what are the causes that generate them. The presence of a recoverable part of the movements is regular and it is addressed to seasonal variation. It is of interest that this variation be contained. The discussed non-recoverable part of movements instead must be carefully examined.

The monitoring of the movements at the top of the dams and the determination of the deterioration mechanisms that concrete is undergoing, are fundamental steps in the light of diagnosing the actual structure problem. The diagnostic phase will give the means, to skilled and aware engineers, to predict the future behaviour of the dams and hence setting the management of the maintenance plans. A great help comes from the modelling of the movements.

In the analysed dams, movements of collimation and levelling are modelled with the equation proposed by Aguado (1993). The parameters of the model can be related to specific issues of the degradation expansive phenomena. Movements always show up with three distinctive phases: initiation, development, stabilization. The model is able to characterize all of them adequately.

The robustness of the model is checked: portions of movements data are adjusted with the model and it is found out that the first part is not usually representative of the whole movements trend, i.e. it doesn't contain information on the future total expected displacement, neither on the time needed by the movements to completely show up. Therefore, a first conclusion is related to the time needed for the monitoring of the dam. Being the chemical reaction and the subsequent expansions of very slow character, many years of measurements are necessary in order to show signs of deterioration. It's hence of clear importance that auscultation systems are placed immediately after the dam construction.

The central part of the movements' data is more representative than the first one in terms of the whole displacement history. This part shows movements increasing at the highest rate. The importance of this central stage is in the inversion of trend of displacement increase, represented by parameter C, that is usually measured after 300-450 months (i.e. 25-37 years) from the dam commissioning. Having the two expansive phenomena different speed of development (ISA and ASR), the time at which there is an inversion of movement enhancement's rate is indicative of what of the two reaction is predominant. Information on speed of reactive development and movements happening is containe din the central part.

The final part of the movements resulted to be the most indicative part when compared to the whole displacement history. To obtain this, nevertheless, some constraints on the model had to be assumed, i.e. the value of parameter A. Setting the parameter A to 0 turned out to not altering the modelling of the whole data significantly. In addition it allowed the modelling of the last portion of data to reproduce quite accurately the whole displacement history. The main implication of this result is the capability to estimate the amplitude of the total displacements in a given direction (i.e. parameter B).

The last result allowed to estimate the movements history of the Toràn dam, whose movements turned out to be not enough for a modelling. Given the similarity with the Graus dam, in terms of material (concrete), dimensions and expansive phenomena (ISA and ASR), assumptions on parameters A, C and P, allowed to estimate the entity of the expected total movements of each block of the Toràn dam (i.e. parameters B).

The modelling of the movements with the equation proposed by Aguado showed good robustness, and hence it can be applied to registered movements data of a dam, once the deterioration mechanisms would have been identified in Internal Sulphate Attack or Alkali-Silica Reaction or a combination of the two and if sufficiently long data sets are available. Nevertheless, other information must be collected, e.g. extraction of cores and widespread laboratory analysis on the concrete.

Moreover, the parameters of the model proposed by Aguado have a precise physical meaning in the regards of the expansive characters of the phenomena, that have been described in chapter 5. The physical modelling of parameters, from a conceptual point of view, allowed to relate mathematical entities to physical and measurable aspects of the degradation phenomena, such as content of reactive aggregates, availability of oxidizing agents.

In the cases of Graus and Tavascan dams there seemed to be a good correlation between the entity of displacements and the geometry of the blocks, as was already assessed by Aguado et al. (1993). The potential total displacements (parameter B) could be modelled according to the direction: the vertical movements being caused to both ISA and ASR phenomena, the horizontal ones due to ISA only. The relation is proposed only at a conceptual level and tries to relate the amount of reactive agents (pyrrhotite, pyrite for ISA, and alkali oxides for ASR) to the strain that their expansion can provoke (equations (12) and (15)). Accounting for the geometry then, from the strain one move to the displacements, estimate them, and relate to the monitored one (chapter 5.3.1).

In the case of the Paso Nuevo dam, there seemed to be good correlation between the quantity of contaminated concrete of the 1st phase and height of the blocks and the expected total movements of that block. Geometry alone could not be related to the movements, therefore there was the need to introduce other variables, for example to account for local effects. Function g is introduced for this purpose. The function has still to be defined. In this stage only a conceptual view of what it could it be related to is proposed, e.g. presence of lateral abutments and induced change in stresses and stiffness of a block toward certain actions, or quantity of contaminated concrete in each block.

Parameter P, expressing the speed of reactions and movements developments, seemed correlated to the availability of oxidizing agents (oxygen and water) of the two expansive phenomena, inside the concrete cross-section. The physical relations of parameters P of the model are referred to the type of reaction (ISA and/or ASR) and

have been conceptually related to the access and diffusion of the oxidizing agents in the transversal direction (chapter 5.3.2). In the vertical direction, a weight function (equation (20)), could express the proportion of importance of the two expansive reactions.

6.2 Future perspectives

The physical modelling of the parameters has been carried out only at a conceptual level. The parameters of the model could be related to the physical parameters already mentioned with a higher level of detailing. For example, geometrical aspects could be addressed with more precision, or with characteristics different from the blocks' height. A parameter that could adequately describe the parameters of the mathematical model of Aguado is the contents of the ISA and ASR reactive components, that could be quantified from block to block. As well, local effects could be addressed into the model.

Numerical analysis could lead to more appropriate results when trying to estimate the total displacements of a point, caused by imposed strain. Alternatively, it could act as a control operator, assessing the goodness of the physical relations.

Kinetic has not been considered adequately, so it could be introduced into the modelling. It may have a relevant influence on the description and on the modelling of parameters C and P.

The analytical model proposed by Aguado is robust enough to be applied to dams for which only the last portions of data series are available. Still, other assumptions have to be made.

BIBLIOGRAPHY – REFERENCES

Aguado et al. (2014) "Estudio del comportamiento de la presa de Graus". Informe Final del Convenio CTT 8400, Barcelona, UniversitatPolitècnica de Catalunya.

Aguado et al. (2018) "Estudio del comportamiento de la presa de Tavascan". Informe Final del Convenio CTT 10572, Barcelona, Universitat Politècnica de Catalunya.

Aguado et al. (2020) "Re-evaluación del comportamiento de la presa de Paso Nuevo". Informe Final del Convenio CTT 11130, Barcelona, Universitat Politècnica de Catalunya.

Aguado, A.; López, C. Mª.; Casanova, I.; Agulló, L. (1996): Avances en el análisis del comportamiento de presas de hormigón. Cemento y Hormigón, Barcelona, pp. 832-852.

Aguado, A.; Agulló, L.; Casanova, I.; López, C. M. (1998): Estudio de fenómenos expansivos en presas de hormigón. De la micro a la macro estructura. Comité Español de Grande Presas. Premio José Torán, 103 p.

Aguado, A.; Agulló, L.; Bastus E.; Chinchón, S.; López, C; M., Vázquez, E.; Ayora, C. (1993): Estudio del comportamiento de las presas de Graus y Tabescan. Barcelona: Documento interno UPC. Convenio UPC. C-1327.

Araújo, G.S.; Chinchón, S.; Aguado, A. (2008): Comportamiento de presas de gravedad de hormigón con problemas de ataque interno por sulfatos. Revista Ibracon de estruturas e materiais. Volume 1, Number 1, p. 84 – 112

ASTM C1260-07 (2007): Standard test method for potential Alkali reactivity of aggregates (Mortar Bar method), American Society for Testing and Materials, Annual book of ASTM standards, p. 5.

Ayora, C.; Chichón, J. S.; Aguado, A.; Guirado, F. (1998): Weathering of iron-sulfides and concrete alteration: thermodynamic model and observation in dams from Central Pyrenees, Spain. Cement and Concrete Research, v 28, p. 1223-1235.

Bazant, Z. P.; Wittman, F. H. (1982), "Creep and shrinkage in concrete structures." John Wiley and Sons Ltd. New York, 374 pp.

Belzile, N.; Chen, Y.; Cai, M.; Li, Y. (2004): A review on pyrrhotite oxidation. Journa l of Geochemical Exploration, v. 84, pp. 65-76.

Bérubé, Ma.; Duchesne, J.; Dorion, J. F.; Rivest, M. (2002): Laboratory assessment of alkali contribution by aggregates to concrete and application to concrete structures affected by alkali– silica reactivity. Cement and Concrete Research, v. 32, n. 8, p. 1215-1227.

Campos de Moura, A. (2012): Análisis numérico de presas de hormigón bajo acciones expansivas. (PhD thesis), Barcelona, Universitat Politècnica de Catalunya.

Campos, A.; López, C.; Blanco, A.; Aguado, A. (2016): Structural diagnosis of a concrete dam with cracking and high non-recoverable displacements. Journal of Performance of Constructed Facilities 30 (5).

Casanova, I.; Agulló, L.; Aguado, A. (1996a), "Aggragate expansivity due to sulfide oxidation – I. Reaction system and rate model." Cement and Concrete Research, vol. 26, pp. 993-998.

Casanova, I.; Aguado, A.; Agulló, L.; Vázquez, E. (1996b), "Physico-chemical analysis of expansive phenomena in concrete dams." Dam Engineering, vol. 07, pp. 249-270.

Casanova, I.; Aguado, A.; Agulló, L. (1997): Aggregate expansivity due to sulfide oxidation - II. Physico-chemical modeling of sulfate attack. Cement and Concrete Research, v. 27, n. 11, p. 1627– 1632.

Chinchón, J. S.; Ayora, C.; Aguado, A.; Guirado, F. (1995), "Influence of weathering of iron sulfides contained in aggregates on concrete durability", Cement and Concrete Research, vol. 25, pp. 1264-1272.

del Hoyo, R.; Alonso, J. M.; Losada, J.; Velasco Pascual, J.; Baztán, J., (2002): Auscultación de presas de hormigón con problemas expansivos. VII Jornadas Españolas de Presas, Comité Nacional Español de Grandes Presas, vol. 3, Zaragoza, pp. 259-266.

Díez-Cascón, J.; Bueno, F. (2001), "Ingeniería de presas. Presas de fábrica." Servicio de publicaciones de la Universidad de Cantabria, Santander, 2 v., 929 p.

Divet, L. (2001) Les reactions sulfatiques internes au beton. Contribution a l´etude d es mecanismes de la formation differee de l´ettringite. Tesis Doctoral, Conservatoire National des Arts et Metiers, Paris, 227 p.

EN 206-1 Concrete – Part 1 (2001): Specification, performance, productivity and conformity.

Espinós, J.; Río, F.; Campos, A.; Oliveira I.; Aguado A. (2008): Hipótesis de partida del comportamiento de la presa de Paso Nuevo. VIII Jornadas Españolas de Presas. GECOLD. 26-28 Noviembre 2008, Córdoba, España ISBN: 978-84-380-0406-7. D.L.: M 50.342-2008 pp.: 43 and pp.: 1-10

Espinós, J.; Aguado A.; López, C.Mª.; Campos, A., Chinchón-Payá. S. (2010) Expansion studies for the Paso Nuevo dam. Proceedings of the 2nd International Congress on Dam Maintenance and Rehabilitation, Zaragoza, Spain, 23-25.11. 2010 CRC Press Taylor and Francis Group. Balkema. Editores: Rafael Romero et al. pp.: 143-152. ISBN 9780-415-61648-5.

Fournier, B.; Berubé, M. (2000): Alkali-aggregate reaction in concrete: a review of basic concepts and engineering implications. Canadian Journal of Civil Engineering, v. 27, n. 2, p. 167-191.

Gobbi, A. (2019): Reacciones expansivas internas: estudio de los áridos y hormigón de presas. (PhD thesis), Barcelona, Universitat Politècnica de Catalunya.

Gómez Arruche, J. (1989): Instrumentación y comportamiento de las presas de hormigon, (Cap.12), en Instrumentación de obras. E. Alonso, A. Gens, Editores. Edición de la Universitat Politécnica de Catalunya.

Guirguis B.; Shehata M. H.; Duchesne J.; Fournir B.; Durant B.; Rivard P. (2018): The application of new mortar bar test to mixtures containing different cementing systems. Construction and Building Materials 173, pp 775.785.

Hobbs, D. W. (1988): Alkali-silica reaction in concrete. Michigan: Telford.

Lindgård, J; Andiç.-Çakir, O.; Borchers I.; Broekmans M.; Brouard E.; Fernandes I.; Giebson C.; Pedersen B.; Pierre C.; Røniing T.F.; Thomas M.D.A.; Wigum B.J. (2011): RILEM TC 219-ACS-P: Literature survey on performance testing, COIN project report 27, pp. 164

Lutz M.; Müller R.; Pougatsch H.; Steiger K.; Straubhaar R. (2006): Swiss Committee on Dams on the occasion of the 22nd Congress of the International Commission on Large Dams, Barcelona.

Martinez Roig, J.M.; Aguado, A.; Agullo, L.; And Vazquez, E. (1991): Diagnostic of the behavior of the Graus and Tabescan dams. Seventeenth International Congress on Large Dams. Viena (Austria). Junio. I.S.B.N. 0254-0703. pp. 603-617.

Neville, A. M. (2002): Properties of concrete. Longman Group UK Limited.

Oliveira, I. (2011).; Reacción sulfática interna en presas de hormigón: cinética del comportamiento (PhD thesis), Barcelona, Universitat Politècnica de Catalunya.

Pardo, F. (2009): Estudio del diagnóstico y del tratamiento de presas de hormigón con expansiones. Barcelona: Tesina de final de carrera, Universidad Politécnica de Catalunya, 193 p.

Río, F.; Lopez, Ma. C.; Araujo, G.; Aguado, A. (2008): Análisis de la fisuración orient ada encoronación: interacción estribo-estructura. VIII Jornadas Españolas de Presas. GECOLD, Córdoba, España.

Rodrigues A.; Duchesne J.; Fournier B. (2015): A new accelerated mortar bar test to assess the potential deleterious effect of sulfide-bearing aggregates in concrete. Cement and Concrete Research 75, pp. 96-110.

Schmidt, T.; Leemann, A.; Gallucci, E.; Scrivener, K. L. (2011): physical and microstructural aspects of iron sulfide degradation in concrete. Cement and concrete research, 41, 263-269.

Skalny, J.; Marchand, J.; Odler, I. (2002): Sulfate Attack on Concrete. 10. ed. London: Spon Press.

Stankowski, T. (1990). Numerical simulation of progressive failure in particle composites. PhD thesis, University of Colorado, Boulder, EEUU.

Stanton, T. E. (1940): Expansion of concrete through reaction between cement and aggregate. American Society of Civil Engeneerings, New York, v. 66, p. 1781-1811.

Swamy I. (1992): The Alkali-Silica Reaction in Concrete. Department of Mechanical and Process Engineering, University of Sheffield, Blackie and Son Ltd.

TagnitHamou, A.; SaricCoric, M.; Rivard, P. (2005): Internal deterioration ofconcret e by the oxidation of pyrrhotitic aggregates. Cement and Concrete Research 35, pp. 99-107.

Ulm, F. J; Coussy, O.; Kefei, L.; Larive, C. (2000): "Thermo-chemo-mechanics of ASR expansion in concrete structures." Journal of Engineering Mechanics, vol. 126, pp. 233-242.

ANNEXES

ANNEX 1: SPLITTING OF THE DATASETS

In this annex are reported the data regarding the splitting of the data of the measurements.

The tables attached below report some of the measurements' information, for each block:

- Number of measurements N
- Years Y
- Density of measurements $\frac{N}{Y}$

Graus dam: Levelling

Levelling	**number of measurements**	**years**	**number of years**	**measurements/year**
block 1	245	1983-2018	36	6.8
block 2 - 3 - 4 - 5 - 6	252	1981-2018	38	6.6
block 7	69	2000-2018	19	3.6

3 PARTS, same number of years	**number of measurements**	**years**	**number of years**	**measurements/year**
block 1	245	1983-2018	36	
part 1	116	1983-1994	12	9.67
part 2	84	1995-2006	12	7.00
part 3	45	2007-2018	12	3.75
block 2 - 3 - 4 - 5 - 6	252	1981-2018	38	
part 1	111	1981-1993	13	8.54
part 2	97	1994-2006	13	7.46
part 3	48	2007-2018	12	4.00
block 7	69	2000-2018	19	
part 1	36	2000-2009	10	3.60
part 2	33	2010-2018	9	3.67

3 PARTS, same number of measurements	number of measurements	years	number of years	measurements/year
block 1	245	1983-2018	36	
part 1	82	1983-1991	9	9.11
part 2	82	1992-1999	8	10.25
part 3	81	2000-2018	19	4.26
block 2 - 3 - 4 - 5 - 6	252	1981-2018	38	
part 1	84	1981-1990	10	8.40
part 2	84	1991-1999	9	9.33
part 3	84	1999-2018	20	4.20
block 7	69	2000-2018	19	
part 1	23	2000-2006	7	3.29
part 2	23	2006-2012	7	3.29
part 3	23	2012-2018	7	3.29

blocks of 10 years	number of measurements	years	number of years	measurements/year
block 1	245	1983-2018	36	
first 10 years	97	1983-1993	10	9.70
second 10 years	88	1993-2003	10	8.80
third 10 years	38	2003-2013	10	3.80
fourth 10 years	22	2013-2018	6	3.67
block 2 - 3 - 4 - 5 - 6	252	1981-2018	38	
first 10 years	85	1981-1991	10	8.50
second 10 years	100	1991-2001	10	10.00
third 10 years	39	2001-2011	10	3.90
fourth 10 years	28	2011-2018	8	3.50
block 7	69	2000-2018	19	
first 10 years	36	2000-2009	10	3.60
second 10 years	33	2010-2018	9	3.67

blocks of cumulative 10 years	number of measurements	years	number of years	measurements/year
block 1	245	1983-2018	36	
cumulative 20 years	177	1983-2003	20	8.85
cumulative 30 years	216	1983-2013	30	7.20
block 2 - 3 - 4 - 5 - 6	252	1981-2018	38	
cumulative 20 years	185	1981-2001	20	9.25
cumulative 30 years	224	1981-2011	30	7.47

Graus dam: Collimation (only block 2 and 3 are reported)

Collimation	number of measurements	years	number of years	measurements/year
block 1	244	1983-2018	36	6.8
block 2 - 3	248	1983-2018	36	6.9
block 4	249	1981-2018	38	6.6
block 5	244	1981-2018	38	6.4
block 6	246	1981-2018	38	6.5
block 7	122	1999-2018	20	6.1

3 PARTS, same number of years	number of measurements	years	number of years	measurements/year
block 2 - 3	248	1983-2018	36	
part 1	119	1983-1994	12	9.92
part 2	89	1995-2006	12	7.42
part 3	40	2007-2018	12	3.33

3 PARTS, same number of measurements	number of measurements	years	number of years	measurements/year
block 2 - 3	248	1983-2018	36	
part 1	83	1983-1991	9	9.22
part 2	83	1991-1999	9	9.22
part 3	82	1999-2018	20	4.10

blocks of 10 years	number of measurements	years	number of years	measurements/year
block 2 - 3	248	1983-2018	36	
first 10 years	99	1983-1993	10	9.90
second 10 years	94	1993-2003	10	9.40
third 10 years	36	2003-2013	10	3.60
fourth 10 years	19	2013-2018	6	3.17

blocks of cumulative 10 years	number of measurements	years	number of years	measurements/year
block 2 - 3	248	1983-2018	36	
cumulative 20 years	196	1983-2003	20	9.80
cumulative 30 years	230	1983-2013	30	7.67

Tavascan dam: Levelling (only block 2, 3, 4 and 5 are reported)

3 PARTS, same number of years	number of measurements	years	number of years	measurements/year
block 2 - 3 - 4 - 5	490	1966-2018	53	
part 1	240	1966-1983	18	13.33
part 2	183	1984-2001	18	10.17
part 3	67	2002-2018	17	3.94

3 PARTS, same number of measurements	number of measurements	years	number of years	measurements/year
block 2 - 3 - 4 - 5	490	1966-2018	53	
part 1	164	1966-1976	11	14.91
part 2	163	1976-1991	16	10.19
part 3	163	1991-2018	28	5.82

blocks of 10 years	number of measurements	years	number of years	measurements/year
block 2 - 3 - 4 - 5	490	1966-2018	53	
first 10 years	158	1966-1975	10	15.80
second 10 years	105	1976-1985	10	10.50
third 10 years	104	1986-1995	10	10.40
fourth 10 years	72	1996-2005	10	7.20
fifth 10 years	51	2006-2018	13	3.92

blocks of cumulative 10 years	number of measurements	years	number of years	measurements/year
block 2 - 3 - 4 - 5	490	1966-2018	53	
cumulative 20 years	274	1966-1986	20	13.70
cumulative 30 years	378	1966-1996	30	12.60
cumulative 40 years	443	1966-2006	40	11.08

Tavascan dam: Collimation (only block 1, 2, 3 and 4 are reported)

3 PARTS, same number of years	number of measurements	years	number of years	measurements/year
block 1 - 2 - 3 - 4	497	1966-2018	53	
part 1	240	1966-1983	18	13.33
part 2	190	1984-2001	18	10.56
part 3	67	2002-2018	17	3.94

3 PARTS, same number of measurements	number of measurements	years	number of years	measurements/year
block 1 - 2 - 3 - 4	497	1966-2018	53	
part 1	166	1966-1976	11	15.09
part 2	166	1976-1991	16	10.38
part 3	165	1991-2018	28	5.89

blocks of 10 years	number of measurements	years	number of years	measurements/year
block 1 - 2 - 3 - 4	497	1966-2018	53	
first 10 years	158	1966-1975	10	15.80
second 10 years	105	1976-1985	10	10.50
third 10 years	104	1986-1995	10	10.40
fourth 10 years	78	1996-2005	10	7.80
fifth 10 years	52	2006-2018	13	4.00

blocks of cumulative 10 years	number of measurements	years	number of years	measurements/year
block 1 - 2 - 3 - 4	497	1966-2018	53	
cumulative 20 years	275	1966-1986	20	13.75
cumulative 30 years	378	1966-1996	30	12.60
cumulative 40 years	449	1966-2006	40	11.23

Paso Nuevo dam: Levelling and Collimation (all blocks)

3 PARTS, same number of years	number of measurements	years	number of years	vector position	measurements/year
block 1 to 8	81	1984-2018	35	1 81	
part 1	20	1984-1995	12	1 20	1.67
part 2	22	1996-2007	12	21-42	1.83
part 3	39	2008-2018	11	43-81	3.55

3 PARTS, same number of measurements	number of measurements	years	number of years	measurements/year
block 1 to 8	81	1984-2018	35	
part 1	27	1984-2001	18	1.50
part 2	27	2002-2012	11	2.45
part 3	27	2012-2018	7	3.86

blocks of 10 years	number of measurements	years	number of years	measurements/year
block 1 to 8	81	1984-2018	35	
first 10 years	19	1984-1993	10	1.90
second 10 years	14	1994-2003	10	1.40
third 10 years	32	2004-2013	10	3.20
fourth 10 years	16	2014-2018	5	3.20

blocks of cumulative 10 years	number of measurements	years	number of years	vector position	measurements/year
block 1 to 8	81	1984-2018	35	1 81	
cumulative 20 years	33	1984-2004	20	1 33	1.65
cumulative 30 years	65	1984-2014	30	1 65	2.17

ANNEX 2: RESULTS OF MODELLING OF PORTIONS OF MOVEMENTS

In this annex are reported the data of the modelling of the movements of levelling and collimation with the equation

$$y = A + B \cdot \left(1 - \exp\left(-\left(\frac{t}{C}\right)^{p}\right)\right)$$

for all the four dams investigated. The equation above is applied to different portions of data, that have been split in 4 different ways, to compare the different parts of the movements and their associated phase of the expansive phenomena. The splitting is explained in chapter 4.4.2.

The results of the modelling of portions of data are reported in this way:

- Parameters obtained from fitting each one of the 3 parts (A<0), having divided the data in 3 parts having the same number of measurements
- Parameters obtained from fitting each one of the 3 parts (A=0), having divided the data in 3 parts having the same number of measurements
- Parameters obtained from fitting each one of the 3 parts (A<0), having divided the data in 3 parts having the same number of years
- Parameters obtained from fitting each one of the 3 parts (A=0), having divided the data in 3 parts having the same number of years
- Difference between A=0 and A<0 cases
- Difference between parts of the data and whole data set fittings
- Same procedure, but splitting in blocks of 10 years
- Same procedure, but splitting in blocks of the first 20-30-40 years

Not all the data have been reported, only the modelling of a representative block. The attached data include: GRAUS block 5, TAVASCAN block 2 and PASO NUEVO block 7. Both levelling and collimation are reported.

The plots are reported only in for the Graus splitting data.

Graus dam: B5 Levelling. 3 parts: (A<0), (A=0), differences, differences with whole data set in the case A=

B5 - LEVELLING - SAME NUMBER OF MEASUREMENTS			
A = 0	part 1	part 2	part 3
a	0	0	0
b	73.79	61.76	134.3
c	357.2	334.9	448.7
p	3.613	3.673	3.406
R^2	0.9915	0.9932	0.9993
SSE	10.04	27.25	36.91
RMSE	0.352	0.58	0.6879

B5 - LEVELLING - SAME NUMBER OF YEARS			
A < 0	part 1	part 2	part 3
a	-0.1705	-5.0E-8	-90.96
b	111.7	185.3	251.1
c	414.1	516.2	405
p	3.448	3.188	1.81
R^2	0.9793	0.9984	0.9958
SSE	84.45	33.67	37.7
RMSE	0.8885	0.6017	0.9589

A < 0	part 1	part 2	part 3
a	-4.7E-12	-0.0208	-47.26
b	68.27	61	205.1
c	348.2	333	441.7
p	3.627	3.692	2.122
R^2	0.9915	0.9933	0.9994
SSE	10.04	27.25	30.11
RMSE	0.352	0.5837	0.6253

A = 0	part 1	part 2	part 3
a	0	0	0
b	84.97	175.4	137.4
c	374.2	504	454.4
p	3.587	3.219	3.288
R^2	0.9793	0.9984	0.9958
SSE	84.47	33.67	37.68
RMSE	0.8844	0.5985	0.9472

DIFFERENCE	part 1	part 2	part 3
b	8.1	1.2	-34.5
c	2.6	0.6	1.6
p	-0.4	-0.5	60.5
R^2	0.00	-0.01	-0.01
SSE	0.00	0.00	22.58
RMSE	0.00	-0.63	10.01

DIFFERENCE	part 1	part 2	part 3
b	-23.9	-5.3	-45.3
c	-9.6	-2.4	12.2
p	4.0	1.0	81.7
R^2	0.00	0.00	0.00
SSE	0.02	0.00	-0.05
RMSE	-0.46	-0.53	-1.22

B5 - LEVELLING - SAME NUMBER OF MEASUREMENTS			
DIFFERENCE WITH RESPECT TO WHOLE DATA SET (A=0)	part 1	part 2	part 3
b	-50.0	-55.3	50.3
c	-23.1	-26.4	-2.4
p	8.5	10.4	-36.5
R^2	-0.8	-0.7	-0.1
SSE	-67.4	-11.4	-2.1
RMSE	-0.7	64.7	76.4

B5 - LEVELLING - SAME NUMBER OF YEARS			
DIFFERENCE WITH RESPECT TO WHOLE DATA SET (A=0)	part 1	part 2	part 3
b	-37.8	28.5	0.7
c	-17.3	11.4	0.4
p	7.3	-3.7	-1.6
R^2	-2.1	-0.2	-0.4
SSE	174.5	9.4	22.5
RMSE	149.5	68.9	167.3

Graus dam: B5 Collimation. 3 parts: (A<0), (A=0), differences, differences with whole data set in the case A=0

B5 - COLLIMATION - SAME NUMBER OF MEASUREMENTS			
A < 0	part 1	part 2	part 3
a	-5.713	-74.58	-202.6
b	372.7	617.9	493.9
c	369.8	583.7	291.6
p	3.387	1.485	1.406
R^2	0.999	0.9963	0.9894
SSE	30.85	123.43	893.93
RMSE	0.6289	1.2661	3.5994

B5 - COLLIMATION - SAME NUMBER OF YEARS			
A < 0	part 1	part 2	part 3
a	-3.983	-66.05	-0.000067
b	143.8	361.4	274.7
c	260.6	360.4	375.9
p	3.95	1.877	2.156
R^2	0.9996	0.9974	0.9189
SSE	29.98	233.71	784.08
RMSE	0.5503	1.5522	5.2918

B5 - COLLIMATION - SAME NUMBER OF MEASUREMENTS			
A = 0	part 1	part 2	part 3
a	0	0	0
b	102.1	216.1	264.8
c	233.2	324.8	367.8
p	4.845	3.073	2.408
R^2	0.9988	0.9961	0.9981
SSE	37.24	130.49	163.51
RMSE	0.6866	1.2934	1.5283

B5 - COLLIMATION - SAME NUMBER OF YEARS			
A = 0	part 1	part 2	part 3
a	0	0	0
b	121	237	278.4
c	247.5	342.3	379
p	4.579	2.898	2.068
R^2	0.9996	0.9973	0.9172
SSE	35.64	240.39	800.48
RMSE	0.597	1.5662	5.2538

DIFFERENCE	part 1	part 2	part 3
b	-72.6	-65.0	-46.4
c	-36.9	-44.4	26.1
p	43.0	106.9	71.3
R^2	-0.02	-0.02	0.88
SSE	20.71	5.72	-81.71
RMSE	9.17	2.16	-57.54

DIFFERENCE	part 1	part 2	part 3
b	-15.9	-34.4	1.35
c	-5.0	-5.0	0.82
p	15.9	54.4	-4.08
R^2	0.00	-0.01	-0.19
SSE	18.88	2.86	2.09
RMSE	8.49	0.90	-0.72

DIFFERENCE WITH RESPECT TO THE WHOLE DATA SET (A=0)	part 1	part 2	part 3
b	-56.5	-8.0	12.7
c	-31.2	-4.2	8.5
p	57.0	-0.4	-22.0
R^2	-0.1	-0.4	-0.2
SSE	-89.2	-62.3	-52.8
RMSE	-43.7	6.1	25.4

DIFFERENCE WITH RESPECT TO THE WHOLE DATA SET (A=0)	part 1	part 2	part 3
b	-48.5	0.9	18.5
c	-27.0	0.9	11.8
p	48.4	-6.1	-33.0
R^2	0.0	-0.2	-8.3
SSE	-89.7	-30.6	131.1
RMSE	-51.0	28.5	330.9

Graus dam: B5 Levelling. Blocks of 10 years: (A<0), (A=0), differences, differences with whole data set in the case A=0

B5 - LEVELLING - BLOCKS OF 10 YEARS				
A < 0	B5 - first 10	B5 - second 10	B5 - third 10	B5 - fourth 10
a	-2.8E-14	-1.088	-114.6	-2.4E-14
b	50.38	2870	538.3	130.9
c	314.6	1635	935.8	451.8
p	3.701	2.666	1.048	4.015
R^2	0.9919	0.9965	0.9963	0.9756
SSE	10.01	29.47	24.12	45.56
RMSE	0.3493	0.554	0.8302	1.4391

A = 0	B5 - first 10	B5 - second 10	B5 - third 10	B5 - fourth 10
a	0	0	0	0
b	50.39	594.5	135	130.9
c	314.6	853.2	450	451.7
p	3.701	2.833	3.303	4.003
R^2	0.9919	0.9964	0.9959	0.9756
SSE	10.01	29.8	26.33	45.56
RMSE	0.3493	0.5543	0.8552	1.4391

DIFFERENCE	B5 - first 10	B5 - second 10	B5 - third 10	B5 - fourth 10
b	0.0	-79.3	-74.9	0.0
c	0.0	-47.8	-51.9	0.0
p	0.0	6.3	215.2	-0.3
R^2	0.00	-0.01	-0.04	0.00
SSE	0.00	1.12	9.16	0.00
RMSE	0.00	0.05	3.01	0.00

DIFFERENCE WITH RESPECT TO THE WHOLE DATA SET (A=0)	B5 - first 10	B5 - second 10	B5 - third 10	B5 - fourth 10
b	-62.7	339.7	-0.1	-3.2
c	-30.2	89.3	-0.2	0.2
p	9.9	-15.9	-1.9	18.9
R^2	-0.8	-0.4	-0.4	-2.4
SSE	-68.1	-5.1	-16.1	45.1
RMSE	-2.2	55.2	139.4	302.9

Graus dam: B5 Collimation. Blocks of 10 years: (A<0), (A=0), differences, differences with whole data set in the case A=0

B5 - LEVELLING - SAME NUMBER OF MEASUREMENTS				
A < 0	first 10	second 10	third 10	fourth 10
a	-3.619	-11.23	-4E-12	-5.6E-07
b	130.3	265.3	237.9	247.7
c	251.5	351.1	342.9	443.9
p	4.091	2.618	2.876	10.42
R^2	0.9988	0.9972	0.988	0.9222
SSE	29.61	194.01	130.2	152.23
RMSE	0.6283	1.3999	1.9569	3.4219
A = 0	first 10	second 10	third 10	fourth 10
a	0	0	0	0
b	95.41	228.7	236.7	247.7
c	227.9	335.2	342.1	443.7
p	4.97	2.976	2.905	10.4
R^2	0.9986	0.9971	0.9878	0.9205
SSE	34.23	197.35	131.96	155.49
RMSE	0.6711	1.4048	1.9701	3.3326
DIFFERENCE	first 10	second 10	third 10	fourth 10
b	-26.8	-13.8	-0.5	0.0
c	-9.4	-4.5	-0.2	0.0
p	21.5	13.7	1.0	-0.2
R^2	-0.02	-0.01	-0.02	-0.18
SSE	15.60	1.72	1.35	2.14
RMSE	6.81	0.35	0.67	-2.61
DIFFERENCE WITH RESPECT TO THE WHOLE DATA SET (A=0)	first 10	second 10	third 10	fourth 10
b	-59.4	-2.6	0.8	5.4
c	-32.8	-1.2	0.9	30.8
p	61.0	-3.6	-5.9	237.0
R^2	-0.1	-0.3	-1.2	-7.9
SSE	-90.1	-43.0	-61.9	-55.1
RMSE	-45.0	15.2	61.6	173.3

Graus dam: B5 Levelling. Blocks of the first 20-30-40 years: (A<0), (A=0), differences, differences with whole data set in the case A=0

B5 - LEVELLING - BLOCKS OF 20 AND 30 YEARS		
A < 0	B5 - cumulative 20	B5 - cumulative 30
a	-0.5115	-0.299
b	114.3	144.3
c	429.6	464.2
p	3.246	3.283
R^2	0.9993	0.9998
SSE	22.59	24.03
RMSE	0.3533	0.3305

A = 0	B5 - cumulative 20	B5 - cumulative 30
a	0	0
b	93.68	139.4
c	394.3	457.1
p	3.453	3.337
R^2	0.9993	0.9998
SSE	23.15	24.05
RMSE	0.3567	0.3299

DIFFERENCE	B5 - cumulative 20	B5 - cumulative 30
b	-18.0	-3.4
c	-8.2	-1.5
p	6.4	1.6
R^2	0.00	0.00
SSE	2.48	0.08
RMSE	0.96	-0.18

DIFFERENCE WITH RESPECT TO THE WHOLE DATA SET (A=0)	B5 - cumulative 20	B5 - cumulative 30
b	-30.7	3.1
c	-12.5	1.4
p	2.5	-0.9
R^2	-0.1	0.0
SSE	-26.3	-23.4
RMSE	-0.1	-7.6

Graus dam: B5 Collimation. Blocks of the first 20-30-40 years: (A<0), (A=0), differences, differences with whole data set in the case A=0

B5 - COLLIMATION - BLOCKS OF 20 AND 30 YEARS		
A < 0	**B5 - cumulative 20**	**B5 - cumulative 30**
a	-11.82	-18.53
b	211.6	259.4
c	304.9	335.8
p	3.052	2.633
R^2	0.9999	0.9992
SSE	39.71	727.31
RMSE	0.4737	1.8435
A = 0	**B5 - cumulative 20**	**B5 - cumulative 30**
a	0	0
b	172.4	220.8
c	287.8	326.5
p	3.844	3.327
R^2	0.9998	0.9972
SSE	83.24	2435.7
RMSE	0.6838	3.3658
DIFFERENCE	**B5 - cumulative 20**	**B5 - cumulative 30**
b	-18.5	-14.9
c	-5.6	-2.8
p	26.0	26.4
R^2	-0.01	-0.20
SSE	109.62	234.89
RMSE	44.35	82.58

DIFFERENCE WITH RESPECT TO THE WHOLE DATA SET (A=0)	**B5 - cumulative 20**	**B5 - cumulative 30**
b	-26.6	-6.0
c	-15.1	-3.7
p	24.6	7.8
R^2	0.0	-0.3
SSE	-76.0	603.2
RMSE	-43.9	176.1

Tavascan dam: B2 Levelling. 3 parts: (A<0), (A=0), differences, differences with whole data set in the case A=0

B2 - LEVELLING - SAME NUMBER OF MEASUREMENTS			
A < 0	B2 - part 1	B2 - part 2	B2 - part 3
a	-2.5E-14	-7.95	-4.4E-14
b	3.524	419.7	82.07
c	47.34	1962	494.3
p	1.546	1.351	2.103
R^2	0.5416	0.9962	0.9937
SSE	180.44	27.53	151.96
RMSE	1.0586	0.4161	0.9746

B2 - LEVELLING - SAME NUMBER OF YEARS			
A < 0	B2 - part 1	B2 - part 2	B2 - part 3
a	-2.4E-14	-12.39	-2.2E-14
b	994.7	297.4	82.63
c	3059	1490	495.6
p	1.674	1.266	2.084
R^2	0.987	0.9897	0.978
SSE	37.36	154.02	65.09
RMSE	0.397	0.9276	1.0085

A = 0	B2 - part 1	B2 - part 2	B2 - part 3
a	0	0	0
b	3.526	36.49	82.07
c	47.38	293	494.3
p	1.545	2.847	2.103
R^2	0.5417	0.9961	0.9937
SSE	180.42	28.4	151.96
RMSE	1.0586	0.4213	0.9746

A = 0	B2 - part 1	B2 - part 2	B2 - part 3
a	0	0	0
b	993.8	73.27	83.61
c	3057	453.2	502.4
p	1.674	2.238	2.055
R^2	0.987	0.9893	0.9716
SSE	37.36	159.72	84.09
RMSE	0.397	0.942	1.1462

DIFFERENCE	B2 - part 1	B2 - part 2	B2 - part 3
b	0.1	-91.3	0.0
c	0.1	-85.1	0.0
p	-0.1	110.7	0.0
R^2	0.02	-0.01	0.00
SSE	-0.01	3.16	0.00
RMSE	0.00	1.25	0.00

DIFFERENCE	B2 - part 1	B2 - part 2	B2 - part 3
b	-0.09	-75.36	1.19
c	-0.07	-69.58	1.37
p	0.00	76.78	-1.39
R^2	0.00	-0.04	-0.65
SSE	0.00	3.70	29.19
RMSE	0.00	1.55	13.65

DIFFERENCE WITH RESPECT TO THE WHOLE DATA SET (A=0)	B2 - part 1	B2 - part 2	B2 - part 3
b	-95.6	-54.7	1.8
c	-90.3	-39.8	1.5
p	-28.2	32.4	-2.2
R^2	-45.8	-0.4	-0.6
SSE	522.6	-2.0	424.4
RMSE	333.9	72.7	299.4

DIFFERENCE WITH RESPECT TO THE WHOLE DATA SET (A=0)	B2 - part 1	B2 - part 2	B2 - part 3
b	1132.7	-9.1	3.7
c	528.0	-6.9	3.2
p	-22.2	4.0	-4.5
R^2	-1.3	-1.1	-2.8
SSE	28.9	451.1	190.2
RMSE	62.7	286.1	369.8

Tavascan dam: B2 Collimation. 3 parts: (A<0), (A=0), differences, differences with whole data set in the case A=0

B2 - COLLIMATION - SAME NUMBER OF MEASUREMENTS			
A < 0	C2 - part 1	C2 - part 2	C2 - part 3
a	-1.143	-1.1E-06	-0.4834
b	14.67	32.39	26.6
c	307.2	358	302
p	1.064	2.111	2.557
R^2	0.6889	0.9951	0.8446
SSE	155.52	13.6	209.51
RMSE	0.9798	0.2898	1.1407

B2 - COLLIMATION - SAME NUMBER OF YEARS			
A < 0	C2 - part 1	C2 - part 2	C2 - part 3
a	-0.65	-7.9E-09	-0.0326
b	1092	26.35	25.91
c	6691	304.1	395.5
p	1.378	2.431	9.772
R^2	0.8944	0.9535	0.0908
SSE	235.16	173.66	98.49
RMSE	0.9982	0.9637	1.2503

B2 - COLLIMATION - SAME NUMBER OF MEASUREMENTS			
A = 0	C2 - part 1	C2 - part 2	C2 - part 3
a	0	0	0
b	4.401	31.84	26.1
c	103.1	353.3	304
p	2.562	2.125	2.594
R^2	0.648	0.9953	0.8447
SSE	175.95	13.09	209.41
RMSE	1.039	0.2834	1.137

B2 - COLLIMATION - SAME NUMBER OF YEARS			
A = 0	C2 - part 1	C2 - part 2	C2 - part 3
a	0	0	0
b	46.89	26.44	25.88
c	519.4	305	395.5
p	1.746	2.423	9.763
R^2	0.8855	0.9535	0.0908
SSE	254.96	173.76	98.49
RMSE	1.0372	0.964	1.2405

DIFFERENCE	C2 - part 1	C2 - part 2	C2 - part 3
a	-	-	-
b	-70.0	-1.7	-1.9
c	-66.4	-1.3	0.7
p	140.8	0.7	1.4
R^2	-5.94	0.02	0.01
SSE	13.14	-3.75	-0.05
RMSE	6.04	-2.21	-0.32

DIFFERENCE	C2 - part 1	C2 - part 2	C2 - part 3
a	-	-	-
b	-95.7	0.3	-0.12
c	-92.2	0.3	0.00
p	26.7	-0.3	-0.09
R^2	-1.00	0.00	0.00
SSE	8.42	0.06	0.00
RMSE	3.91	0.03	-0.78

DIFFERENCE	C2 - part 1	C2 - part 2	C2 - part 3
a	-	-	-
b	-83.7	17.8	-3.4
c	-66.8	13.7	-2.1
p	15.1	-4.5	16.6
R^2	-34.3	0.8	-14.4
SSE	-69.7	-97.7	-63.9
RMSE	-4.2	-73.9	4.9

DIFFERENCE	C2 - part 1	C2 - part 2	C2 - part 3
a	-	-	-
b	73.5	-2.2	-4.3
c	67.2	-1.8	27.3
p	-21.5	8.9	338.8
R^2	-10.3	-3.4	-90.8
SSE	-56.1	-70.1	-83.0
RMSE	-4.3	-11.1	14.4

Tavascan dam: B2 Levelling. Blocks of 10 years: (A<0), (A=0), differences, differences with whole data set in the case A=0

B2 - LEVELLING - BLOCKS OF 10 YEARS					
A < 0	first 10	second 10	third 10	fourth 10	fifth 10
a	-3.1E-14	-6.451	-15.76	-43.04	-1.153
b	3.492	88.09	167.7	156.5	87.87
c	46.46	539.5	828.9	525.2	515
p	1.563	1.532	1.28	1.103	1.938
R^2	0.5272	0.9833	0.97	0.964	0.9881
SSE	180.7	32.88	88.27	63.29	14.48
RMSE	1.0797	0.5706	0.9395	0.9647	0.555

A = 0	first 10	second 10	third 10	fourth 10	fifth 10
a	0	0	0	0	0
b	3.492	18.48	53.84	67.69	86.18
c	46.46	205.3	367.8	427.2	515.7
p	1.563	3.603	2.555	2.511	1.978
R^2	0.5272	0.9833	0.9693	0.9628	0.9881
SSE	180.7	32.93	90.21	65.44	14.47
RMSE	1.0797	0.5682	0.9451	0.9739	0.5491

DIFFERENCE	first 10	second 10	third 10	fourth 10	fifth 10
b	0.00	-79.02	-67.90	-56.75	-1.92
c	0.00	-61.95	-55.63	-18.66	0.14
p	0.00	135.18	99.61	127.65	2.06
R^2	0.00	0.00	-0.07	-0.12	0.00
SSE	0.00	0.15	2.20	3.40	-0.07
RMSE	0.00	-0.42	0.60	0.95	-1.06

DIFFERENCE WITH RESPECT TO THE WHOLE DATA SET (A=0)	first 10	second 10	third 10	fourth 10	fifth 10
b	-95.7	-77.1	-33.2	-16.0	6.9
c	-90.5	-57.8	-24.4	-12.2	5.9
p	-27.3	67.5	18.8	16.7	-8.0
R^2	-47.3	-1.7	-3.1	-3.7	-1.2
SSE	523.5	13.6	211.3	125.8	-50.1
RMSE	342.5	132.9	287.3	299.1	125.0

Tavascan dam: B2 Collimation. Blocks of 10 years: (A<0), (A=0), differences, differences with whole data set in the case A=0

B2 - COLLIMATION - BLOCKS OF 10 YEARS					
A < 0	first 10	second 10	third 10	fourth 10	fifth 10
a	-1.165	-1.9E-06	-11.74	-5.2E-05	couldn't fit, this last portion of data show decreasing movement trend, so the R^2 correlation was anyways negative (see graph)
b	46.44	48.67	88.75	56.39	
c	1188	465.9	780	760.9	
p	0.9892	2.001	1.033	1.053	
R^2	0.65641	0.9825	0.9062	0.6221	
SSE	154.57	12.42	79.29	90.14	
RMSE	1.0019	0.3507	0.8904	1.1037	

A = 0	first 10	second 10	third 10	fourth 10	fifth 10
a	0	0	0	0	couldn't fit, this last portion of data show decreasing movement trend, so the R^2 correlation was anyways negative (see graph)
b	5.631	41.92	37.95	56.53	
c	121.9	424.5	405	765	
p	2.318	2.027	1.976	1.05	
R^2	0.6073	0.9825	0.905	0.6221	
SSE	175.48	12.43	80.27	90.14	
RMSE	1.064	0.349	0.8915	1.0963	

DIFFERENCE	first 10	second 10	third 10	fourth 10	fifth 10
b	-87.87	-13.87	-57.24	0.25	-
c	-89.74	-8.89	-48.08	0.54	-
p	134.33	1.30	91.29	-0.28	-
R^2	-7.48	0.00	-0.13	0.00	-
SSE	13.53	0.08	1.24	0.00	-
RMSE	6.20	-0.48	0.12	-0.67	-

DIFFERENCE WITH RESPECT TO THE WHOLE DATA SET (A=0)	first 10	second 10	third 10	fourth 10	fifth 10
b	-79.17	55.09	40.40	109.14	-
c	-60.75	36.67	30.39	146.30	-
p	4.18	-8.90	-11.19	-52.81	-
R^2	-38.47	-0.46	-8.31	-36.97	-
SSE	-69.77	-97.86	-86.17	-84.47	-
RMSE	-1.85	-67.80	-17.76	1.13	-

Tavascan dam: B2 Levelling. Blocks of the first 20-30-40 years: (A<0), (A=0), differences, differences with whole data set in the case A=0

B2 - LEVELLING - BLOCKS OF 20-30-40 YEARS			
A < 0	B2 - cum 20	B2 - cum 30	B2 - cum 40
a	-2.4E-14	-2.6E-14	-2.3E-14
b	2718	248	83.24
c	3987	966.2	497.8
p	1.843	1.96	2.135
R^2	0.9945	0.9992	0.9997
SSE	36.4	32.28	29.74
RMSE	0.3665	0.2934	0.26

A = 0	B2 - cum 20	B2 - cum 30	B2 - cum 40
a	0	0	0
b	2701	255.6	83.24
c	3974	984.1	497.8
p	1.843	1.956	2.135
R^2	0.9945	0.9992	0.9997
SSE	36.4	31.89	29.74
RMSE	0.3665	0.2916	0.26

DIFFERENCE	B2 - cum 20	B2 - cum 30	B2 - cum 40
b	-0.63	3.06	0.00
c	-0.33	1.85	0.00
p	0.00	-0.20	0.00
R^2	0.00	0.00	0.00
SSE	0.00	-1.21	0.00
RMSE	0.00	-0.61	0.00

DIFFERENCE WITH RESPECT TO THE WHOLE DATA SET (A=0)	B2 - cum 20	B2 - cum 30	B2 - cum 40
b	3250.29	217.04	3.25
c	716.35	102.16	2.26
p	-14.32	-9.07	-0.74
R^2	-0.53	-0.06	-0.01
SSE	25.60	10.04	2.62
RMSE	50.20	19.51	6.56

Tavascan dam: B2 Collimation. Blocks of the first 20-30-40 years: (A<0), (A=0), differences, differences with whole data set in the case A=0

B2 - COLLIMATION - BLOCKS OF 20-30-40 YEARS			
A < 0	C2 - cum 20	C2 - cum 30	C2 - cum 40
a	-0.4755	-0.401	-0.0373
b	1749	60.9	29.55
c	5945	588.2	334.4
p	1.558	1.729	2.099
R^2	0.9386	0.9991	0.9995
SSE	272.41	15.66	17.21
RMSE	1.0026	0.2046	0.1966

A = 0	C2 - cum 20	C2 - cum 30	C2 - cum 40
a	0	0	0
b	1720	43.73	29.25
c	4312	454.2	332
p	1.736	1.898	2.116
R^2	0.9357	0.9992	0.9995
SSE	285.48	15.26	16.38
RMSE	1.0245	0.2017	0.1916

DIFFERENCE	C2 - cum 20	C2 - cum 30	C2 - cum 40
a	-	-	-
b	-1.66	-28.19	-1.02
c	-27.47	-22.78	-0.72
p	11.42	9.77	0.81
R^2	-0.31	0.01	0.00
SSE	4.80	-2.55	-4.82
RMSE	2.184321	-1.4174	-2.54323

DIFFERENCE WITH RESPECT TO THE WHOLE DATA SET (A=0)	B2 - cum 20	B2 - cum 30	B2 - cum 40
b	6263.30	61.78	8.21
c	1288.28	46.23	6.89
p	-21.98	-14.70	-4.90
R^2	-5.20	1.24	1.27
SSE	-50.82	-97.37	-97.18
RMSE	-5.49	-81.39	-82.32

Paso Nuevo dam: B7 Levelling. 3 parts: (A<0), (A=0), differences, differences with whole data set in the case A=0

B7 - LEVELLING - SAME NUMBER OF MEASUREMENTS			
A < 0	part 1	part 2	part 3
a	-29.89	-4.9E-14	-0.000000012
b	45.46	19.36	74.75
c	174.1	421.4	1051
p	0.8055	10.76	1.567
R^2	0.7045	0.6328	0.456
SSE	77.96	106.49	52.45
RMSE	1.8411	2.1065	1.5101

B7 - LEVELLING - SAME NUMBER OF YEARS			
A < 0	part 1	part 2	part 3
a	-11.22	-0.000000017	-0.000098
b	39.3	538.7	104.1
c	477.3	1247	1418
p	1.143	3.413	1.481
R^2	0.6498	0.7623	0.5876
SSE	44.05	93.02	111.64
RMSE	1.6593	2.2733	1.812

A = 0	part 1	part 2	part 3
a	0	0	0
b	7.881	19.2	84.95
c	276.1	422.4	1190
p	5.849	12.04	1.512
R^2	0.6906	0.6128	0.4553
SSE	81.64	112.29	52.52
RMSE	1.8444	2.1631	1.5111

A = 0	part 1	part 2	part 3
a	0	0	0
b	7.205	569.7	289.9
c	260.9	1242	3575
p	6.678	3.478	1.339
R^2	0.6269	0.7592	0.5876
SSE	46.94	94.23	111.62
RMSE	1.6616	2.227	1.7858

DIFFERENCE	part 1	part 2	part 3
a	-	-	-
b	-82.7	-0.8	13.6
c	58.6	0.2	13.2
p	626.1	11.9	-3.5
R^2	-1.97	-3.16	-0.15
SSE	4.72	5.45	0.13
RMSE	0.18	2.69	0.07

DIFFERENCE	part 1	part 2	part 3
a	-	-	-
b	-81.7	5.8	178.5
c	-45.3	-0.4	152.1
p	484.3	1.9	-9.6
R^2	-3.5	-0.4	0.0
SSE	6.6	1.3	0.0
RMSE	0.1	-2.0	-1.4

B7 - LEVELLING - SAME NUMBER OF MEASUREMENTS			
DIFFERENCE WITH RESPECT TO THE WHOLE DATA SET (A=0)	part 1	part 2	part 3
a	-	-	-
b	-74.1	-36.9	179.3
c	-44.7	-15.4	138.5
p	81.5	273.7	-53.1
R^2	-27.3	-35.4	-52.0
SSE	-70.7	-59.7	-81.2
RMSE	-3.1	13.6	-20.6

B7 - LEVELLING - SAME NUMBER OF YEARS			
DIFFERENCE WITH RESPECT TO THE WHOLE DATA SET (A=0)	part 1	part 2	part 3
a	-	-	-
b	-76.3	1773.4	853.3
c	-47.7	148.9	616.4
p	107.3	7.9	-58.4
R^2	-34.0	-20.0	-38.1
SSE	-83.2	-66.2	-60.0
RMSE	-12.7	17.0	-6.2

Paso Nuevo dam: B7 Collimation. 3 parts: (A<0), (A=0), differences, differences with whole data set in the case A=0

B7 - COLLIMATION - SAME NUMBER OF MEASUREMENTS			
A < 0	B7 - part 1	B7 - part 2	B7 - part 3
a	0.7682	99.05	1.6E-09
b	-20.31	-172.2	-3092
c	322.3	337.3	2866
p	6.322	1.436	2.512
R^2	0.9083	0.8646	0.8649
SSE	119.47	144.46	125.09
RMSE	2.2792	2.5062	2.3321

B7 - COLLIMATION - SAME NUMBER OF YEARS			
A < 0	B7 - part 1	B7 - part 2	B7 - part 3
a	2.6E-14	0.00000023	4.6E-12
b	-13.27	-50.15	-1370
c	295.1	433.4	3037
p	16.78	5.331	1.925
R^2	0.77	0.9285	0.8604
SSE	110.36	135.51	237.07
RMSE	2.5479	2.7438	2.6026

B7 - COLLIMATION - SAME NUMBER OF MEASUREMENTS			
A = 0	B7 - part 1	B7 - part 2	B7 - part 3
a	0	0	0
b	-19.14	-56	-2848
c	319.9	451.9	2852
p	7.525	4.027	2.469
R^2	0.9067	0.8605	0.8638
SSE	121.64	148.84	126.12
RMSE	2.2513	2.4903	2.3417

B7 - COLLIMATION - SAME NUMBER OF YEARS			
A = 0	B7 - part 1	B7 - part 2	B7 - part 3
a	0	0	0
b	-13.23	-50.31	-1370
c	294.9	433.9	2990
p	16.82	5.319	1.943
R^2	0.77	0.9285	0.8603
SSE	110.38	135.56	237.24
RMSE	2.5482	2.6711	2.6035

DIFFERENCE	B7 - part 1	B7 - part 2	B7 - part 3
b	-5.8	-67.5	-7.9
c	-0.7	34.0	-0.5
p	19.0	180.4	-1.7
R^2	-0.18	-0.47	-0.13
SSE	1.82	3.03	0.82
RMSE	-1.22	-0.63	0.41

DIFFERENCE	B7 - part 1	B7 - part 2	B7 - part 3
b	-0.30	0.3	0.0
c	-0.07	0.1	-1.5
p	0.24	-0.2	0.9
R^2	0.00	0.00	-0.01
SSE	0.02	0.04	0.07
RMSE	0.01	-2.65	0.03

DIFFERENCE WITH RESPECT TO THE WHOLE DATA SET (A=0)	B7 - part 1	B7 - part 2	B7 - part 3
b	-69.5	-10.7	4443.7
c	-33.6	-6.2	492.2
p	91.9	2.7	-37.0
R^2	-7.2	-12.0	-11.6
SSE	-83.1	-79.3	-82.5
RMSE	-26.3	-18.5	-23.4

DIFFERENCE WITH RESPECT TO THE WHOLE DATA SET (A=0)	B7 - part 1	B7 - part 2	B7 - part 3
b	-78.9	-19.7	2085.7
c	-38.8	-9.9	520.8
p	328.9	35.6	-50.5
R^2	-21.2	-5.0	-12.0
SSE	-84.7	-81.2	-67.0
RMSE	-16.6	-12.6	-14.8

Paso Nuevo dam: B7 Levelling. Blocks of 10 years: (A<0), (A=0), differences, differences with whole data set in the case A=0

B7 - LEVELLING - BLOCKS OF 10 YEARS				
A < 0	B7 - first 10	B7 - second 10	B7 - third 10	B7 - fourth 10
a	-3.9E-08	-4.5E-07	3.552	-3E-13
b	5.64	139.8	25	50.92
c	237.7	997.1	434.2	719.5
p	10.97	2.702	11.41	1.909
R^2	0.6256	0.516	0.5534	0.3732
SSE	36.84	76.89	116.49	12.54
RMSE	1.567	2.773	2.0042	1.0223

A = 0	B7 - first 10	B7 - second 10	B7 - third 10	B7 - fourth 10
a	0	0	0	0
b	5.814	249.9	21.31	69.1
c	238.5	1271	439.5	952.6
p	10.98	2.654	13.44	1.65
R^2	0.616	0.5167	0.5519	0.3711
SSE	37.79	76.77	116.89	12.58
RMSE	1.5369	2.6418	2.0077	1.0241

DIFFERENCE	B7 - first 10	B7 - second 10	B7 - third 10	B7 - fourth 10
b	3.1	78.8	-14.8	35.7
c	0.3	27.5	1.2	32.4
p	0.1	-1.8	17.8	-13.6
R^2	-1.53	0.14	-0.27	-0.56
SSE	2.58	-0.16	0.34	0.32
RMSE	-1.92	-4.73	0.17	0.18

DIFFERENCE WITH RESPECT TO THE WHOLE DATA SET (A=0)	B7 - first 10	B7 - second 10	B7 - third 10	B7 - fourth 10
b	-80.9	721.8	-29.9	127.2
c	-52.2	154.7	-11.9	90.9
p	240.8	-17.6	317.1	-48.8
R^2	-35.1	-45.6	-41.9	-60.9
SSE	-86.5	-72.5	-58.1	-95.5
RMSE	-19.3	38.8	5.5	-46.2

Paso Nuevo dam: B7 Collimation. Blocks of 10 years: (A<0), (A=0), differences, differences with whole data set in the case A=0

B7 - COLLIMATION - BLOCKS OF 10 YEARS				
A < 0	B7 - first 10	B7 - second 10	B7 - third 10	B7 - fourth 10
a	4.1E-14	7.4E-07	2.3E-14	0.00014
b	-143.5	-2019	-50.47	-162.4
c	401.9	1244	433.3	755.6
p	9.341	3.886	4.719	3.253
R^2	0.7542	0.9004	0.8219	0.8137
SSE	97.71	92.53	142.65	46.07
RMSE	2.4711	3.0419	2.2178	2.0465

A = 0	B7 - first 10	B7 - second 10	B7 - third 10	B7 - fourth 10
a	0	0	0	0
b	-90.41	-1961	-50.47	-199.5
c	379.2	1247	433.4	833.3
p	9.614	3.85	4.725	3.06
R^2	0.7528	0.8999	0.8219	0.8117
SSE	98.25	92.97	142.65	46.57
RMSE	2.4781	2.9072	2.2179	1.97

DIFFERENCE	B7 - first 10	B7 - second 10	B7 - third 10	B7 - fourth 10
a	-	-	-	-
b	-37.0	-2.9	0.0	22.8
c	-5.6	0.2	0.0	10.3
p	2.92	-0.93	0.13	-5.93
R^2	-0.19	-0.06	0.00	-0.25
SSE	0.55	0.48	0.00	1.09
RMSE	0.28	-4.43	0.00	-3.74
DIFFERENCE WITH RESPECT TO THE WHOLE DATA SET (A=0)	B7 - first 10	B7 - second 10	B7 - third 10	B7 - fourth 10
b	44.2	3028.6	-19.5	218.3
c	-21.3	158.9	-10.0	73.0
p	145.1	-1.8	20.5	-22.0
R^2	-23.0	-7.9	-15.9	-17.0
SSE	-86.3	-87.1	-80.2	-93.5
RMSE	-18.9	-4.9	-27.4	-35.5

Paso Nuevo dam: B7 Levelling. Blocks of the first 20-30-40 years: (A<0), (A=0), differences, differences with whole data set in the case A=0

B7 - LEVELLING - BLOCKS OF 20 - 30 YEARS		
A < 0	**B7 - cum 20**	**B7 - cum 30**
a	-1.698	-0.6348
b	40.66	31.06
c	599.9	497.6
p	2.286	2.975
R^2	0.8143	0.9294
SSE	122.89	265.09
RMSE	2.0585	2.0847

A = 0	**B7 - cum 20**	**B7 - cum 30**
a	0	0
b	39.94	27.78
c	572.7	477
p	3.025	3.361
R^2	0.8086	0.9293
SSE	126.62	265.28
RMSE	2.0544	2.0685

DIFFERENCE	**B7 - first 10**	**B7 - second 10**
b	-1.8	-10.6
c	-4.5	-4.1
p	32.3	13.0
R^2	-0.70	-0.01
SSE	3.04	0.07
RMSE	-0.20	-0.78

DIFFERENCE WITH RESPECT TO THE WHOLE DATA SET (A=0)	**B7 - first 10**	**B7 - second 10**
b	31.3	-8.6
c	14.8	-4.4
p	-6.1	4.3
R^2	-14.8	-2.1
SSE	-54.6	-4.9
RMSE	7.9	8.7

Paso Nuevo dam: B7 Collimation. Blocks of the first 20-30-40 years: (A<0), (A=0), differences, differences with whole data set in the case A=0

B7 - LEVELLING - BLOCKS OF 20 - 30 YEARS		
A < 0	B7 - cum 20	B7 - cum 30
a	2.724	1.312
b	-4485	-51.95
c	1993	430.9
p	3.169	4.551
R^2	0.9445	0.9814
SSE	229.87	389.78
RMSE	2.8154	2.5278

A = 0	B7 - cum 20	B7 - cum 30
a	0	0
b	-111.8	-50.46
c	557.8	433.5
p	4.181	4.732
R^2	0.9398	0.9809
SSE	249.18	400.71
RMSE	2.882	2.5423

DIFFERENCE	B7 - first 10	B7 - second 10
b	-97.5	-2.9
c	-72.0	0.6
p	31.9	4.0
R^2	-0.50	-0.05
SSE	8.40	2.80
RMSE	2.37	0.57

DIFFERENCE WITH RESPECT TO THE WHOLE DATA SET (A=0)	B7 - first 10	B7 - second 10
b	78.4	-19.5
c	15.8	-10.0
p	6.6	20.7
R^2	-3.9	0.3
SSE	-65.4	-44.3
RMSE	-5.7	-16.8

GRAUS B5 PLOTS:

B5 – 3 parts - same number of measurements
X axis: months
Y axis: displacements (levelling or collimation) [mm]

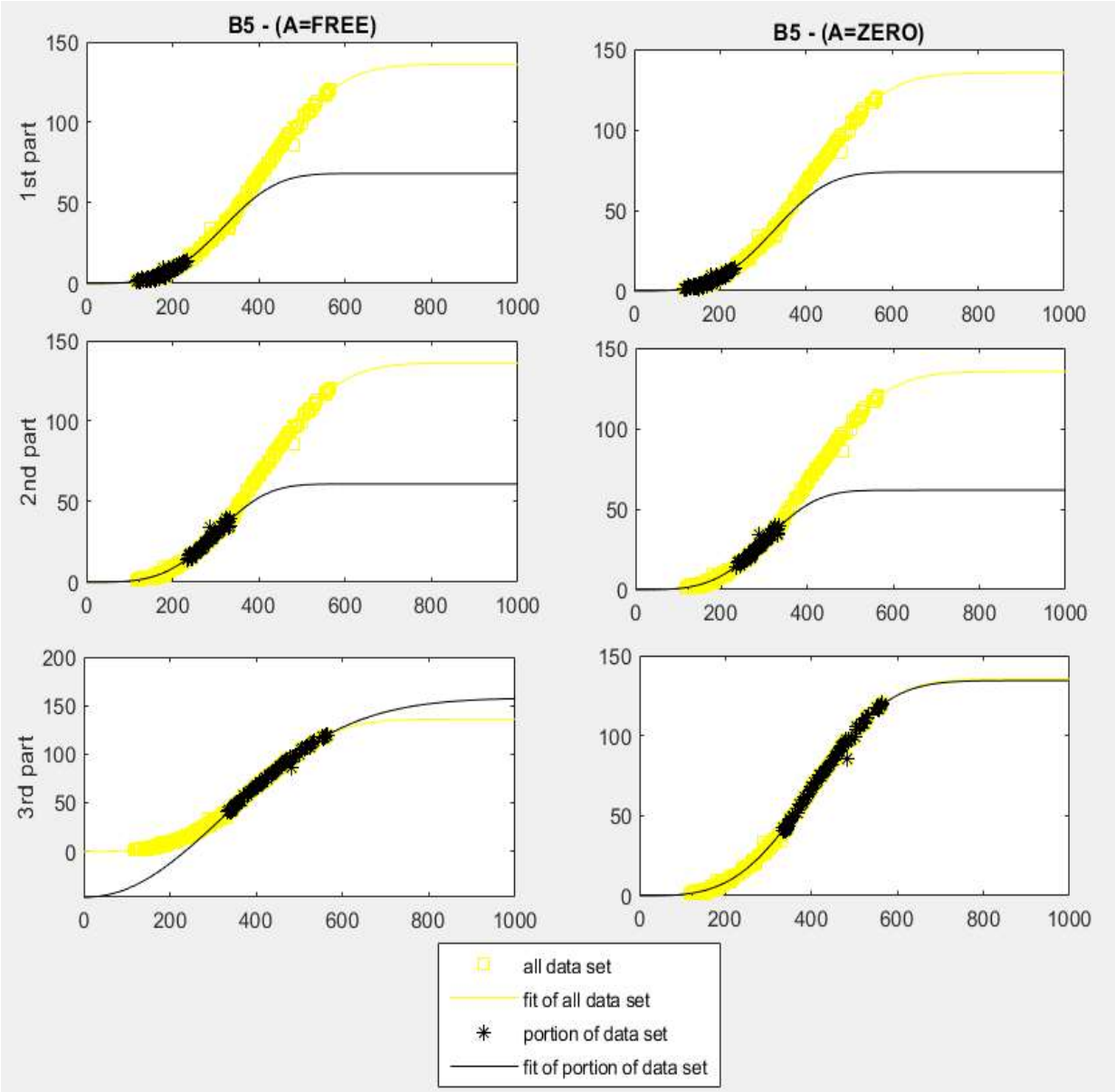

B5 – 3 parts - same number of years

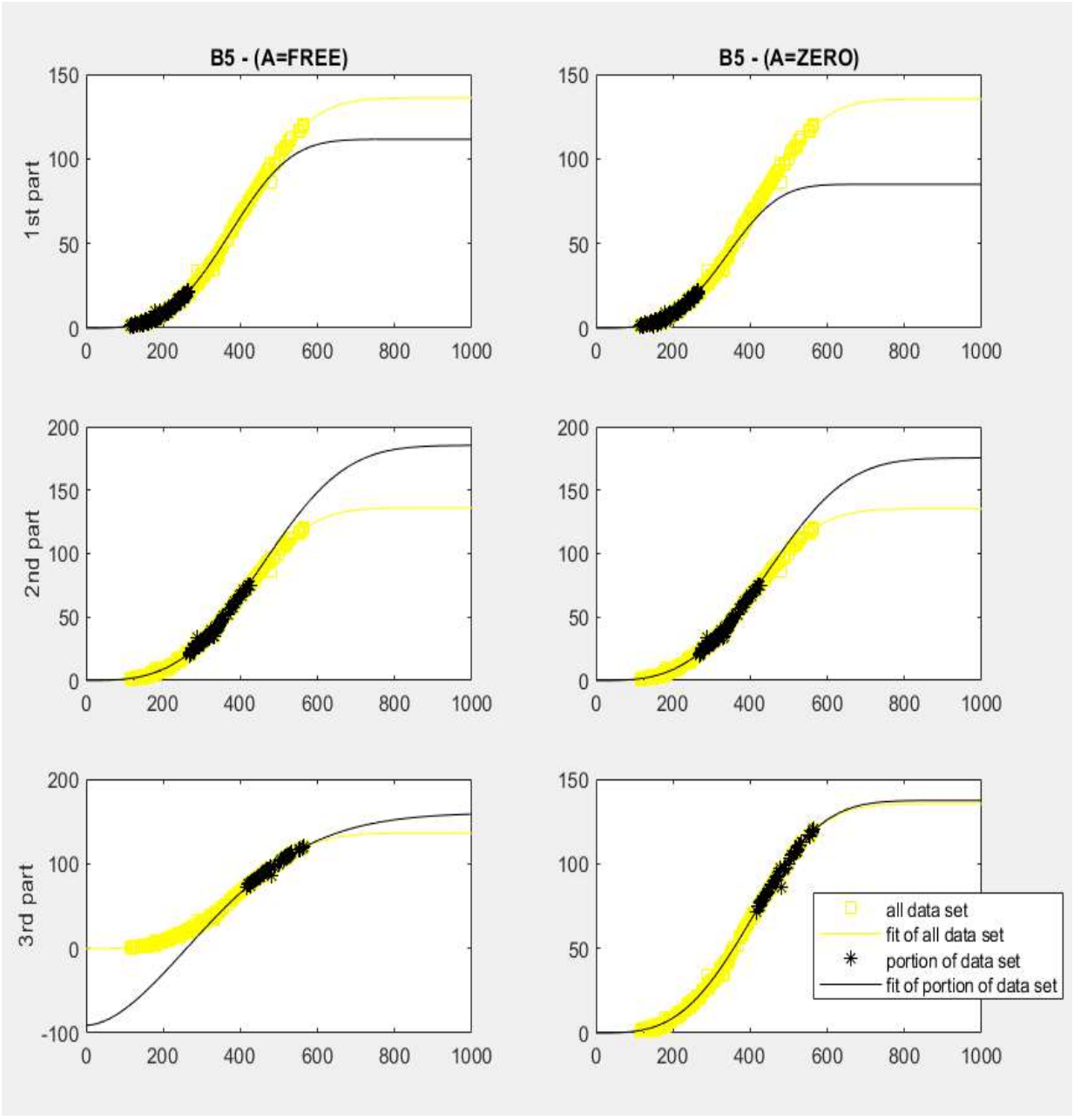

B5 - blocks of 10 years (A=ZERO)

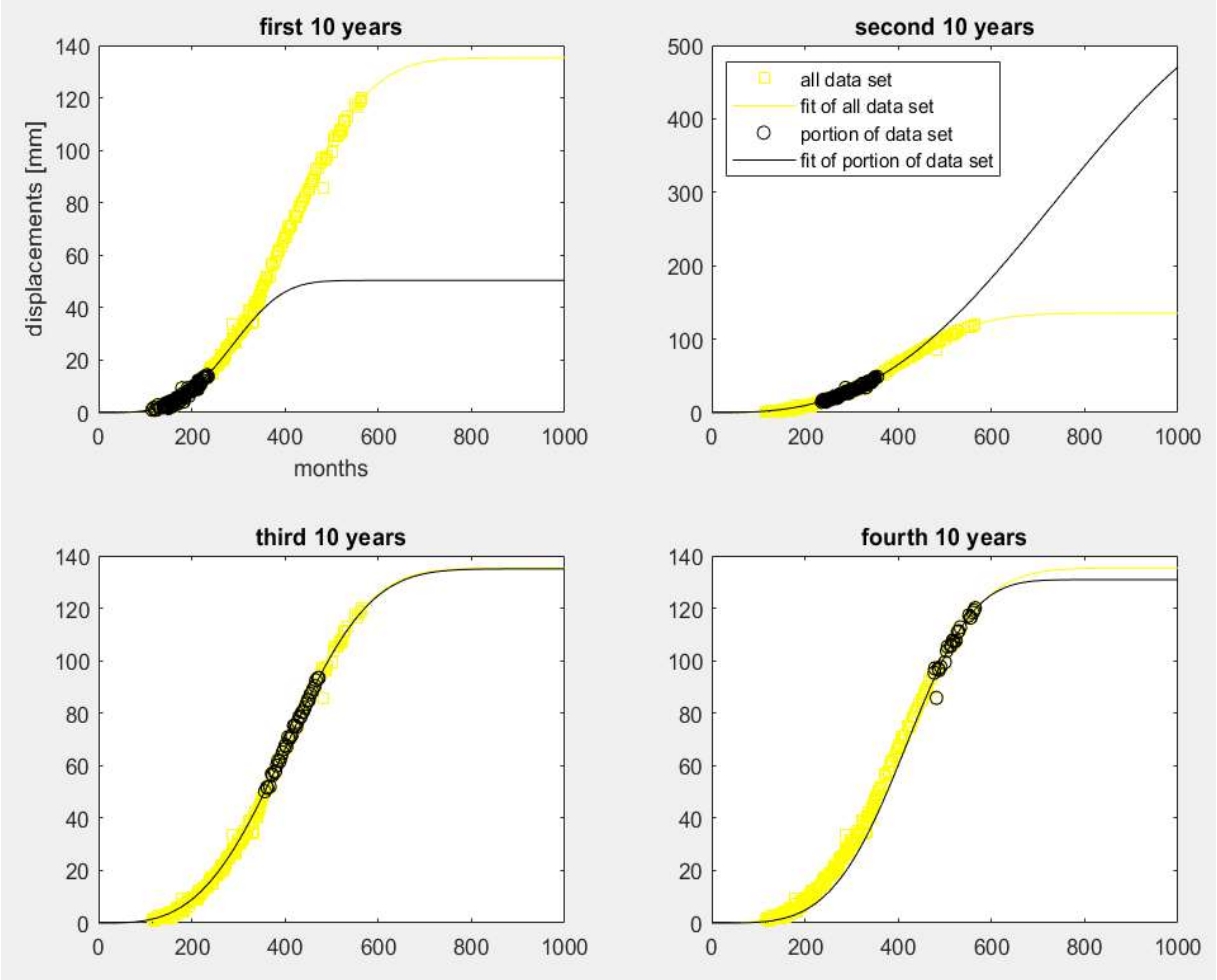

B5 - blocks of 10 years (A<0)

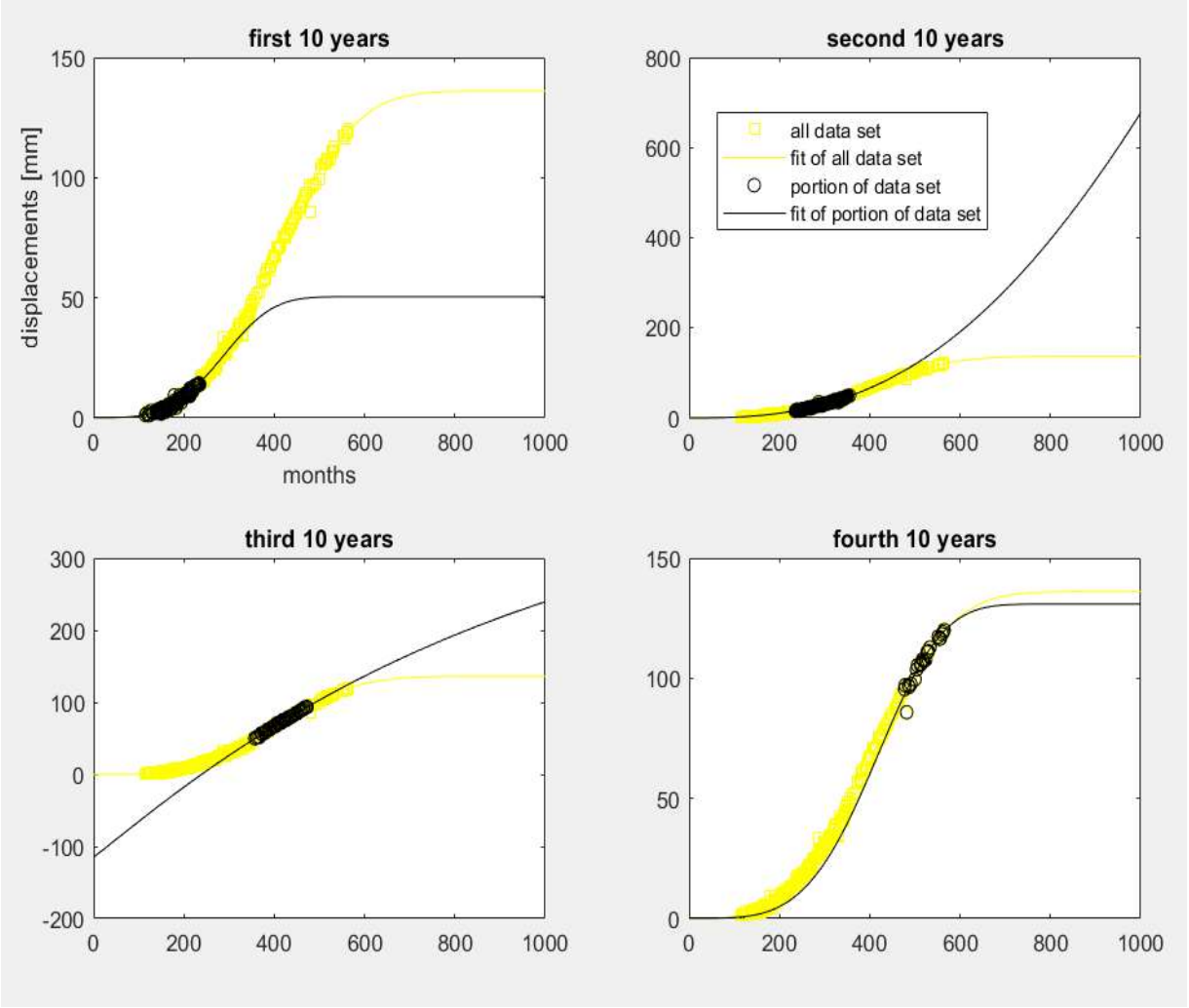

B5 - blocks of 20 and 30 years (A<0 on the left, A=0 on the right)